Screening, mutagenesis and gene expression analysis for improving fucoxanthin biosynthesis in the marine diatom *Phaeodactylum tricornutum*.

Sean Macdonald Miller

July 2023

C3 (Climate Change Cluster)

Faculty of Science

University of Technology Sydney

Submitted in partial fulfilment of the requirements for the degree of Doctor of Philosophy (PhD) at the University of Technology Sydney (UTS)

CERTIFICATE OF ORIGINAL AUTHORSHIP

I, Sean Macdonald Miller, declare that this thesis is submitted in fulfilment of the requirements for the award of Doctor of Philosophy, in the School of Life Sciences at the University of Technology Sydney.

This thesis is wholly my own work unless otherwise referenced or acknowledged. In addition, I certify that all information sources and literature used are indicated in the thesis.

This document has not been submitted for qualifications at any other academic institution.

This research is supported by the Australian Government Research Training Program.

Signature:

Production Note:
Signature removed prior to publication.

Date: 21/07/2023

Acknowledgements

The first I have to thank, considering all that has gone into finishing my PhD, are my mother **Eila** and brother **Evander** for their eternal encouragement to that curly-haired little boy.

I thank the team I was introduced to on Heron Island, including **Audrey Commault**, **David Suggett** and (especially) **Michele Fabris** who gave a lecture on synthetic biology late one night to which I scribbled feverishly.

I humbly thank **Peter Ralph**, for challenging me to see if I had what it took – but more so for being one of those very exceptional people who is forging, tenaciously, a future worth being a part of.

Mathieu Pernice for his support despite my inconsistency, his skilful adaptation to my weaknesses and fraternal encouragement of my strengths, but mostly for his time and dedication to seeing me succeed, without which I would certainly have failed.

Raffaela Abbriano (-Burke), whose rare mix of unending patience and uncompromising expertise allowed me to find my feet during my honours and PhD, I certainly would have given up without her guidance and I can only ever hope to be half the scientist she is.

A very special thanks goes out to **Alexandra Thomson** who has been a mentor and guide for my study woes, an encourager of my teaching abilities and a stellar person.

Andrei Herdean for being a scientist I will always look up to and an generally great guy.

Anna Segečová, Richard Banati, Brandon Signal and **Vishal Gupta** for their admirable work on manuscripts.

Unnikrishnan Kuzhiumparambil, **Helen Price**, **Kun Xiao** and **Taya Lapshina** for their vast knowledge (and reagents).

I'm thankful for making friends with some great people and very fine scientists, particularly **Shawn Price**, **Nine Le Reun**, **Matthias Windhagauer** and **Erin Browne**.

As well as those who made my time more enjoyable – **Kirsty**, **Abeeha**, **Kieran**, **Taya**, **Nathan**, **Gemma**, **Rachael**, **Paige**, **Billy**, **Dominic**, **Artur** …

I would also like to thank my people outside of university - especially **Dillon** for always checking in on me, if not just to compare our experiences in academia.

Finally, I would like to thank **Eloise** for backing me even when I was harping on or complaining about my day - I felt like I could achieve anything with her by my side.

List of publications included

Chapter 2

Macdonald Miller, S., Abbriano, R. M., Segecova, A., Herdean, A., Ralph, P. J., & Pernice, M. (2022). Comparative Study Highlights the Potential of Spectral Deconvolution for Fucoxanthin Screening in Live *Phaeodactylum tricornutum* Cultures. Marine drugs, 20(1), 19.

Chapter 3

Macdonald Miller, S., Abbriano, R. M., Herdean, A., Banati, R., Ralph, P. J., & Pernice, M. (2023). Random mutagenesis of Phaeodactylum tricornutum using ultraviolet, chemical, and X-radiation demonstrates the need for temporal analysis of phenotype stability. *Scientific Reports*, *13*(1), 22385.

Chapter 4

Macdonald Miller, S., Herdean, A., Gupta, V., Signal, B., Abbriano, R. M., Ralph, P. J., & Pernice, M. (2023). Differential gene expression in a subpopulation of Phaeodactylum tricornutum with enhanced growth and carotenoid production after FACS-mediated selection. *Journal of Applied Phycology*, *35*(6), 2777-2787.

I also contributed to the following publication as a co-author during my time as a PhD candidate at UTS, however, this article does not constitute a stand-alone data chapter of this thesis:

Herdean, A., Hall, C. C., Pham, L. L., Macdonald Miller, S., Pernice, M., & Ralph, P. J. (2021). Action Spectra and Excitation Emission Matrices reveal the broad range of usable photosynthetic active radiation for *Phaeodactylum tricornutum*. *Biochimica et biophysica acta. Bioenergetics*, 1862(9), 148461.

Statement of contribution of authors

Chapter 2

Comparative study highlights the potential of spectral deconvolution for fucoxanthin screening in live Phaeodactylum tricornutum cultures.

Sean Macdonald Miller[1,*], Raffaela M. Abbriano[1], Anna Segecova[1, 2], Andrei Herdean[1], Peter J. Ralph[1] and Mathieu Pernice[1]

[1] Faculty of Science, Climate Change Cluster (C3), University of Technology Sydney, Sydney, NSW 2007, Australia;

[2] Affiliation 2; Global Change Research Institute of the Czech Academy of Sciences

***Marine Drugs* – In press**

Contributions:

Conceptualization, Sean Macdonald Miller, Raffaela M. Abbriano and Mathieu Pernice; Data curation, Sean Macdonald Miller and Anna Segecova; Formal analysis, Sean Macdonald Miller; Investigation, Sean Macdonald Miller; Methodology, Sean Macdonald Miller, Raffaela M. Abbriano, Andrei Herdean and Mathieu Pernice; Project administration, Peter Ralph and Mathieu Pernice; Resources, Peter Ralph and Mathieu Pernice; Software, Sean Macdonald Miller and Anna Segecova; Supervision, Raffaela M. Abbriano, Andrei Herdean, Peter Ralph and Mathieu Pernice; Visualization, Sean Macdonald Miller and Anna Segecova; Writing – original draft, Sean Macdonald Miller; Writing – review & editing, Sean Macdonald Miller, Raffaela M. Abbriano, Anna Segecova, Andrei Herdean, Peter Ralph and Mathieu Pernice.

Sean Macdonald Miller — Production Note: Signature removed prior to publication.

Raffaela Abbriano — Production Note: Signature removed prior to publication.

Anna Segecova — Production Note: Signature removed prior to publication.

Andrei Herdean — Production Note: Signature removed prior to publication.

Peter Ralph — Production Note: Signature removed prior to publication.

Mathieu Pernice — Production Note: Signature removed prior to publication.

Chapter 3

Random mutagenesis of *Phaeodactylum tricornutum* using ultraviolet, chemical, and X-radiation demonstrates the need for temporal analysis of phenotype stability.

Sean Macdonald Miller[1,*], Raffaela M. Abbriano[1], Andrei Herdean[1], Richard Banati[2, 3, 4], Peter J. Ralph[1] and Mathieu Pernice[1]

[1] Faculty of Science, Climate Change Cluster (C3), University of Technology Sydney, Sydney, NSW 2007, Australia;

[2] Australian Nuclear Science and Technology Organisation (ANSTO), Kirrawee DC, New South Wales 2232, Australia

[3] Faculty of Medicine and Health, University of Sydney, Camperdown, NSW 2006, Australia

[4] Santuari di San Giovanni D'andorno, Frazione San Giovanni 8, Biella, Italy

Scientific Reports **– In press**

Contributions:

Sean Macdonald Miller, Raffaela M. Abbriano and Mathieu Pernice conceived the study and designed the experiments. Raffaela M. Abbriano, Andrei Herdean, Mathieu Pernice and Peter Ralph guided data and manuscript approach. Richard Banati carried out X-ray treatments. Sean Macdonald Miller carried out the preparation, culturing, ultraviolet (UV) and ethyl methanesulfonate (EMS) treatment, sampling, screening, High Performance Liquid Chromatography (HPLC) and statistical analyses. Andrei Herdean assisted with culture physiology measurements. Sean Macdonald Miller wrote the manuscript, all authors assisted in editing the manuscript. We thank Dr. Justin Davies, Manager, Gamma Irradiations at Australian Nuclear Science and Technology Organisation (ANSTO) for assistance in x- irradiation and dosimetry. We also thank Dr. Unnikrishnan Kuzhiumparambil for assistance with HPLC.

Sean Macdonald Miller Production Note: Signature removed prior to publication.

Raffaela Abbriano Production Note: Signature removed prior to publication.

Andrei Herdean Production Note: Signature removed prior to publication.

Richard Banati Production Note: Signature removed prior to publication.

Peter Ralph Production Note: Signature removed prior to publication.

Mathieu Pernice Production Note: Signature removed prior to publication.

Chapter 4

Differential gene expression in a subpopulation of *Phaeodactylum tricornutum* with enhanced growth and carotenoid production after FACS-mediated selection.

Sean Macdonald Miller[1,*], Andrei Herdean[1], Vishal Gupta[1], Brandon Signal[2], Raffaela M. Abbriano[1,2], Peter J. Ralph[1] and Mathieu Pernice[1]

[1] Faculty of Science, Climate Change Cluster (C3), University of Technology Sydney, Sydney, NSW 2007, Australia;

[2] School of Medicine, College of Health and Medicine, University of Tasmania, Hobart, TAS 7000, Australia

Journal of Applied Phycology **– In press**

Contributions:

Conceptualization, Sean Macdonald Miller and Mathieu Pernice; Data curation, Sean Macdonald Miller; Formal analysis, Sean Macdonald Miller, Brandon Signal and Vishal Gupta; Investigation, Sean Macdonald Miller; Methodology, Sean Macdonald Miller, Brandon Signal, Vishal Gupta and Mathieu Pernice; Project administration, Peter Ralph, Mathieu Pernice and Andrei Herdean; Software, Sean Macdonald Miller, Brandon Signal and Vishal Gupta; Supervision, Raffaela Abbriano-Burke, Andrei Herdean, Peter Ralph and Mathieu Pernice; Visualization, Sean Macdonald Miller; Writing – original draft, Sean Macdonald Miller; Writing – review & editing, all authors. The authors would like to humbly thanks Dr. Unnikrishnan Kuzhiumparambil and Dr. Taya Lapshina for their indispensable expertise on HPLC.

Sean Macdonald Miller Production Note: Signature removed prior to publication.

Vishal Gupta Production Note: Signature removed prior to publication.

Andrei Herdean Production Note: Signature removed prior to publication.

Brandon Signal Production Note: Signature removed prior to publication.

Raffaela Abbriano Production Note: Signature removed prior to publication.

Peter Ralph Production Note: Signature removed prior to publication.

Mathieu Pernice Production Note: Signature removed prior to publication.

Table of Contents

List of Figures and tables

Figure 3.2. **Fluorescence Activated Cell Sorting (FACS) gating strategy.** FSC (forward scatter) is plotted on the x-axis against PerCP-Cy5.5.5-A on the y-axis. The latter has previously shown to have high correlation to fucoxanthin content measured using HPLC. The top 1% cells are selected for single-cell sorting (box A).

Figure 3.3. Mortality and fluorescence assessment examples for selected treatments. (**a**) UV-C (Note that data is missing for day 3 6-second treatment), (**b**) EMS and (**c**) X-ray treatments over a 7-day period, $n = 3$. For clarity not all treatments from the mortality assessment are included. (**d**) Chlorophyll fluorescence measured using the flow cytometry B690 channel as proxy at day 3 for treatments from each mutagen used for downstream analysis of mutants (6-second UV, 30-minute EMS and 1,000Gy X-ray). The positive control is healthy WT *Phaeodactylum tricornutum* cells while the negative control is the same cells boiled on a hot plate until dead.

Figure 3.4. Spectral deconvolution, biomass and fucoxanthin data (**a**) results of spectral deconvolution screening method on WT, UV, EMS and X-ray treated populations (note that this is after FACS-sorting for higher fluorescence in mutagen-treated populations) with coloured dots indicating strains selected for further subculturing and culture and chemical analysis, (**b**) Biomass productivity (mg dry biomass after lyophilisation per L per day) and fucoxanthin productivity results of top strain chosen from each mutagen, (**c**) fucoxanthin content (mg per g dry weight) of top strains, and (**d**) temporal analysis using HPLC over a 6-month period. U denotes UV treated strains, E denotes EMS treated strains and X denotes X-ray treated strains with asterisks denoting statistical significance with one-way ANOVA, $n = 3$ for month 0, $n = 5$ for months 2, 4 and 6.

Figure 4.1. Conceptual diagram of workflow used in this study: from Fluorescence-Activated Cell Sorting (FACS) to culturing, pigment detection using High-Performance Liquid Chromatography (HPLC), and RNA sequencing and analysis.

Figure 4.2. Biomass, growth and pigment data for WT and F cultures of *P. tricornutum*, with (**a**) cell counts measured using flow cytometry, (**b**) chlorophyll *a* and fucoxanthin pigment content measured using HPLC, (**c**) specific growth rate (μ), (**d**) relative fucoxanthin productivity and (**e**) biomass (mg per L). Asterisks denote statistical significance, $n = 5$.

Figure 4.3. Multi-Dimensional Scaling (MDS) plot showing similarities between RNA samples (leading LogFC dimension 1 compared to leading LogFC dimension 2. WT = wild-type, F = FACS). Made using Degust.

Figure 4.4. Gene Ontology (GO) enrichment analysis results with a minimum pathway size of 10 and FDR cut-off = 0.05. Pink bars indicate pathways with 25 – 50 % of genes in that pathway being represented by the gene set, blue indicates 50% of genes being represented. GO term IDs are in parentheses.

Figure 4.5. Genes differentially expressed over a threshold of 1 logFC and $p < 0.05$ in pathways related to pigment biosynthesis and growth. Nineteen genes were differentially regulated between F and WT populations.

Figure 4.6. Pigment pathways with coinciding gene expression values comparing F cultures with WT cultures of *P. tricornutum*.. (**a**) Carotenoid / fucoxanthin pathway from upstream MEP pathway and (**b**) tetrapyrrole pathway to chlorophyll *a*. Red-coloured terms indicate genes over threshold of 1 logFC, while grey terms indicate genes within threshold of 1 logFC. Asterisks denote genes with expression p-value < 0.05. Reactions involving more than one gene are shown as averages unless p-values are either side of 0.05; e.g MgCh_H and MgCh_D are averaged to 1.98 and listed simply as MgCh as both had $p < 0.05$.

Figure 5.1. Hypothetical directed evolution methodology for improving pigments in microalgal cultures. Once a starting population is established using FACS, cells are treated and sorted again, after which they are screened, mutated and sorted continually.

List of Tables

List of Supplementary figures

List of Supplementary Tables

Thesis abstract

Advancements in agricultural technology have been a prevailing feature of exponential human population growth since the Neolithic revolution [5]. Plants have long been recognised as providers of vital services in the form of food, raw materials, and compounds for health [6]. However, there is a growing appreciation of the need to transform current agricultural practices that are strongly associated with high water demand, pollution of soil and waterways, and biodiversity loss [7,8].

Microalgae harbour enormous potential as sustainable contributors to a wide array of industries and technologies, including the production of useful molecules for health and food, sequestration of atmospheric carbon, wastewater treatment, and production of sustainable biofuels [9,10].

This thesis is focused on the marine diatom *Phaeodactylum tricornutum* as a production platform for the primary carotenoid fucoxanthin, which is a pigment currently used in the food and pharmaceutical sectors [11]. Each chapter represents proof of concept studies for, and betters understanding of, critical areas of microalgae biotechnology – high-throughput screening, untargeted mutagenesis, artificial selection and gene expression for pigment biosynthesis.

In Chapter 1, a reliable, inexpensive, and fast high-throughput screening method was developed for detecting fucoxanthin in *P. tricornutum*. In Chapter 2, three mutagens were evaluated for the ability to increase fucoxanthin in *P. tricornutum* mutants. Fluctuating pigment content detected over six months in three mutant lines and one strain displaying a 35% increase in fucoxanthin at four months highlighted the critical need for temporal phenotype stability for studies of this kind. In Chapter 3, a FACS-based method was used to artificially isolate a population of *P. tricornutum* with increased growth, pigment content, and fucoxanthin productivity under an industry-relevant culturing regime. Additionally, gene expression analysis and gene pathway enrichment analysis were used to highlight genes of potential interest to chlorophyll and fucoxanthin biosynthesis. It was found that the tetrapyrrole pathway was significantly enriched

and likely responsible for upregulated chlorophyll, while only three genes along the carotenoid pathway were upregulated, indicating only a few critical rate-limiting steps in fucoxanthin biosynthesis.

Chapter 1: Introduction

1.1 Microalgae as an emerging platform for biotechnological applications

Microalgae are a polyphyletic group of unicellular, photosynthetic organisms that can be either prokaryotic (cyanobacteria) or eukaryotic, exhibiting vast differences in morphology, lifestyle traits, growth, habitats, and cellular biochemistry [12,13]. Marine microalgae make up the phytoplankton community which despite constituting only 0.2% of the photosynthetically active carbon biomass on Earth, are responsible for about half of net primary production [14,15]. These organisms optimise processes like photosynthesis, non-photochemical quenching (NPQ), nutrient acquisition and the utilisation of specialist genes which contributes to their ecological success [16].

Interest in the potential of microalgae for biotechnological applications has increased significantly in the last two decades due to their ability to produce compounds of interest, such as polyunsaturated fatty acids, terpenoids, alkaloids, polyphenols, peptides, proteins, carbohydrates, antioxidants, and pigments [17,18]. These are valuable compounds relevant to many different sectors, including biofuel, health supplement, pharmaceutical, cosmetic, agriculture, food and aquaculture industries [19-21].

Microalgae are preferable as cell factories for valuable compounds because they can be grown heterotrophically, autotrophically, or mixotrophically, which allows for diverse culturing approaches [22]. They also convert sunlight into biomass and fix CO_2 at considerably higher rates than terrestrial plants [23] when grown under autotrophic conditions, have the ability to recover and utilise nutrients from wastewater, can be cultivated on non-arable land throughout the year, and are amenable to relatively rapid strain development [19]. Additionally, microalgae produce a diverse range of valuable bioactive compounds of which they exhibit high potency [24,25]. Despite these many benefits, industrial cultivation of microalgae is still often restricted by physiological constraints [26] and the cost of production techniques and infrastructure [19,27], although these

limitations can be overcome through optimisation of culture conditions and through genetic engineering [28].

1.2 *Phaeodactylum tricornutum*

Diatoms (Bacillariophyceae) constitute a significant portion of global microalgae populations, with around 100,000 species [29]. The marine diatom *Phaeodactylum tricornutum* is the only species in the *Phaeodactylum* genus and is notable for rare or unique characteristics like its relative hardiness during culture, lack of silica requirement and multiple morphotypes, factors which make it interesting for research [30,31]. Additionally, *P. tricornutum* is one of few species to have an entirely sequenced genome [32]. This fact benefits projects undertaking genetic manipulation or analysis, and indeed the species has been used to explore cell processes, to improve target compounds like poly-unsaturated fatty acids, lipids and pigments as well as for analysis of carbon fixing mechanisms [33-38] .

While *Arthrospira* (Spirulina) and *Chlorella* compose the majority of the microalgal biomass produced and used in industry, *P. tricornutum* is of great interest not only for research but also for biotechnological applications [39,40]. This is mostly because *P. tricornutum* contains considerably more fucoxanthin than other microalgal species and up to 100 times more than seaweed (macroalgae) at around 59 mg g^{-1}under optimal conditions and typically range between 10 – 20 mg g^{-1} in algal species compared to 1 -2 mg g^{-1} for seaweed (Khaw et al. 2022; Susanto et al. 2016)[189]. This is important considering the current primary source of industrial fucoxanthin is seaweed [41, 44].

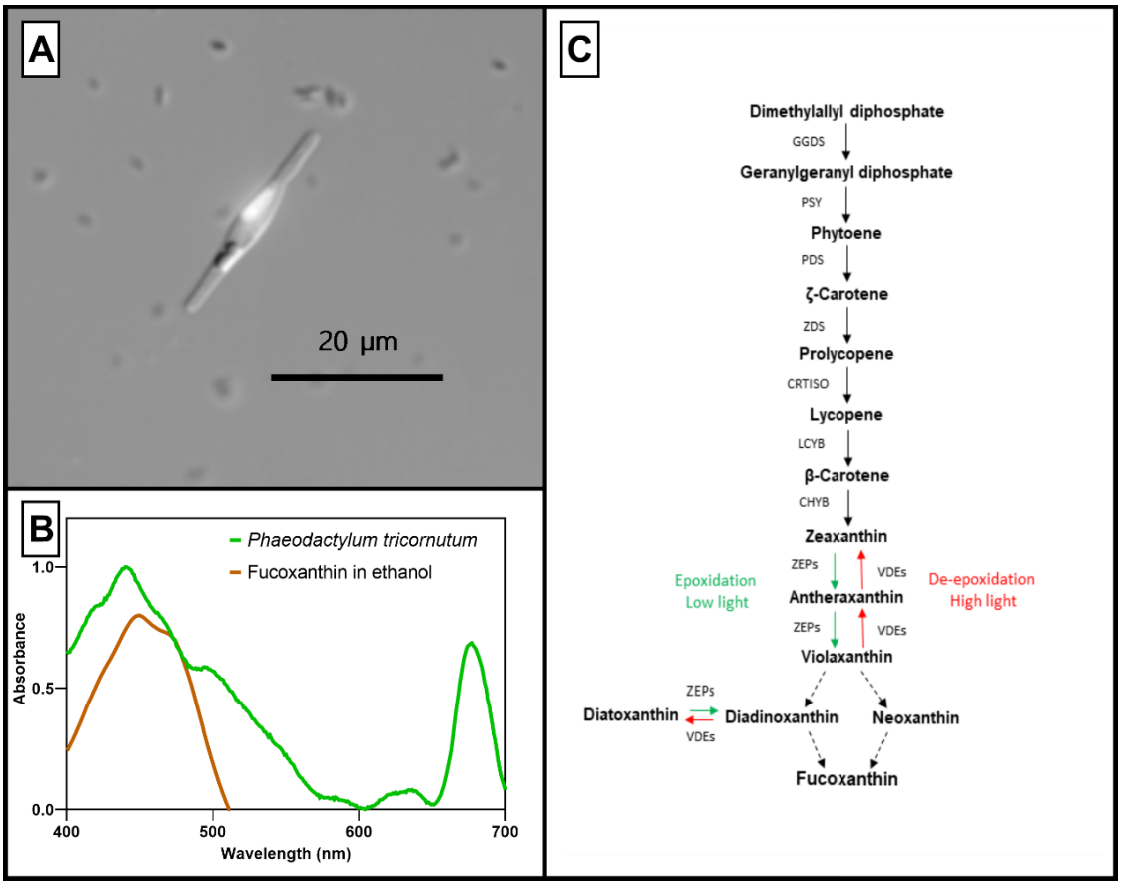

Figure 1.1 (**a**) Nile red-stained fluorescence microscope image of exponential-phase *P. tricornutum* cell with fusiform variation (lipid highlighted), (**b**) visible spectrum *P. tricornutum* culture absorbance with fucoxanthin absorbance (in ethanol), and (**c**) *P. tricornutum* fucoxanthin pathway as illustrated by Manfellotto, et al. 2020 [1].

1.3 The biological importance of pigments

Pigments are molecules with selective absorption of visible light (**Figure 1.1b**) that are found across every taxonomic domain, and are utilised in photosynthetic organisms for light harvesting and photoprotection [45]. Chlorophylls, carotenoids and phycobilins are the primary photosynthetic pigments used for light absorption in the photosynthetic apparatus, including in microalgae [46]. These pigments are attached to light-harvesting complexes to trap light for conversion to usable energy at photosystems I and II [47].

In diatoms, fucoxanthin-chlorophyll proteins bind the primary pigments of chlorophyll *a* and chlorophyll *c* along with fucoxanthin in high stoichiometric ratios, providing the cells with a

larger absorption in the blue-green region of the electromagnetic spectrum [48-50].

In plants, prenols and isoprenoids are synthesized with two independent pathways, the plastidic methylerythritol 4- phosphate (MEP) and cytosolic mevalonic acid pathway (MVA) originating in the plastid and cytosol, respectively. Further to this, carotenoids are synthesised in *P. tricornutum* through the MEP and MVA pathways from isopentenyl diphosphate (IPP) and dimethylallyl diphosphate (DMAPP), via the carotenoid precursor geranylgeranyl diphosphate (GGPP) and then phytoene via the phytoene synthase (PtPSY) gene (**Figure 1.1c**)[51,52].

1.4 Natural pigments for industry

Pigments sourced from photosynthetic organisms like microalgae are used in a range of industries including food, cosmetics, fashion, textiles and human health [53-56]. Pigments contribute to the health supplement sector primarily for their antioxidant properties, as well as to improve eye health and support pro-vitamin A function [57]. Furthermore, microalgal pigments have been used for decades in aquaculture production to improve the colouration of farmed seafood [56,58,59].

While some pigments are produced synthetically for economic reasons, concerns over food safety, pollution and sustainability make microalgal-sourced alternatives promising [60,61]. Microalgae-sourced pigments receiving the most research and industry attention are phycocyanin, chlorophylls, β-carotene, and astaxanthin using the species' *Chlorella vulgaris*, *Spirulina platensis*, *Haematococcus pluvialis*, and *Dunaliella salina* [62]. Microalgal biofactories offer a promising alternative platform for producing pigments while addressing safety and sustainability issues.

1.5 Fucoxanthin

Carotenoids are yellow, orange and red pigments comprised of two groups: carotenes which are purely hydrocarbons, and xanthophylls. Xanthophylls are oxygenated carotenoids, the most commonly found and/or highly researched being violaxanthin, neoxanthin, zeaxanthin, lutein,

astaxanthin, fucoxanthin, canthaxanthin and spirillocanthin and are most commonly associated with the xanthophyll cycle (violaxanthin, antheraxanthin, diadinoxanthin, diatoxanthin and zeaxanthin) which drive non-photochemical quenching to protect against photoinhibition[63],

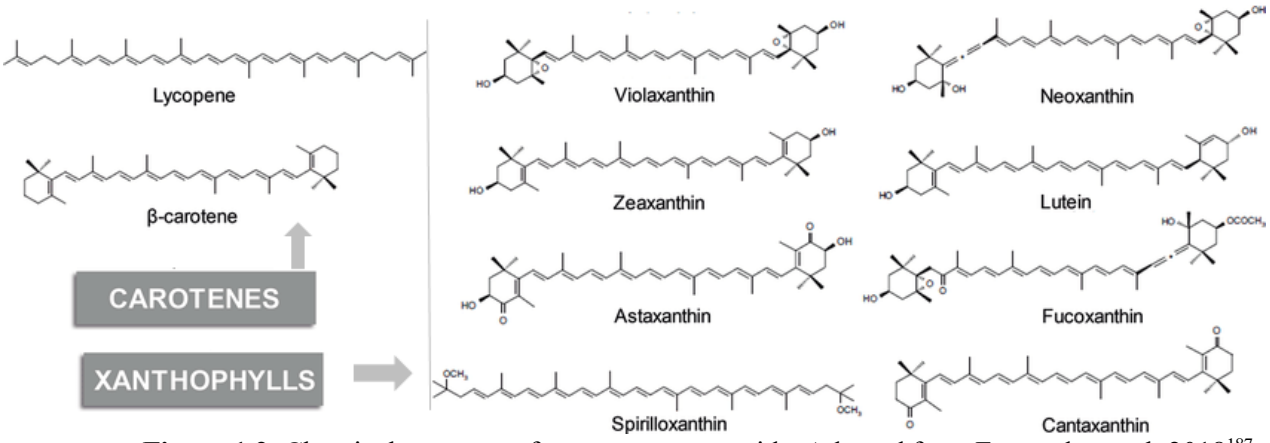

Figure 1.2. Chemical structure of common carotenoids. Adapted from Fernandes et al. 2018[187].

Fucoxanthin is another xanthophyll and one of the most predominant pigments in marine phytoplankton (**Figure 1.3**) [64]. It is an accessory pigment found in the chloroplasts of microalgae where it is protein-bound with chlorophyll to form Fucoxanthin- Chlorophyll Protein complexes (FCPs) to assist in the capture and transfer of energy during photosynthesis [65]. The benefit of fucoxanthin is that is absorbs light in the blue-green region of the visible spectrum with a λ_{max}, or peak wavelength, around 460-570 nm when protein-bound [66].

The unusual molecular structure of fucoxanthin is thought to contribute to its amplified health benefits [67]. Under certain conditions fucoxanthin has a higher antioxidant activity than other common antioxidants like β-carotene including 13.5 × that of α-tocopherol due to the allenic bond and possibly due to greater molecular oxygen content [67-69]. This antioxidant property has important implications for human health and disease treatment as oxidative stress is a common feature of most diseases and chronic disorders [70].

Fucoxanthin additionally could reduce the likelihood of obesity and related illnesses like diabetes primarily by upregulation of uncoupling protein 1 (UCP1) in white adipose tissue, to drive thermogenesis and therefore weight regulation [71-73].

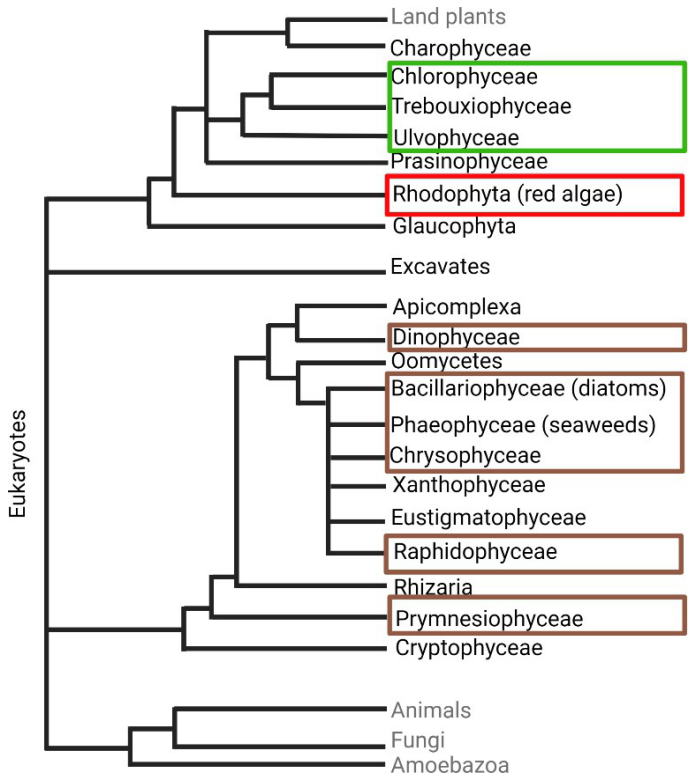

Figure 1.3. Phylogenetic tree depicting Eukaryote lineages with the green square indicating green alga, red depicting red alga and brown squares indicating classes containing fucoxanthin. Adapted from Stiger-Pouvreau and Zubia 2020[2].

1.6 Strain limitations in algal biotechnology

The usefulness of a particular microalgal strain is limited by its physiological characteristics that make growing and harvesting unviable. Improving target traits through optimised cultivation and genetic modification is therefore critical for overcoming high operational, maintenance, harvesting and conversion costs [18,74]. Targeted genetic engineering is an invaluable tool for improving strains, while random mutagenesis is a more cost- and time- effective strategy [75,76]. This is because genetic engineering projects require a larger time investment while also falling under strict legislation regarding GMOs (Genetically Modified Organisms) because they are

strains created by introduction of foreign genetic material [75].

There are major gaps in our understanding of the effects of untargeted mutagens on microalgal cultures and downstream effects on strain stability. In addition there is virtually no consensus on best practices for utilising untargeted mutagenesis to increase yield of target compounds in microalgae. Therefore exploration of the effects of various untargeted DNA modification strategies on strain stability and yield of target compounds is crucial, and will assist in the discovery of target genes and the mapping of biosynthetic pathways.

1.7 DNA modification for creating microalgae strains

Every single organism is constantly under threat of undergoing genetic alterations from numerous sources. Endogenous causes, namely polymerase copy error, hydrolysis and reactive oxygen species (ROS), are omnipresent factors with the potential to naturally induce DNA (deoxyribonucleic acid) damage, as are exogenous chemical and physical agents like UV light ubiquitous within the biosphere [77]. Essentially, no species is entirely detached from experiencing genetic mutation, and while that is a threat substantial to individuals, genetic variation forms the basis of evolutionary adaptation on Earth [78].

Research in genetics enables the process of guided evolution, leading to the development of genetic modification tools. These tools have proven to be invaluable as they permit the alteration of a species to execute advantageous functions or improve preferred traits. In this context, targeted genetic engineering can be seen as an extension of selective breeding, and has provided important services like medical therapies and improved agricultural yields [79]. Targeted genome editing systems include ZFN (zinc-finger nucleases), TALEN (transcription activator-like effector nucleases) and CRISPR (clustered regularly interspaced short palindromic repeats) that have the potential to make impactful changes to industry, but are often complex and can exhibit off-target effects. While these genetic engineering platforms requires the editing of specific segments of an organism's genome, random mutagenesis is the utilisation of physical and chemical mutagens to induce alteration of DNA, after which

desirable strains can be screened and selected for. The common theme among mutagens is that they all introduce changes in the DNA sequence that can lead to incorrect pairing of nucleotides during DNA replication, which, if not repaired by the cell's DNA repair mechanisms (for example direct reversal of DNA damage, excision repair, mismatch repair or the SOS response), can result in altered phenotypic traits [80]. However, the specific type and extent of the DNA damage, as well as the cell's response to the damage, can vary depending on the type of mutagen and the specific conditions.

One of the most common exogenous mutagenic agents is UV light, with the sun delivering UV-A (320-400 nm), and to a lesser extent UV-B (290-320 nm), to the surface of the Earth [81] and therefore existing as one of the most pervasive origins of genetic mutation. UV-C light (<290 nm) however is absorbed by the atmosphere, yet can be reproduced artificially for germicidal and research purposes. The effectiveness of UV light at forming molecular lesions in the DNA depends on wavelength, with the highest rate of damage occurring at 260 nm [81], and the most common wavelength used for research being 254 nm [82]. Aside from the potency of UV-C light, it has the additional benefit that, generally speaking, organisms have not evolved protective mechanisms against UV-C because of its absorbance into the atmosphere, thereby serving as a valuable tool for mutagenesis. Ninety-five percent of UV-induced molecular lesions are attributable to pyrimidine dimers: cyclobutane pyrimidine dimers (CPDs – 85%) and pyrimidine-pyrimidone (6-4) photoproducts (6-4PPs – 10%), which in turn account for the majority of genetic effects from UV radiation [83]. Cyclobutane pyrimidine dimers occur through photoaddition when adjacent pyrimidines (thymine or cytosine) form covalent linkages in the area of their 5,6 double bonds, resulting in a 4-membered carbon ring between them [84] with most mutations arising from photoaddition being C-T and CC-TT transition mutations [85].

The mutagenic chemical EMS has been used widely for genetic mutation research primarily for its potency, ease of use, and consistent mutation rates independent of genome size [86]. EMS is in the alkylating agent category of chemical mutagens because it alkylates guanine bases, forming O^6-ethylguanine, resulting in mispairing of guanine bases with thymine instead of cytosine [87].

X-ray mutagenesis occurs primarily via single and double strand breaks along the phosphate-sugar backbone, as well as from secondary sources like reactive oxygen species [88,89]. X-radiation is the emittance of charged photons which collide into and transfer energy into other molecules, exciting electrons which are then released in unequal distributions until captured elsewhere, as well as the production of radical species and other molecular products in the location surrounding affected DNA [90]. The DNA disruption described is illustrated in **Figure 1.4**.

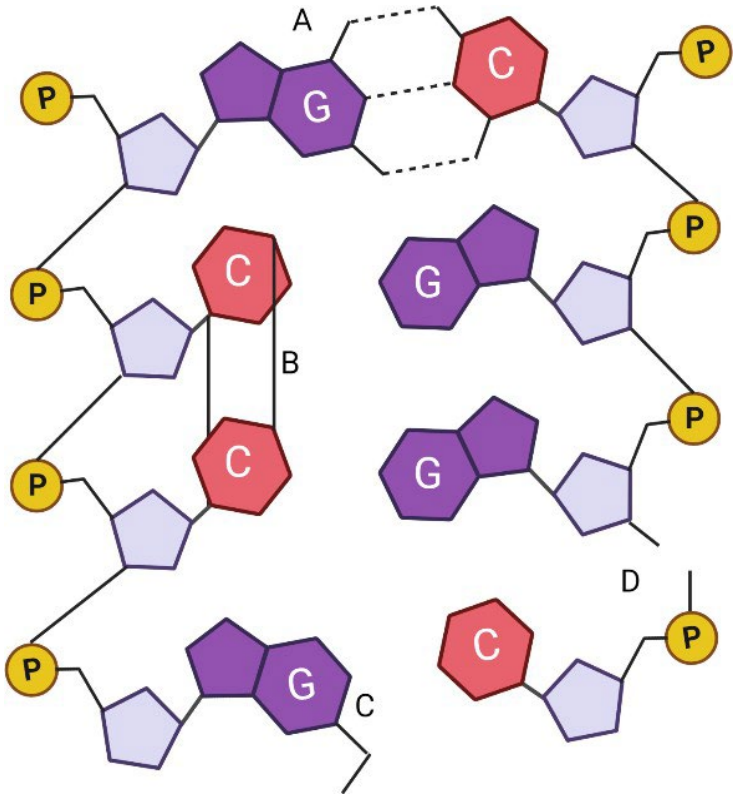

Figure 1.4. Genetic products of mutagenic agents within the DNA double helix. (**a**) normal base pairing between guanine (G) and cytosine (C), (**b**) a cyclobutane pyrimidine dimer (CPD) is one of the most common products of UV radiation, (**c**) 0^6-ethylguanine is formed by ethyl methanesulfonate (EMS) and (**d**) depicts a single strand break caused by ionising radiation. Figure adapted from Friedberg et al. 2005[77].

1.8 Aims and objectives

This work covers three crucial areas of microalgal biotechnology: high-throughput screening, random mutagenesis and gene expression differences of elite strains, which are covered by the following aims (Figure 1.5):

1. **To develop a high-throughput selection and screening method for high yield fucoxanthin mutants of *Phaeodactylum tricornutum* for further analysis.**

   The objective for Chapter 1 is that with the development of a high-throughput screen for fucoxanthin in this species, this work will also act as a proof of concept to further pigment screening for microalgal biotechnology as applicable to other target pigments and other species of interest.

2. **To alter pigment biosynthesis in *Phaeodactylum tricornutum* using short UV radiation, EMS and X-radiation to create pigment hyper-producing strains.**

   The second objective is to enhance our understanding of mutagens used in projects of this type, to understand how cultures respond as well as to better understand phenotype instability after treatments, to better inform on projects undertaking this type of methodology either in research or industry.

3. **To identify the gene expression changes responsible for improved non-mutant pigment phenotypes using FACS-sorting and Illumina RNA sequencing in *Phaeodactylum tricornutum*.**

   The third objective is to generate a more comprehensive knowledge of gene expression differences driving increase in fucoxanthin biosynthesis, in order to develop a more complete understanding of how pigment content is up or downregulated in *P. tricornutum*.

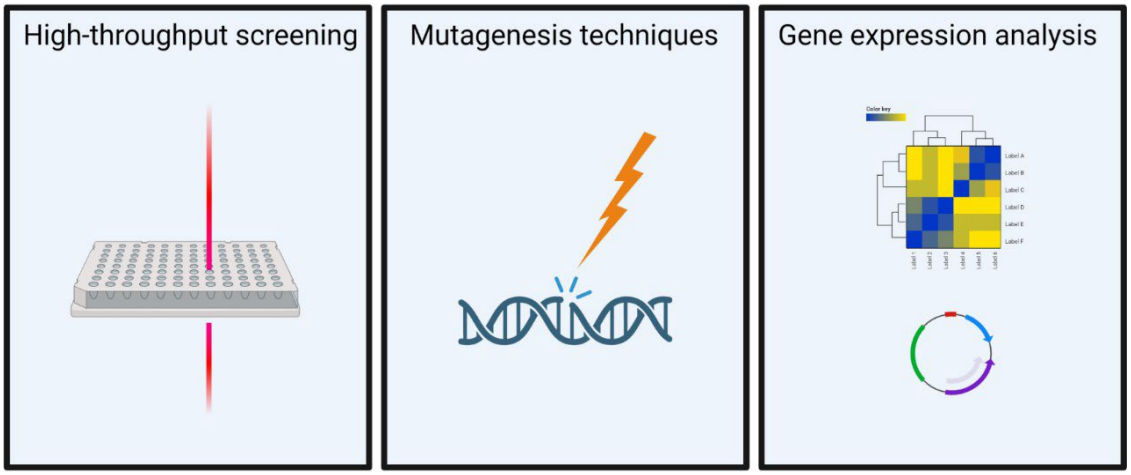

Figure 1.5. The three primary areas of focus for this thesis are high-throughput screening, untargeted mutagenesis and gene expression analysis.

Chapter 2

Comparative study highlights the potential of spectral deconvolution for fucoxanthin screening in live *Phaeodactylum tricornutum* cultures.

Published in *Marine Drugs* in the Special Issue *Biotechnology Applications of Microalgae*

December 2021

Sean Macdonald Miller[1,*], Raffaela M. Abbriano[1], Anna Segecova[1,2], Andrei Herdean[1], Peter J. Ralph[1] and Mathieu Pernice[1]

[1] Faculty of Science, Climate Change Cluster (C3), University of Technology Sydney, Sydney, NSW 2007, Australia;

[2] Affiliation 2; Global Change Research Institute of the Czech Academy of Sciences

2.1 Abstract

Microalgal biotechnology shows considerable promise as a sustainable contributor to a broad range of industrial avenues. The field is however limited by processing methods which have commonly hindered the progress of high throughput screening, and consequently development of improved microalgal strains. We tested various microplate reader and flow cytometer methods for monitoring the commercially relevant pigment fucoxanthin in the marine diatom *Phaeodactylum tricornutum.* Based on accuracy and flexibility, we chose one described previously [4] to adapt to live culture samples using a microplate reader and achieved a high correlation to HPLC ($R^2 = 0.849$), effectively removing the need for solvent extraction. This was achieved by using new absorbance spectra inputs, reducing the detectable pigment library and changing pathlength values for the spectral deconvolution method in microplate reader format. Adaptation to 384-well microplates and removal of the need to equalize cultures by density further increased the screening rate. This work is of primary interest to projects requiring detection of biological pigments, and could theoretically be extended to other organisms and pigments of interest, improving the viability of microalgae biotechnology as a contributor to sustainable industry.

2.2 Introduction

Fucoxanthin is the most abundant marine carotenoid pigment, accounting for more than 10% of the total carotenoids produced naturally [91]. Fucoxanthin is of commercial interest for its antioxidant, anti-inflammatory, antibacterial and anti-obesity characteristics [42,70,92,93], as well as having potential in inhibiting cancer cell growth [94]. Due to these beneficial properties, fucoxanthin is an established nutraceutical currently sourced from seaweed [71,95]. However, the marine pennate diatom *Phaeodactylum tricornutum* exhibits up to 100 times higher fucoxanthin content (mg g^{-1} DW) than seaweed, which makes it an attractive alternative for commercial purposes. *P. tricornutum* has also been used extensively across a wide area of research and has full genome

data [32]. This species has demonstrated genetic manipulability [33,96,97], which further supports its utility as a biofactory template for fucoxanthin. Fucoxanthin in *P. tricornutum* can reach up to 59.2 mg g^{-1} under optimal growth conditions [44], has been improved by 69.3% (mg g^{-1} DW) in chemically-induced mutants [98] and by 45% per cell by introduction of the PSY (phytoene synthase) gene [99] compared to the wild-type strain.

Strategies that generate large mutant or transformant libraries (hundreds to thousands of clones) necessitate high-throughput methods to screen novel strains for pigments because the current benchmark of pigment detection is high-performance liquid chromatography (HPLC), which while being accurate, is very expensive and time-consuming. Several approaches to screening fucoxanthin in *P. tricornutum* were investigated here and compared in terms of the accuracy of their prediction as compared to HPLC, as well as the effort invested to produce that result. Because fucoxanthin and chlorophyll *a* are associated with light harvesting, chlorophyll screening methods were included as fucoxanthin proxies alongside direct fucoxanthin quantifiers, and their assessment included both microplate reader and flow cytometer formats. Flow cytometry provides a means of analyzing samples at the resolution of individual cells - which negates effects from culture density and can be attached to fluorescence-activated cell sorting (FACS), while the microplate reader format provides an inexpensive and non-invasive way of analyzing many samples in a short period of time, therefore both systems were included.

Three microplate reader methods and three flow cytometry methods were chosen for this study. First, two estimates for chlorophyll and fucoxanthin autofluorescence were measured using flow cytometry to investigate whether various excitation/emission gates could accurately predict average fucoxanthin content through analysis of single cells. A third flow cytometry method using Nile Red dye was included to investigate if dye fluorescence can improve the detection of fucoxanthin based on its relationship to lipids [100] and correlation to total carotenoids [98]. One approach for estimating chlorophyll in ethanol was tested as a proxy for measuring fucoxanthin in microplate format from Ritchie [101]. The second microplate reader method investigated in this study is theoretically similar to the equations from Ritchie [101], except that it aims to quantify

fucoxanthin directly by using equations based on specific wavelength absorbance of pigment extracts related to fucoxanthin, rather than using chlorophyll as a proxy, found in Wang et al. [3]. The final microplate reader method is from Thrane et al. [4], developed from earlier work [102,103], and uses spectral deconvolution of absorbance spectra obtained from samples extracted using an organic solvent like ethanol. All samples were compared during exponential growth phase, as this is the easiest point to detect pigment content differences without compounding effects from media changes and cell senescence, and enables the screening methods with the best resolution to be highlighted accordingly.

This study aims to reconcile accuracy with practical considerations of screening methods, and to further optimize a promising method for high-throughput screening of fucoxanthin in *P. tricornutum*. Six published methods using two common pieces of analytical equipment were used to assess their correlation to HPLC, one being chosen for further optimisation based on this correlation as well as practical considerations like ease of use compared to cost and time investment. This work contributes to the field of microalgal biotechnology by improving the rate at which novel strains of *P. tricornutum* can be selected based on improved fucoxanthin content.

2.3 Materials and Methods

2.3.1 Stock culturing

Axenic *Phaeodactylum tricornutum* (CCAP 1055/1) stock cultures were grown in Artificial Sea Water (ASW) medium (Darley & Volcani, 1969) under fluorescent light (200 µmol photons m^{-2} s^{-1}) with a 24:0 light cycle in shaking Erlenmeyer flasks (95 rpm) kept at 21°C. Treatment flasks were inoculated at 8.5×10^5 cells mL^{-1} from cultures at exponential stage.

2.3.2 Experimental design

Treatment flasks consisted of 250 mL conical flasks containing 100 mL of respective media. Highest fucoxanthin content has been achieved with low light availability and high nitrate availability [44], so combinations of these two factors were used to maximise the expected culture fucoxanthin content range. Cells were inoculated into either nitrate-free ASW media (-N), standard (1xN) nitrate media or media with 10× nitrate (10xN) from KNO3 and placed under either 10 (LL) or 200 (HL) µmol photons m^{-2} s^{-1}. To diminish variances in media composition

introduced by pipetting culture volumes directly into experimental flasks, 30 mL culture aliquots were centrifuged and the pellets were then pipetted into experimental flasks (~2.5×10^7 cells total). Three × 30 mL stock cultures were also centrifuged, washed once with ultrapure water, flash-frozen in LN2, lyophilised and weighed to estimate a starting value for biomass in each experimental flask. The treatments were left until there was a detectable difference observed in the relative chlorophyll *a* fluorescence across treatments.

2.3.3 Sampling

Each day, 200 µL from each flask was transferred into a clear-bottom, black 96-well microplate (Corning Inc.) and a microplate reader (Tecan Infinite M1000 Pro) was used to measure absorbance at 750 nm as well as chlorophyll *a* fluorescence using an excitation wavelength of 440 nm and emission wavelength of 680 nm. Cells were counted daily using flow cytometry (Cytoflex LX, Beckman Coulter) by separating singlets via gating within an XY plot of forward scatter (FSC) and side scatter (SSC). A second plot comparing forward scatter by cell area (FSC- A) to chlorophyll *a* fluorescence (excitation with blue laser at 488 nm with 690-50A optical filter) was constructed to separate singlets into live cells and dead cells/debris.

At the conclusion of the experimental period, flask culture volumes were measured, centrifuged and washed once with ultrapure water to reduce dissolved salts. Previous experiments have shown that this method does not impact the fucoxanthin content while maximizing extraction efficiency (data not shown). Samples were then flash-frozen in liquid nitrogen and lyophilized before being kept at -80°C for measurement using HPLC. The remaining flask media was frozen for nitrate analysis.

Culture aliquots were diluted to 1×10^6 cells mL^{-1}, and pigment extraction of both diluted and undiluted culture aliquots was performed by centrifugation and replacement of supernatant with equal volume of absolute ethanol kept at -30°C. Dilution was made for uniform cell concentration in order to test whether equalised cell concentrations had an effect on the efficacy of a given screen. Extraction was furthered using 3 × 3-second pulses of an ultrasonic homogenizer (Qsonica Q125) at maximum amplitude with centrifugation in between pulses to confirm blanching of

pellets and thus complete extraction of cellular pigments. Extracts and raw culture, both diluted and undiluted, were used to attain data for the various screening methods by pipetting 200 µL into clear-bottom, black 96-well microplates and measuring on microplate reader and by flow cytometry.

2.3.4 Chlorophyll and Fucoxanthin autofluorescence using flow cytometry (method A and B)

Daily plots of chlorophyll *a* fluorescence (excitation with blue laser at 488 nm with 690/50 optical filter) for assisting in cell counts using flow cytometry were also utilized on the day of harvest to retrieve single-cell chlorophyll fluorescence data. A secondary plot for detecting fucoxanthin was also created on this day to assess whether a different excitation/emission arrangement would be more reliable for detecting fucoxanthin than that used for detecting chlorophyll (488/690). Firstly, HPLC data was compared to data for all available flow cytometry channel arrangements, and the channel with highest correlation to fucoxanthin was chosen to be displayed. This was a yellow excitation laser at 561 nm with 710/50 nm optical filter. The mean single-cell fluorescence for both channels was used to compare to fucoxanthin as measured using HPLC. To explore whether chlorophyll *a* fluorescence measured using microplate reader could be sufficient to predict fucoxanthin content, daily chlorophyll *a* measurements from section 2.3 were also compared to fucoxanthin measured using HPLC.

2.3.5 Nile red fluorescence using flow cytometry (method C)

Nile Red fluorescence using both microplate reader and flow cytometry was included to test the sensitivity of this dye in both formats. One mL of each diluted culture sample was dyed with 0.75 µg Nile Red for ~10 minutes and fluorescence was measured using microplate reader Excitation/Emission wavelengths of 484/583 nm, while the cytometry equivalent was measured by retrieving the mean single cell fluorescence using blue excitation laser at 488 nm with 610/20 optical filter. Optimal concentration and wavelength can be seen in **Supplementary figure 2.1** and excitation/emission matrices using Nile Red are visualized in **Supplementary figure 2.2**.

2.3.6 Ritchie (2008) using microplate reader (method D)

The equations for chlorophyll for Ritchie [101] were applied to extracts to test whether they could

reliably predict fucoxanthin in ethanol:

$$\text{Chl } a = -0.9394 \times A_{632} - 4.2774 \times A_{649} + 13.3914 \times A_{665}$$

2.3.7 Wang et al. (2018) using microplate reader (method E)

A similar method to the equations above, yet for direct quantification of fucoxanthin in *P. tricornutum* has also been developed albeit without the need for removal of cell debris after extraction [3]. The equation from the original source is as follows (Cfuc' = Fucoxanthin concentration in mg L^{-1}):

$$Cfuc' = 6.39 \times A_{445} - 5.18 \times A_{663} + 0.312 \times A_{750} - 5.27$$

2.3.8 Thrane et al. (2015) using microplate reader (method F)

The direct quantification method using visible light absorbance spectra developed by Thrane, et al. [4], which while requiring a more complex data analysis, was included to test the potential of 'gauss-peak' fitting originally established by Küpper, et al. [102]. The method is described thoroughly in Thrane, et al. [4]. In short, individual pigment spectra are described by combinations of Gaussian peaks (termed the Gauss-peak spectra method), and are then modelled alongside background noise using non-negative least squares. The method utilizes R software to input coefficients for peak height, wavelength and peak halfwidth to characterize pigments, and then compares this to sample absorbance spectra to estimate pigment content in mg L^{-1} using absorbance and pigment molar extinction coefficients. Thrane, et al. [4] aimed to quantify multi-species pigment samples from lakes, whereas this work aims to adapt the method to a single species in a laboratory setting. The original source includes R scripts for readers to easily perform the method. To test if the method was further applicable to cultures without extraction**,** absorbance spectra obtained using diluted culture aliquots on a microplate reader were used instead of sample extract spectra.

2.3.9 HPLC for pigment detection

Freeze-dried pellet samples were weighed and re-suspended in a solvent ratio of between 2-3 mg of sample (DW) per mL of ethanol and sonicated with an ultrasonic homogenizer (Qsonica Q125) at 100% amplitude for 3 × 3-second pulses before being stored at -20°C overnight once blanching of pellets was confirmed using a centrifuge. They were then filtered using 0.2 µm PTFE 13 mm

syringe filters and stored in -80°C until analysis. HPLC was conducted using an Agilent Technologies 1290 Infinity, equipped with a binary pump with integrated vacuum degasser, thermostatted column compartment modules, Infinity 1290 auto-sampler and PDA detector. Column separation was performed using a 4.6 mm × 150 mm Zorbax Eclipse XDB-C8 reverse-phase column (Agilent Technologies, Inc.) and guard column using a gradient of TBAA (tert-Butyl acetoacetate): Methanol mix (30:70) (solvent A) and Methanol (Solvent B) as follows: 0–22 min, from 5 to 95% B; 22–29 min, 95% B; 29-31 min, 5% B; 31-40 min, column equilibration with 5% B. Column temperature was maintained at 55°C. A complete pigment profile from 270 to 700 nm was recorded using PDA detector with 3.4 nm bandwidth. Example spectra can be seen in **Supplementary figure 2.3**.

2.3.10 Additional measurements

Media nitrate content was analyzed using an automated photometric analyzer (Gallery™ Discrete Analyzer, Thermo Fisher Scientific) by establishing standard calibration curves for nitrite and Total Oxidised Nitrogen (TON) from 0 – 20 mg L^{-1} after which samples from 10 × nitrate flasks were diluted to 1/20th of their original concentration to fit within this range. Spiked recoveries were performed using 3 samples with dissimilar concentrations and these resulted in an average recovery of 100 ± 7.5%.

2.3.11 Statistical analysis

One-way ANOVA with confidence level of 0.05 was performed followed by Tukey's post-hoc to determine significance among samples, using GraphPad Prism version 9.0.2 for Windows, GraphPad Software, San Diego, California USA, www.graphpad.com.

2.4 Results and discussion

2.4.1. Culture characteristics

The 200 µmol photons m^{-2} s^{-1} without nitrate (HL-N) treatment cell growth was statistically significantly higher ($p = 0.0005$) than both other HL treatments (~9.5 × 10^6 compared to an average 6.5× 10^6 cells mL^{-1}) on the final day. While the final pellet weights for all HL treatments were similar, the mean singlet forward scatter (FSC-A) of HL-N cultures was 50% less than the forward scatter of nitrogen-present HL treatments ($p < 0.0001$). Decreased cell size and volume

due to nitrogen

limitation has been observed previously [104] and explains the much higher cell density in HL-N treatments. Importantly, this indicates that *P. tricornutum* has impressive light stress tolerance mechanisms despite low or no nutrient availability, considering the analogous biomass productivity of HL treatments, which averages were significantly higher ($p = 0.0206$) at up to 2 times that of the lowest LL biomass productivities.

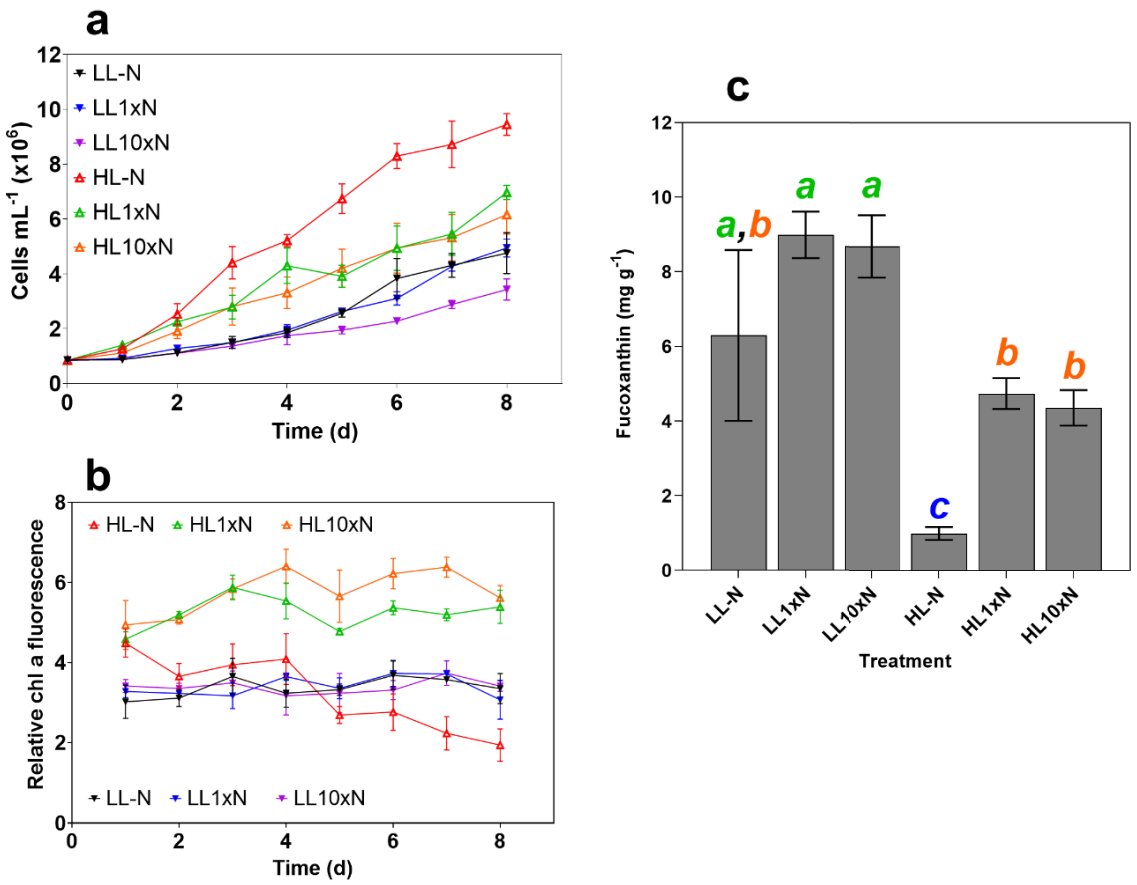

Figure 2.1. Measured culture characteristics over the 8 day experimental period. (a) Cell density in millions mL^{-1}, (b) Relative chlorophyll *a* fluorescence (chlorophyll *a* fluorescence / culture absorbance at 750 nm), which was used to determine optimal experiment termination time point, and (c) fucoxanthin content of freeze-dried samples measured using HPLC (mg g^{-1}). Treatment abbreviations are as follows: nitrate-free ASW media (-N), standard (1xN) nitrate media or media with 10× nitrate (10xN) and either 10 (LL) or 200 (HL) µmol photons m^{-2} s^{-1} of white light. Statistical significance was calculated using one-way ANOVA ($p < 0.05$) with letters denoting non-significant groupings. Error bars denote standard deviation ($n = 3$).

Pigment content was measured by relative chlorophyll *a*, and the experiment was terminated on day 8 when relative chlorophyll *a* was significantly different ($p < 0.0001$, ~1.9 for HL-N

compared to ~3.3 for all LL treatments and ~5.5 for HL treatments with nitrate supplementation).

LL cultures displayed very similar chlorophyll *a* autofluorescence over the experimental period, while there was a clear distinction between nitrogen replete and deplete conditions under HL.

As expected, fucoxanthin content was a function of irradiance, specifically, its role as a light harvesting pigment was demonstrated by its negative correlation with photon availability. Nitrogen limitation decreased overall fucoxanthin content and productivity under 200 µmol photons m^{-2} s^{-1}, while simply increasing the variability under 10 µmol photons m^{-2} s^{-1}. These treatments provided a sufficient range of fucoxanthin contents to assess high-throughput screen viability.

2.4.2 High-throughput screen analysis

Data for live culture chlorophyll *a* autofluorescence on microplate reader were not shown because there was no correlation to HPLC (R^2 <0.002). The microplate reader Nile Red fluorescence data displayed a negative correlation, which can be attributed to disturbance by media noise and other resolution issues, and these were therefore not considered reliable methods.

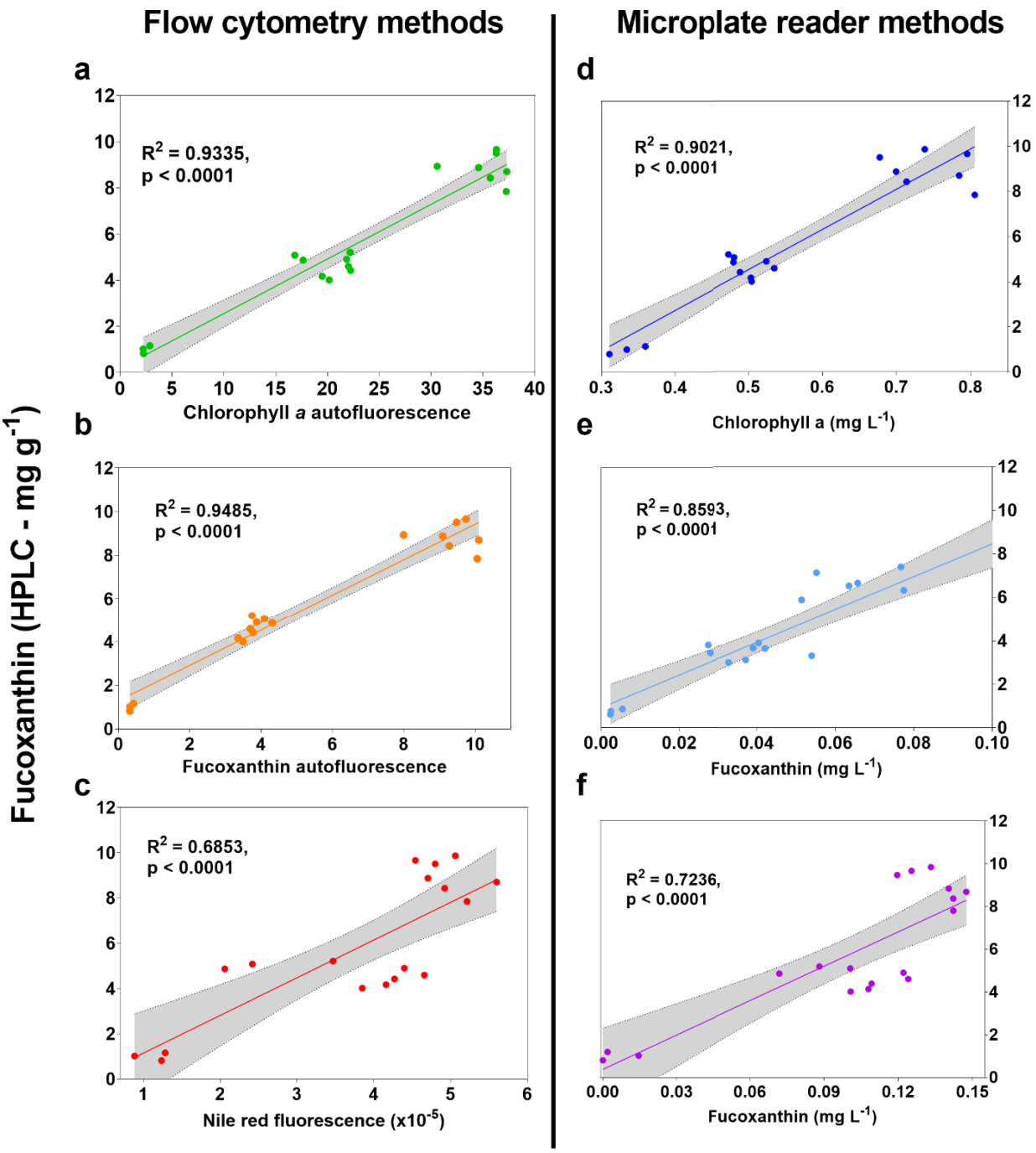

Figure 2.2. High-throughput screen results correlated to fucoxanthin (mg g^{-1}) measured using HPLC. (a) Mean single cell chlorophyll *a* autofluorescence measured on flow cytometer using blue excitation wavelength of 488 nm with 690/50 nm optical filter, (b) mean single cell fucoxanthin autofluorescence measured on flow cytometer using yellow excitation laser at 561 nm with 710/50 optical filter, (c) mean single cell fluorescence measured on flow cytometer using blue excitation laser at 488 nm with 610/20 optical filter after dyeing with Nile Red, (d) chlorophyll *a* content (mg L^{-1}) using equations for ethanol extracts from Ritchie (2008) on a microplate reader, (e) fucoxanthin content (mg L^{-1}) for concentrated ethanol extracts from Wang, et al. [3] on a microplate reader, and (f) spectral deconvolution method from Thrane, et al. [4] using raw culture absorbance spectra on microplate reader. Units on x- axes for d, e and f are simply what the sources for each use to determine fucoxanthin content, while samples for all three were

extracted herein using an equal weight of biomass, effectively making x- axis units as weight of fucoxanthin per unit weight of biomass (like HPLC).

Autofluorescence measurements using flow cytometry displayed highest correlation to HPLC data with $R^2 = 0.9335$ and $R^2 = 0.9485$ for chlorophyll *a* (B690-50, **Figure 2.2a**) and fucoxanthin (Y710-50, **Figure 2.2b**), respectively. These were also higher than both Nile Red and the equations from Ritchie [101] and Wang et al. [3], which require either dyeing or extraction with an organic solvent. While chlorophyll *a* autofluorescence was included to estimate the B690-50 filter reliability at estimating fucoxanthin, using alternatives is likely to give more accurate predictions, as with the Y710-50 filter. Excitation at 561 nm with emission at 710 nm (Y710-50) has generally been avoided in the literature because there is little or no absorption of individual *P. tricornutum* pigments at these wavelengths. However, Premvardhan, et al. [105] have shown a shift in fucoxanthin absorbance when bound in Fucoxanthin-Chlorophyll Protein (FCP) to wider than 561 nm. Because the flow cytometry methods are measuring live cells rather than pigments in extracts, it is appropriate to assess fucoxanthin absorbance characteristics when bound to FCP. Also, an extra emission peak at 710 nm was observed by Fan, et al. [106] in *P. tricornutum*, who confirmed a relationship between emission intensity at 710 nm and fucoxanthin content measured using HPLC [106]. Using these wavelengths has the likely benefit of being able to measure fucoxanthin content by its relationship to cellular FCP rather than by chlorophyll content as a proxy, like when measuring extracts using equations from Ritchie [101]. Despite the overall fluorescence intensity of Y710 being about 25% that of the B690 channel (data not shown), it appears sufficient as not only an accurate indicator, but more reliable in predicting fucoxanthin content than B690-50.

Measuring autofluorescence with flow cytometry is not only accurate for measuring fucoxanthin, it does not require extraction, dilution or dyeing, and this greatly improves screening time. Relevant to many projects that generate large mutant or transformant libraries, FACS can also be attached to this method to further improve screening and selection times, as also found in Gao, et al. [100] and Fan, et al. [106].

The use of Nile Red to correlate polar lipids with fucoxanthin has been performed previously using live cultures of *Tisochrysis lutea* with an R^2 value of 0.88 [100] as well as has the correlation between Nile Red and total carotenoids in *P. tricornutum* [98]. A relationship to HPLC was found herein ($R^2 = 0.69$) for *P. tricornutum* using the average single cell fluorescence of singlets after staining with Nile Red (**Figure 2.2c**). While a correlation was found, using different channels resulted in higher R^2 values without the need to dye first.

Microplate reader formats displayed overall lower correlation to HPLC, with the maximum found using the method from Ritchie [101] (R^2= 0.9021, **Figure 2.2d**).

In our initial analysis, the method from Wang, et al. [3] displayed reduced correlation to HPLC at $R^2 = 0.0292$ when the dilution of 1×10^6 cells mL^{-1} was used. Verification cultures in the original source use a cell density between 20 - 100×10^6 cells mL^{-1} which is likely to have contributed to the sensitivity and therefore accuracy reported therein ($R^2 \geq 0.946$). To improve the resolution of fucoxanthin predictions using the method from Wang, et al. [3], experimental samples were analyzed again at higher cell concentration and an R^2 value of 0.8593 was found (**Figure 2.2e**). Despite this method displaying a slightly lower correlation than in the original source (R^2= 0.8593 compared to $R^2 \geq 0.946$, see Wang, et al. [3], users performing equipment calibration can expect even better results, and should keep in mind the changes to resolution when using low cell densities.

Despite displaying a relatively high correlation of $R^2 = 0.7236$ (**Figure 2.2f**), the spectral deconvolution method from Thrane, et al. [4] did not require solvent extraction. This method also had the greatest potential for calibration and refinement, owing to its use of a much larger dataset and multiple programmable input scripts using R software. Therefore the method was chosen for further optimisation.

2.4.3 Optimisation of spectral deconvolution from Thrane et al. (2015)

The R scripts contained within Thrane, et al. [4] were first tested using absorbance spectra obtained from uniformly-dilute ethanol-extracted experimental samples. It was noticed that predictions for fucoxanthin were either extremely low or 0. To allow the method to attribute lower wavelength

spectral regions to the presence of fucoxanthin, pigments that are not present in *P. tricornutum*, or present in only minute amounts, were removed from the R script "gaussian.peak.parameters.txt" as well as from line 32 of the "pigments.function.R" script. It was found that removing all but the chlorophylls *a*, *c1* and *c2* and fucoxanthin from the method ensured detection of fucoxanthin in every sample. After removal of 'unnecessary' pigments and the reassigning of pathlength in the 'Sediments.R' file to z = 0.625 for microplate reader adaptation, the correlation between the script and the content of fucoxanthin detected using HPLC in mg g^{-1} was $R^2 = 0.801$.

The spectral qualities of a pigment are altered when measured in live cell thylakoid membranes compared to when measured as free-floating molecules in an organic solvent like ethanol. The cumulative effects of the silica frustule of *P. tricornutum*, the lipid layers associated with the thylakoid, effects from saltwater medium, and interference from other cellular components are expected to have substantial effects on fucoxanthin spectral characteristics, so the ethanol-fucoxanthin coefficients used in the original source were replaced. Firstly, the *P. tricornutum* absorbance spectrum from cultures under LL+N (maximum fucoxanthin) were averaged and the spectrum between 400 – 550 nm was used to estimate new fucoxanthin Gaussian peaks using the "chl.b.fit.R" file from the original source. These new coefficients for peak height ("a"), wavelength ("xp") and peak halfwidth ("s") for live cultures were then used instead of the original coefficients for ethanol and used to compare the spectral deconvolution (mg L^{-1}) to fucoxanthin as measured using HPLC (mg g^{-1}), which resulted in an R^2 value of 0.849 (**Figure 2.3a**).

The above method analysis and troubleshooting was performed with pre-diluted culture samples for ease of use and confidence of comparison. To explore the possibility of using microplate well cultures without equalizing by cell density, and to exclude potential effects from differences in individual cell volume amongst a population, an exponential-phase wild type *P. tricornutum* culture was diluted to various densities between approximately 0.5 and 20×10^6 cells mL^{-1} (A_{750} between 0.03 and 0.7) and their predicted fucoxanthin values compared on a 384-well microplate

using spectral deconvolution of individual wavelengths normalized by the absorbance at 750 nm (**Figure 2.3b**), using the following equation:

$$\text{SpeDec Fx (mg L}^{-1}\text{)} = \text{spectra [400 – 700 nm]} / (\text{Sample A}_{750} - \text{ASW A}_{750})$$

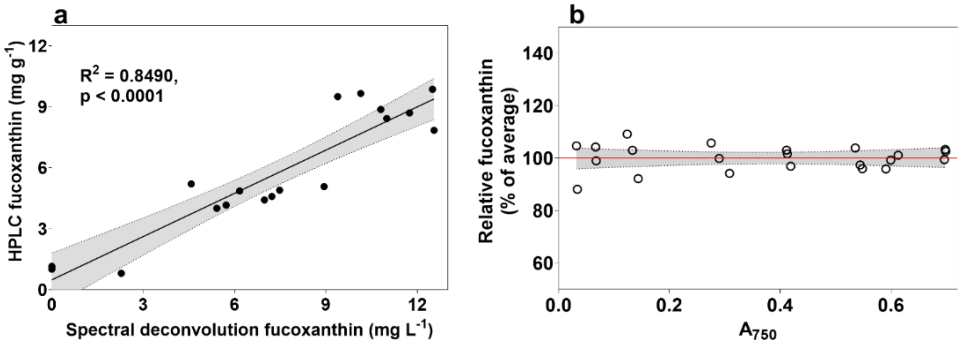

Figure 2.3. Correlation of modified spectral deconvolution method to fucoxanthin measured using HPLC. (a) Correlation after modifying fucoxanthin coefficients, and (b) results after normalizing absorbance spectra to culture density (absorbance at 750 nm) on a 384-well microplate.

Fucoxanthin predictions across replicates were within 8% of each other when only including samples at optical density of 0.4 or above. The success of using the absorbance at 750 nm to normalize the results of the spectral deconvolution method relies on each wavelength of a culture spectrum (400 – 700 nm) being divided by the culture A750 after blanking to culture media absorbance at the same wavelength. This method allows multiple wells to be measured without prior dilution, removing the need to account for screen bias towards denser cultures, but does not account for increased fucoxanthin due to culture shading effects.

The benefit of using this method in comparison to flow cytometry is that the latter is expensive to purchase and run, requires skilled users and most importantly cannot screen using microplate format without a high risk of cross-well contamination. The modified spectral deconvolution method from Thrane, et al. [4]allows users to screen libraries of hundreds to thousands of individuals cost-effectively without removing microplate lids or culture volume to preserve sterility, which also enables temporal evaluation across growth curves and different growth conditions. Method benefits are outlined in Table 2.1.

Table 2.1. Practical considerations of tested high-throughput screens for fucoxanthin in *P. tricornutum.* Culture contact refers to removing vessel lids, pipetting or transferring into measurement vessels.

Fucoxanthin screening method	Method letter	Correlation to HPLC (R^2)	No dyeing required	No extraction required	No skilled equipment operators required	No culture contact required
Flow cytometry / FACS	A/B	0.949	✓	✓		
Nile Red	C	0.685		✓	✓	
Ritchie (2008)	D	0.902	✓		✓	
Wang et al. (2018)	E	0.859	✓		✓	
Thrane et al. (2015)	F	0.849	✓	✓	✓	✓

2.5. Conclusions

Increasing screening rate is a critical factor for high-throughput projects regarding microalgal libraries. In this aspect, the spectral deconvolution method from Thrane, et al. [4] holds great potential because samples can be analyzed with temporal and multiple-condition evaluation of individuals whilst maintaining culture sterility. This method removes the cost of most expendables and reduces the time spent extracting samples, which also reduces the likelihood of variability introduced through solvent evaporation or pipetting. Most notably, once using modified input scripts, the spectral deconvolution method from Thrane, et al. [4] provides researchers with accurate measurement of fucoxanthin in live cultures of *P. tricornutum*, which to our knowledge has never been achieved, and significantly improves the screening rate of novel strains for biotechnological purposes. While this work is limited to fucoxanthin in *P. tricornutum*,

future projects should look to adapting spectral deconvolution to other microalgal species as well as other pigments of interest.

Chapter 3

Random mutagenesis of *Phaeodactylum tricornutum* using ultraviolet, chemical, and X-radiation demonstrates the need for temporal analysis of phenotype stability.

Published in *Scientific Reports*

December 2023

Sean Macdonald Miller[1,*], Raffaela M. Abbriano[1], Andrei Herdean[1], Richard Banati[2, 3], Peter J. Ralph[1] and Mathieu Pernice[1]

[1] Faculty of Science, Climate Change Cluster (C3), University of Technology Sydney, Sydney, NSW 2007, Australia;

[2] Australian Nuclear Science and Technology Organisation (ANSTO), Kirrawee DC, New South Wales 2232, Australia

[3] Faculty of Medicine and Health, University of Sydney, Camperdown, NSW 2006, Australia

3.1 Abstract

We investigated two non-ionising mutagens in the form of ultraviolet radiation (UV) and ethyl methanosulfonate (EMS) and an ionising mutagen (X-ray) as methods to increase fucoxanthin content in the model diatom *Phaeodactylum tricornutum*. We implemented an ultra-high throughput method using fluorescence-activated cell sorting (FACS) and live culture spectral deconvolution for isolation and screening of potential pigment mutants, and assessed phenotype stability by assessing pigment content over six months using high-performance liquid chromatography (HPLC). Both UV and EMS resulted in significantly higher fucoxanthin within the six month period after treatment, likely as a result of phenotype instability. A maximum fucoxanthin content of 135 ± 10 % wild-type found in the EMS strain, a 35% increase. We found mutants generated using all methods underwent reversion to the wild-type phenotype within a six month time period. X-ray treatments produced a consistently unstable phenotype even at the maximum treatment of 1,000 Grays, while a UV mutant and an EMS mutant reverted to wild-type after four months and six months, respectively, despite showing previously higher fucoxanthin than wild-type. This work provides new insights into key areas of microalgal biotechnology, by (i) demonstrating the use of an ionising mutagen (X-ray) on a biotechnologically relevant microalga, and by (ii) introducing temporal analysis of mutants which has substantial implications for strain creation and utility for industrial applications.

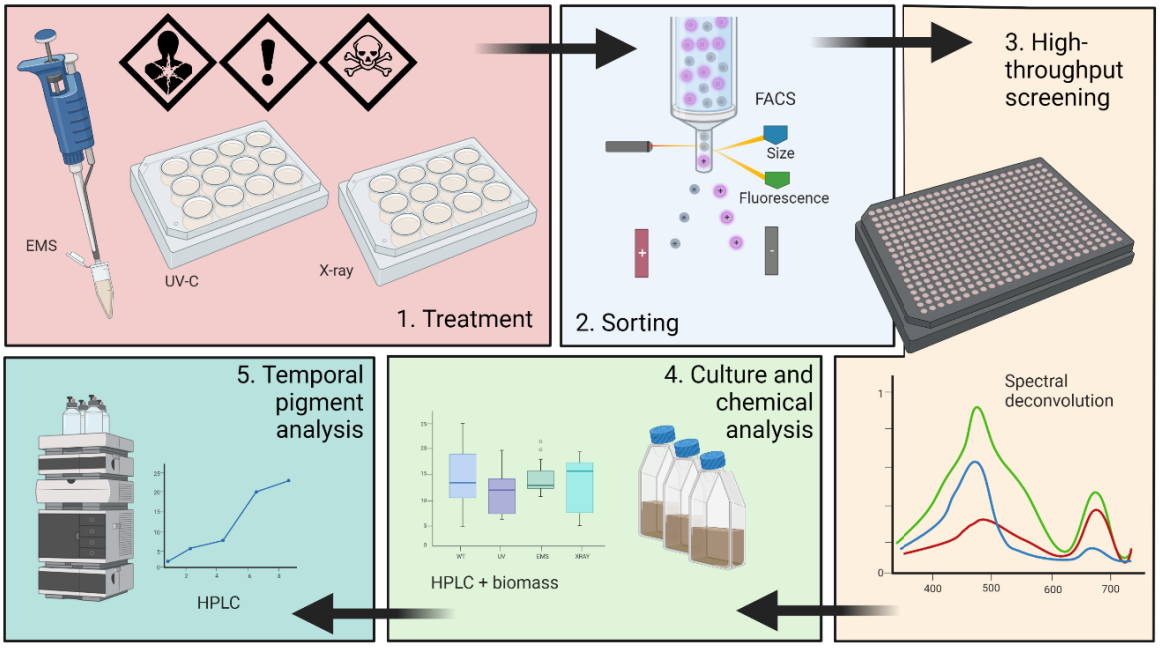

Figure 3.1. Graphical abstract depicting workflow**.** (1) treatment using UV, EMS, and X-ray mutagenesis in microtubes and well plates, (2) single-cell sorting into 384-well plates using FACS for size and fluorescence, (3) sterile high-throughput screening using spectral deconvolution with absorbance obtained using plate reader, (4) growth in tissue culture flasks with standard measurements and chemical analysis of pigments using HPLC, and (5) bimonthly pigment analysis using HPLC over a 6-month period.

3.2 Introduction

Humanity faces an uncertain future at the nexus of environmental damage, climate change and insufficient agricultural yield to support a rapidly growing population [107,108]. The challenge lies in balancing both increasing nutrient-rich agricultural yield and preventing environmental damage typically associated with unsustainable farming practices [109]. Microalgae offer a partial solution to this agricultural puzzle by fixing carbon and serving as a direct source of primary and secondary compounds for human consumption [110,111]. In addition, microalgae are being increasingly recognised as renewable and safe sources of a suite of target compounds like carotenoids [112,113]. This is primarily due to the rapid growth and harvesting of microalgae, as well as unique characteristics like the ability to be grown using wastewater and on non-arable land, thereby providing associated advantages like reduced land use [114,115]. However, microalgal biotechnology in general requires research to improve cultivation techniques and strain performance in order to improve economic viability [116]. Advances in genetic manipulation, cultivation technologies, and automation show promise in improving these economic issues [117].

Genetic engineering targets specific genes to express an enhanced phenotype, however, performing this type of work requires detailed knowledge of microalgal genetics and large infrastructure costs to contain genetically modified organisms. By contrast, experimental or laboratory evolution transcends these challenges by tailoring cells towards improved phenotypes by placing them under a set of conditions in favour of desirable traits [118]. Laboratory evolution can be summarised by the appropriation of two functions of evolution by natural selection – random mutation, which effectively opens new genetic 'space' for novel genotypes, and selection pressure, in the form of growth conditions which favour desired phenotypes. A third – artificial selection, provides an expedient means of picking wanted phenotypes (selective breeding). A combination of all three of these is likely to favour successful laboratory evolution towards elite strains. Benefits to an experimental evolution approach include a genome-wide adaptive response to selective pressures rather than targeting specific sites, and the ability to induce desirable changes to genes and regulatory sequences in tandem [119]. Furthermore, unlike genetic engineering, laboratory evolution is not subject to the same restrictive regulatory frameworks for GMO products that present a hurdle for commercialisation. In this work, we investigate two critical components of laboratory evolution – mutagenesis and artificial selection.

To enable a laboratory evolution approach, mutagens are commonly used as a means to drastically accelerate the natural mutation rate and to generate improved phenotypes for either growth performance or yield of target molecules. Various effects on the genetic material are achievable with different mutagens. In the case of UV mutagenesis, UV-induced molecular lesions are attributable to pyrimidine dimers - cyclobutane pyrimidine dimers and pyrimidine-pyrimidone photoproducts, which in turn account for the majority of genetic effects from UV radiation [83]. EMS is an alkylating agent and alkylates guanine bases, forming O^6-ethylguanine, resulting in mispairing of guanine bases with thymine instead of cytosine [87]. On the other hand, X-rays have a shorter wavelength than UV rays and are therefore more energetic. As a source of ionising radiation, X-rays produce mutations primarily through double-strand breaks [88,89]. It is likely that differences in the DNA modifications imparted by non-ionising and ionising mutagens will also result in differences in mutant stability, with potential implications on the outcome of laboratory evolution experiments. However, the specific efficacy and stability of each mutagenesis approach is underexplored for biotechnology-relevant microalgal strains.

Random physical and chemical mutagenesis strategies have been employed to create novel algae strains for enhancing lipids, docosaehexanoic and eicosapentanoic acid, as well as for improved CO_2

fixation and wastewater treatment [120-123]. Random mutagenesis has also been used to improve bioplastic precursors in cyanobacteria [124]. Specific to the current work, UV light and chemically-induced mutagenesis has been used to increase fucoxanthin in *P. tricornutum* up to 170% of wild-type [97,125]. Although there is a lack of recent information on the use of X-ray mutagenesis on microalgae, previous studies on green algae suggest that algal species respond with immense variance to X-ray mutagenesis: Nybom [126] found 100 Gy to be a lethal dose of X-ray radiation for *Chlamoydomonas reinhardtii*, while Halberstaedter and Back [127] found *Pandorina morum* could survive up to approximately 300,000 Gy. Kumar used X-ray mutagenesis to create antibiotic resistant strains of *Anacystis nidulans* [128], though to our knowledge, there are no instances of this mutagen being successfully used to achieve a target of experimental evolution for biotechnological purposes.

Carotenoid compounds play a vital role in photosynthetic organisms where they assist in light harvesting, energy transfer and protection of cellular machinery against oxidation damage [129]. There exists a wide range of health benefits of carotenoids, chiefly as antioxidant molecules, and therefore they are common in the food, feed and pharmaceutical industries [130,131]. The carotenoid fucoxanthin exemplifies these features and is produced with natural yields up to 59.2 mg g^{-1} in the model diatom *P. tricornutum,* [44] and can be enhanced further by artificial selection [106,132]. For these reasons, fucoxanthin production in *P. tricornutum* was targeted in this study.

This work aims to improve understanding of microalgal biotechnology by including a temporal analysis of confirmed positive strains, to investigate phenotype stability in conjunction with proposed best approaches for creating industrial strains. This includes the first examination of ionising (X-ray) mutagenesis as a potential tool for the creation of novel microalgae strains and supports the use of both FACS and the spectral deconvolution method, which enable the exclusion of solvent extraction in high-throughput screening [132]. This information is essential to future experiments aiming to create novel strains using laboratory evolution for biotechnology purposes, in order to both improve screening and selection rates and importantly to maintain strain stability.

3.3 Materials and methods

3.3.1 Stock culturing

Axenic *P. tricornutum* (CCAP 1055/1) stock cultures were grown in Artificial Sea Water (ASW) medium according to Darley and Volcani [133] under fluorescent incubator light (150 µmol photons m^{-2} s^{-1}) with a 24:0 light cycle in shaking tissue culture flasks (140 rpm) kept at 21°C.

3.3.2 Treatment

Mutagenesis treatments were conducted by first pipetting 3 mL of each species at 2×10^6 cells mL^{-1} into 1 mL volumes. Ultraviolet treatments was conducted in wells in a clear, flat-bottom 48-well microplate (Falcon) and treating without a lid using a 254 nm UV-C Crosslinker (CX-2000, UVP, USA) in triplicate for each treatment time (0, 6, 30 and 300 seconds). X-ray irradiations were also conducted in well plate format as above, and were performed using an XRAD 320 (PXI, USA) x-ray irradiator. The collimator was removed and the machine was set to its maximum settings of peak energy at 320 kVp and beam current at 12.5 mA. Dosimetry was performed with a calibrated ionisation chamber. Taking into account the attenuation of the plastic well plate covering, dose rates were determined to be 155.3 +/- 3.6 mGy/s. This protocol was applied to well plates for multiple doses ranging 4-1000 Gy. A second protocol was applied for lower doses by installing the collimator, reducing the beam current to 10 mA, and increasing the source to sample distance. This dose rate was determined to be 17.9 +/- 0.3 mGy/s and applied to doses 1-3 Gy. For EMS treatments, 1.5 mL of each species was pipetted into 2 mL microtubes and treated with 0.2M EMS for 0, 30 , 60 or 120 minutes before washing with 5% sodium thiosulfate. Cell concentration was determined for before treatments as well as throughout using flow cytometry (CytoFlex LX, Beckman Coulter, USA) by separating cells into singlets by plotting FSC (forward scatter) against SSC (sidescattter) and using the Cytoflex software statistics functions.

All samples were placed in PBS (Phosphate-Buffered Saline) in dark immediately after treatment to limit photorepair of DNA damage[84]. EMS-treated cells were also washed 3 × with 5% sodium thiosulfate to inactivate the EMS before resuspension in PBS. After 24 hours, the samples were placed in ambient light in 384-well microplates at a final volume of 40 µl PBS for the remainder of the experimental period (7 days). The combination of low light, nutrient depletion and lack of mixing and gas exchange was used to limit cell replication, and in order to reduce the effects of increased salinity from evaporation on

mortality, water was pipetted into wells surrounding treated samples while gaps between plate and lids were covered with 2 layers of Parafilm.

3.3.3 Mortality assessment

Mortality curves for *P. tricornutum* were established using UV-C and EMS mutagens and a fluorescent cell dye (Invitrogen LIVE/DEAD fixable Violet 405 nm, Thermo Fisher Scientific, USA). Firstly, cell density was chosen based on two factors: a combination of good mutagen penetration into microplates, and sufficient cell quantity for live/dead staining. Two million cells per mL was chosen as this cell density fit both criteria. In order to develop mortality curves, 3 × 0.5 mL of each treatment was dyed at days 1, 3 and 7 after treatment with LIVE/DEAD dye as per the manufacturer's user guide with slight modification: firstly, the samples were again centrifuged and re-suspended in PBS, then treated with 0.5 µL of LIVE/DEAD dye, vortexed at maximum speed for 5 seconds (Ratek VM1, Australia) and left in the dark for 30 minutes. The cells were then washed twice with 0.5 mL of PBS with 1% bovine serum albumin (BSA) obtained from Sigma Aldrich Corp, USA, and re-suspended in 0.5 mL 1% BSA in PBS. Flow cytometry (CytoFlex LX, Beckman Coulter, USA) was undertaken to determine mortality based on dye fluorescence using a 405 nm laser with a 416/451 excitation/emission range. This method was used to retrieve a standard for live positive control cultures using untreated cells. This method was performed identically for another triplicate set of cultures for each species to attain dead negative control culture references, with the exception that these samples were heated in sealed 30mL glass test tubes to 90°C+ on a hot plate (Major Science MD-01N, USA) for over 10 minutes prior to measurement. Complete culture mortality was confirmed by grouping of at least 98% of cells at ~1% of the chlorophyll fluorescence of wild-type cultures.

3.3.4 Sorting and screening

The treatments chosen for sorting with FACS were 6 seconds (UV), 30 minutes (EMS) and 1,000 Gy (X-ray) as well as a control using WT which were all single-cell sorted on day 7 after treatment. A straight line gate was used for sorting single cells into 384-well microplates using FACS (BD FACS Melody, Beckman Coulter, USA). Firstly, FSC was plotted against SSC to separate singlets after which treated cultures were sorted by gating for the highest fucoxanthin using the PerCP-Cy5.5 channel (**Figure 3.2**). The ~1% highest-fluorescing events were selected for further screening by sorting cells into black, flat-bottom 384-well microplates in ASW at a single cell per well. These cells recovered over a period of ~10 days in

incrementally higher light intensities: ~5, 10, 25, 50 and finally 100 µmol photons m^{-2} s^{-1} white light in a shaking incubator (Climo-Shaker ISF1-XC, Kuhner, Switzerlamd) with a 24:0 light cycle at 95 rpm and 21°C to reduce damaging effects from excessive light on single cells.

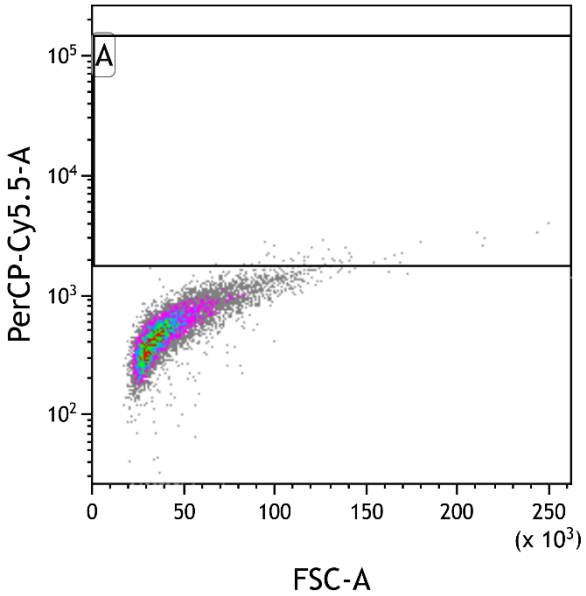

Figure 3.2. **Fluorescence Activated Cell Sorting (FACS) gating strategy.** FSC (forward scatter) is plotted on the x-axis against PerCP-Cy5.5.5-A on the y-axis. The latter is a fluorescence channel that has previously shown to have high correlation to fucoxanthin content measured using HPLC. The top 1% cells are selected for single- cell sorting (box A).

Once surviving wells were between an OD of 0.2 and 1.0 when measured at 750 nm using microplate reader (Infinite M1000 Pro, Tecan, Switzerland), spectra from 400 to 700 nm was measured and used for spectral deconvolution screening, the full method is outlined in our previous work [132]. The top-performing mutants were selected based on both high optical density and spectral deconvolution results. The top-performing strains from each mutagen were measured for biomass and pigment content, after which the top replicate was sub-cultured for 6 months and measured bimonthly for pigment content thereafter, providing a total of 12 rounds of subculturing with 3 points of HPLC measurements throughout.

3.3.5 Measuring culture characteristics and sampling

One strain from each treatment was identified for further analysis of growth characteristics and pigment content. These strains were cultured in ASW under fluorescent light at 150 µmol photons m^{-2} s^{-1} with a 24:0 light cycle at 50 mL in 250 mLshaking tissue culture flasks (140 rpm) kept at 21°C. Daily 1:2 dilutions were included to ensure optimal light and nutrient availability for 3 days, after which the flasks were placed in low light (< 10 µmol photons m^{-2} s^{-1}) without dilution for an additional 5 days to maximise carotenoid content. Cell counts and chlorophyll fluorescence were measured daily using flow cytometry.

At the end of the experimental period, cultures were centrifuged, washed with MQ and flash-frozen in liquid nitrogen before being lyophilised and stored at -80°C for further analysis. Data visualisation was performed using GraphPad Prism version 9.0.2 for Windows (GraphPad Software, San Diego, California USA, www.graphpad.com) and Kaluza Flow Cytometry Analysis Software version 2.1 (Beckman Coulter, USA).

Biomass productivity was measured according to Levasseur et al. (1993)[188] using the equation Productivity = Ln (N_2 / N_1) / (t_2 – t_1) where N is found using absorbance at 750 nm. Fucoxanthin productivity was calculated by multiplying fucoxanthin content by N at any given time point.

3.3.6 High Performance Liquid Chromatography

Freeze-dried pellets were weighed and re-suspended at 2-3 mg dry biomass per mL of chilled ethanol before being sonicated with 1-second pulses using an ultrasonic homogeniser (Qsonica Q125) at 100% amplitude and filtered once extraction was confirmed. Extracts were filtered using 0.2 µm PTFE syringe filters and stored in -80°C until analysis. High Performance Liquid Chromatography (HPLC) was conducted using an Agilent Technologies 1290 Infinity, equipped with a binary pump with an integrated vacuum degasser, thermostatted column compartment modules, Infinity 1290 auto-sampler and PDA detector. Column separation was performed using a 4.6 mm × 150 mm Zorbax Eclipse XDB-C8 reverse-phase column (Agilent Technologies, Inc.) and guard column using a gradient of TBAA (tetrabutyl ammonium acetate): Methanol mix (30:70) (solvent A) and Methanol (Solvent B) as follows: 0–22 min, from 5 to 95% B; 22–29 min, 95% B; 29-31 min, 5% B; 31-40 min, column equilibration with 5% B. Column temperature was maintained at 55°C. A complete pigment profile from 270 to 700 nm was recorded using PDA detector with 3.4 nm bandwidth. Pigment standards were acquired by Sigma-Aldrich (www.sigmaaldrich.com).

3.3.7 Statistical analysis

One-way ANOVA with a confidence level of 0.05 was performed followed by Tukey's post-hoc test to determine significance among samples, using GraphPad Prism version 9.0.2 for Windows, GraphPad Software, San Diego, California USA, www.graphpad.com.

3.4 Results

3.4.1 Mutagen effects on mortality and chlorophyll fluorescence

Cell death and chlorophyll fluorescence were assessed over a 7-day period in order to gain a preliminary understanding of the effects of UV, EMS and X-ray treatments on *P. tricornutum* cultures. Mortality was high for 6 second treatments of UV ($\bar{x}$ = 76 ±14), 30 seconds of UV ($\bar{x}$ = 97 ±7) and 300 seconds (100 %) of UV 7 days after treatment (**Figure 3.3a**). At this time point, mean mortality was 97 % (± 1.5) for 30-minute EMS and 100 % for both 60- and 90- minute EMS treatments (**Figure 3.3b**) and both UV and EMS mortality were similar to what was previously observed in the literature [97,125]. X-ray mortality was irregular across treatment intensity and displayed high errors between treatments, except 1,000 Gy, which resulted in a mean 60 ±5 % mortality (**Figure 3.3c**). Despite the 30-second UV-C treatment having identical mortality as the 30-minute EMS treatment (97%), the slope for 30-second UV-C was still steeply declining at day 7, unlike the 30-minute EMS which is nearing asymptote. For this reason, the 30-minute EMS treatment was chosen whereas 6-second treatment was chosen instead for UV as the appropriate treatment with day 7 selection point for further analysis. The X-ray treatment chosen for further mutagenesis screening was 1,000 Gy as it displayed a combination of high mortality and low error at day 7 ($\bar{x}$ = 60 %, SD = 4.9 %). These treatments were chosen for further analysis because they were generally high and also because based on the shape of the mortality curves it was believed the mortality was likely to continue increasing after day 7 for each treatment. Indeed, mortality increased after single-cell sorting at day 7. The chosen UV treatment exhibited 76% mortality at day 7 after treatment with LIVE/DEAD dye, while the same treatment exhibited 96% mortality after single-cell sorting. The same pattern is seen for the EMS treatment with 97% mortality on day 7 and 99.7% mortality after sorting. This is not true however for X-ray treatments which showed 60% mortality on day 7 and only 11% after single-cell sorting. Whether this mortality after sorting is due to increased stress from the sorting process or from ongoing effects from mutagenesis is not certain.

While EMS and UV treatments showed defined differences in mortality between treatment intensities as well as low error (**Figure 3.3a and b**), X-ray treatments did not show distinct mortality statistics based on treatment intensity (with 500 Gy displaying a higher mean mortality than 1,000 Gy) and often displayed high variability (**Figure 3.3c**). In addition, chlorophyll *a* fluorescence declined evenly throughout the 7 days after treatment with UV-C and EMS-treated cultures, whereas X-ray treated samples showed a more

complex separation of the fluorescence into two separate populations. This can be seen best on day 3, with one group firmly embedded within the negative control group (dead) and a second towards the positive control group (alive, **Figure 3.3d**).

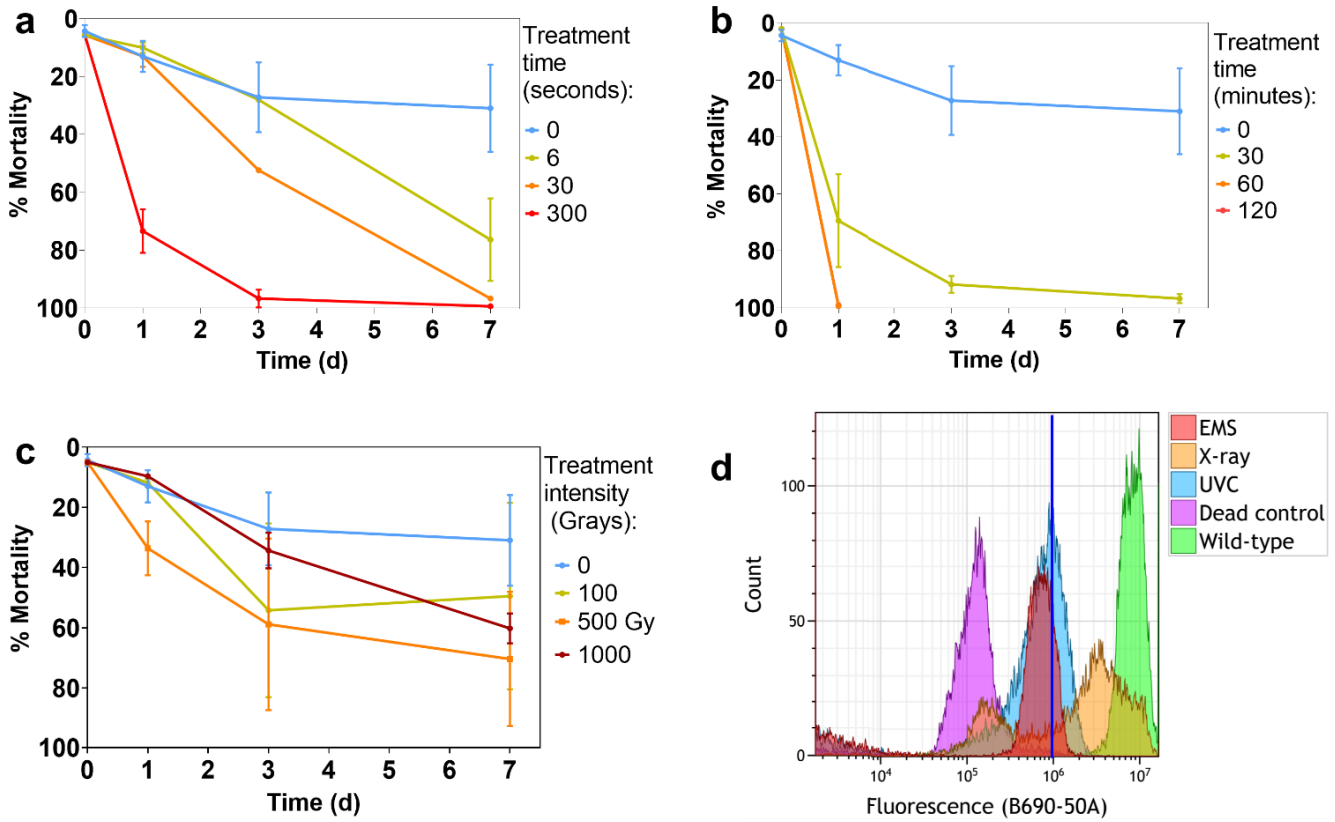

Figure 3.3. Mortality and fluorescence assessment examples for selected treatments. (**a**) UV-C (Note that data is missing for day 3 6-second treatment), (**b**) EMS and (**c**) X-ray treatments over a 7-day period, $n = 3$. For clarity not all treatments from the mortality assessment are included. (**d**) Chlorophyll fluorescence measured using the flow cytometry B690 channel as proxy at day 3 for treatments from each mutagen used for downstream analysis of mutants (6-second UV, 30-minute EMS and 1,000Gy X-ray). The positive control is healthy WT *Phaeodactylum tricornutum* cells while the negative control is the same cells boiled on a hot plate until dead.

These results suggest that UV-C and EMS produce more consistent results within a culture, while X-ray asymmetrically affects cell survival and fluorescence. While both UV-C and EMS mutagens produced visibly different trends between treatment intensities, X-ray treatments often overlapped and had high variability.

3.4.2 Screening and HPLC

The recovery of FACS-sorted single cells in 384-well plates is related to the mortality of a given treatment and was calculated by dividing the number of wells exhibiting at least some colour visible to

the naked eye by the number of wells that had a single cell sorted into them. For example, UV showed a 76 % mortality at day 7 and a 96 % cell mortality after single-cell sorting while EMS had a 97 % mortality and 99.7 % survival after sorting. These are both contrasted to X-ray, which showed a 60 % mortality and 11 % survival after single-cell sorting. After cell recovery and screening, cells were chosen based on high OD and high fucoxanthin content as indicated using the spectral deconvolution method (**Figure 3.3a**). The top performer from each mutagen were selected based on the highest fucoxanthin (mg L^{-1}) compared to WT and subcultured in tissue culture flasks to measure culture characteristics and chemical analysis of pigment content. The sample ID for each was U3I3 (UV), E2F13 (EMS) and X4E20 (X-ray).

These top performers were between 200 - 300% of WT (strain mean fluorescence divided by WT mean fluorescence) fucoxanthin when measured using spectral deconvolution (**Figure 3.4a**), yet these strains were between 111 – 115% of WT fucoxanthin when measured on HPLC several weeks later (**Figure 3.4c**). This difference could be due to multiple factors including exaggeration of pigment results from the spectral deconvolution method, reduction in cellular pigment content after screening and differences in shading effects from growth flask formats. As a result, no strain was significantly higher than WT at time 0 (One-way ANOVA with p-value threshold < 0.05). However, one strain (U5E8) showed significantly higher relative volumetric biomass productivity (121 % WT, $p = 0.0302$, data not shown). All 3 chosen strains displayed a higher mean relative biomass productivity than WT with E2F13 having 131 % (SD = 15 %) WT, although none were statistically significant (**Figure 3.3b**). Neither U3I3 nor X4E20 had over 110% WT fucoxanthin productivity where E2F13 which had 115% (SD = 15%) WT relative volumetric fucoxanthin productivity (**Figure 3.4b**).

Spectral deconvolution results showed a range of fucoxanthin from near 0 to over 300% WT even after sorting top cells using FACS with multiple weeks of incubation. Also, the standard deviation was larger in mutant populations (13 – 17 %) compared to WT (7 %) even after a further month of cultivation and measurement using HPLC, and it was presumed that strains were still undergoing genome instability[134].

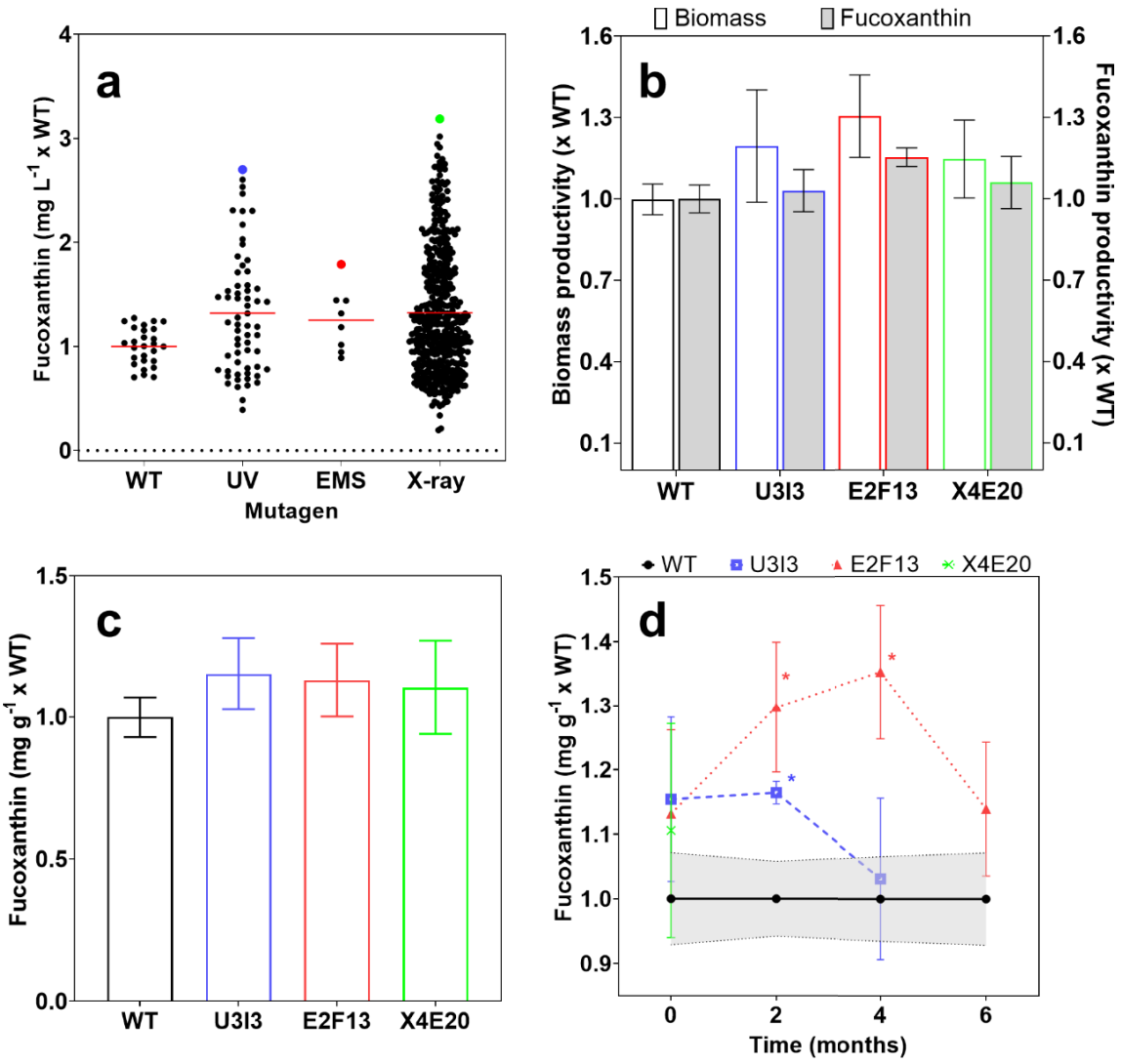

Figure 3.4. Spectral deconvolution, biomass and fucoxanthin data (**a**) results of spectral deconvolution screening method on WT, UV, EMS and X-ray treated populations (note that this is after FACS-sorting for higher fluorescence in mutagen-treated populations) with coloured dots indicating strains selected for further subculturing and culture and chemical analysis, (**b**) Biomass productivity (mg dry biomass after lyophilisation per L per day) and fucoxanthin productivity results of top strain chosen from each mutagen, (**c**) fucoxanthin content (mg per g dry weight) of top strains, and (**d**) temporal analysis using HPLC over a 6-month period. U denotes UV treated strains, E denotes EMS treated strains and X denotes X-ray treated strains with asterisks denoting statistical significance with one-way ANOVA, $n = 3$ for month 0, $n = 5$ for months 2, 4 and 6.

The top UV-C generated strain (U3I3) was stable for up to 2 months ($\bar{x}$ = 115%, SD = 13% WT for month 0 and $\bar{x}$ = 116%, SD = 2% WT for month 2), before dropping for month 4 ($\bar{x}$ = 103%, SD = 13% WT). The top EMS strain (E2F13) increased from 113% WT with a SD of 13% at month 0 to 130%, 135% and 114% WT at months 2, 4 and 6, respectively (all with SD = 10%). The top X-ray strain (X4E20) displayed 111% WT with a SD of 17% at month 0 (**Figure 3.4d**). Due to fluctuations in

fucoxanthin content, E2F13 was significantly higher than WT at months 2 and 4, while U3I3 was significantly higher at month 2 (one-way ANOVA, significance level 0.05, **Figure 3.4d**).

3.5 Discussion

3.5.1 Mutagen effects on mortality and fluorescence

While mortality is a useful statistic for determining mutagen effects on cell cultures, combined mortality (**Figure 3.3a – c**) and chlorophyll *a* fluorescence data (**Figure 3.3d**) offers a complete view of populations generated by different mutagens. Chlorophyll *a* fluorescence is a simple measurement of photosynthetic health and serves to provide a reliable preliminary assessment of the effects of a given mutagen over time (**Figure 3.3d**). Differences between mortality and chlorophyll fluorescence kinetics indicate that cells do not respond consistently to X-rays like they do with the non-ionising mutagens. While X-rays appear to either kill cells or not to have a significant effect on them as indicated by the split fluorescence populations (**Figure 3.3d**), UV and EMS show a uniform loss of fluorescence throughout the 7 days after treatment. While this could be dose-dependent, the comparable mortality between X-rays and UV treatments indicates that cultures respond unevenly to X-ray exposure. In addition, Myung and Kolodner [135] found that 0.7% EMS exposure for 2 hours had a 10-fold higher GCR (Gross Chromosomal Rearrangement) induction than 100 Gy gamma radiation in *Saccharomyces cerevisiae*. EMS may be merely a more efficient tool for creating stable mutants, and this is reflected in EMS being used in 43% of reports where researchers used random mutagenesis to improve microalgae performance [75]. This could be due to EMS providing doses on shorter timeframes, for example EMS was used here to treat cells for 30 minutes, whereas 1,000 Gy X-ray was delivered at 157 mGy/s for 1hr 46 mins. It is important to note here that no statistical comparison between the mutagens is not included here as their effects on cells are expected to differ considerably, rendering comparison between them difficult. Additionally, treatments displayed dissimilar mortality statistics, further making the task of comparison untenable. Therefore in this work all comparisons are merely observational. Other consideration are also important, such as the ease and cost of different methods. X-radiation should be incorporated as a mutagen in further research, with consideration for its more lengthy and potentially cost-heavy involvement comparative to other methods.

While there was no intraspecific comparison of single-cell survivability between treatment intensities herein, treatments that result in higher mortality are expected to increase the proportion of surviving cells with mutations. Thus increasing the likelihood of finding a mutant with the desired trait in downstream analysis, despite the lower total cells screened. This can be seen in the screening of 8 EMS strains with 1 displaying significantly higher fucoxanthin in the temporal analysis and 62 UV strains being screened with 1 displaying significantly higher fucoxanthin in the temporal analysis whereas 445 X-ray strains were screened without any showing significantly higher fucoxanthin. This topic remains purely discussion in this work as there are no comparative measurements of UV-C radiation and X-radiation, nor between these and EMS, on cellular functioning and response. It is, however important to note that, in the process of creating mutants, there exists a balance between obtaining high mortality to maximise the possibility of mutations in surviving cells and preventing the elimination of the culture completely. There is also the consideration that researchers should take care when deciding on a recovery point after treatment, considering the additional balance between the goal of filtering out undesired strains while simultaneously avoiding wasting screening and selection effort on the same strain multiple times, or 'doubling down'.

3.5.2 Sorting and screening

Fluorescence-Activated Cell Sorting is being widely recognised as a pivotal tool for the artificial selection of microbial cells, and indeed has been used to select for superior pigment-producing strains of microalgae [100,136,137]. The inclusion of FACS in this work also shows the immense utility of this tool as a means of sorting single cells, and therefore potentially distinct genomes, into individual wells for further culturing and analysis. Another vital function of FACS is to provide a relatively simple means of artificial selection for a target phenotype, and restricts the pool of mutant cells to a much higher threshold for that target phenotype. This is evident here in the increase of average spectral deconvolution results for fucoxanthin to 125 – 133% WT in mutant populations that have undergone single-cell sorting with FACS with an appropriate channel.

Including a secondary high-throughput screen in the form of spectral deconvolution allowed for sterile, non-invasive mathematical assessment of both culture density and a secondary filtering of strains based on fucoxanthin content. This was essential when considering 34 % of cells screened using spectral deconvolution were lower than WT, further suggesting phenotype instability caused reversion to WT

fucoxanthin contents between FACS-sorting and spectral deconvolution screening stages of the experiment. Choosing wells with low OD and high fucoxanthin predictions after spectral deconvolution is likely to select for higher fucoxanthin content regardless of biomass-related productivity, while selecting for high OD is likely to select for productivity. By comparison, selecting for high OD with high relative fucoxanthin is optimal but difficult to assess when WT wells used for comparison are of a similar density. It is unclear whether just genome instability or exaggeration of fucoxanthin in spectral deconvolution is the cause of high variance in spectral deconvolution results, but it is likely a combination of the two. The spectral deconvolution method here enabled the successful selection of 2 strains with significantly higher fucoxanthin than WT when assessed over 6 months, and the combination of FACS with spectral deconvolution screening in 384-well microplates enabled straightforward and effective isolation of strains from a vast pool of mutated cells (near 5,000 cells sorted). Considering the complexity of carotenoid biosynthesis across genes and related regulatory mechanisms, the likelihood of creating a strain with improved carotenoid production is small. This work highlights the need to ensure high mortality in treatments to increase the proportion of DNA in a culture being affected by a given mutagen, as well as the importance of researchers maximising the quantity of cells screened after treatment. There is also potential to expand beyond single-event mutagenesis and to incorporate other strategies such as iterative mutagenesis and adaptive laboratory evolution.

3.5.3 Pigment measurement

The HPLC results for the temporal analysis supported previous indications that the top strain pigment phenotypes were unstable, and in fact during subculturing, we observed both decrease and increase in the average pigment content despite maintaining constant growth and sampling regimes over a 6-month period, which indicates the cultures were still highly heterogenous. Bulankova, et al. [134] investigated the nature of clonal variability in *P. tricornutum* haplotypes and found that mitotic interhomolog recombination rates were in excess of 10 × that of *Saccharomyces cerevisiae*, indicating that genomic diversity is rapidly accumulated in *P. tricornutum* clonal cultures. It is probable that cells with higher pigment expression outcompeted others, and may have been outcompeted themselves later in the growth cycle. Mitotic recombination was found to increase under oxidative stress in *P. tricornutum*, [134] and reversion to wild-type pigment expression levels may also have been caused by eventual loss of a response to stress conditions brought on by exposure to mutagens. Secondary effects such as interactions with Reactive Oxygen Species (ROS) are also responsible for damage to DNA, and differences between

the levels of direct mutations and secondary effects, as well as activity of DNA repair mechanisms, might explain the differing success with isolation of elite phenotypes between different mutagens[75,77,138]. Note that temporal measurements are from a single population inoculated for each 2-month HPLC cycle and not replicate flasks separately subcultured. This suggests ongoing sorting and screening, and possibly even mutagenesis, is essential for maintaining successful hyper-performing cultures over long periods of time.

This work proposes genome instability as the cause of high error in HPLC measurements of fucoxanthin and as the reason for fluctuating fucoxanthin content over the 6 month experimental period. It is important to note that experimental conditions of light, culture container and cell concentration were all repeated to reduce erroneous effects from self-shadowing on pigment content. Future studies are however needed to assess the exact cause of fluctuating population dynamics as a suspected result of mutation at the single-cell level. Additional measurements of ROS damage as secondary damaging effects as well as SOS repair would aid in this assessment as genomic stability after DNA damage is dependent on cellular repair mechanisms [84,139].

3.6 Conclusion

Both short timeframe (days to weeks) and long timeframe (months) reversion of selected strains to WT pigment levels suggest that ongoing laboratory evolution would be preferable for creating novel strains. Sustained selection pressure and artificial selection using FACS are both likely to encourage the continued expression of desired phenotypes. In addition, X-ray mutagenesis should be further investigated alongside laboratory evolution methods by the increase of treatment intensity as well as cell-level investigation of the dynamic effects of mutations in cultures. In the future, a more detailed comparison of ionising and non-ionising mutagens will reveal the benefits and disadvantages of utilising additional mutagenic mechanisms in evolution experiments.

Chapter 4

Differential gene expression in a subpopulation of *Phaeodactylum tricornutum* with enhanced growth and carotenoid production after FACS-mediated selection.

Published in *Journal of Applied Phycology*

October 2023

Sean Macdonald Miller[1,*], Andrei Herdean[1], Vishal Gupta[1], Brandon Signal[2], Raffaela M. Abbriano[1,2], Peter J. Ralph[1] and Mathieu Pernice[1]

[1] Faculty of Science, Climate Change Cluster (C3), University of Technology Sydney, Sydney, NSW 2007, Australia;

[2] School of Medicine, College of Health and Medicine, University of Tasmania, Hobart, TAS 7000, Australia

[3]Leidos Innovations Center, San Diego, CA 92121, United States

4.1 Abstract

Fluorescence-Activated Cell Sorting (FACS) is a powerful method with many applications in microalgal research, especially for screening and selection of cells with improved phenotypes. However, the technology requires further investigation to determine the phenotypic stability and gene expression changes of sorted populations. *Phaeodactylum tricornutum* cells were sorted using FACS with excitation/emission parameters targeted to favouring the industrially-relevant carotenoid fucoxanthin. The resulting cultures showed significantly higher growth rate (1.10 ×), biomass (1.30 ×), chlorophyll *a* levels (1.22 ×) and fucoxanthin productivity (1.41 ×) relative to the wild-type strain. RNA-seq was used to elucidate the underlying molecular-level regulatory changes associated with these traits, and represents the first study do so on FACS-sorted microalgal cultures. Transcriptome analysis corroborated evidence of increased chlorophyll *a* and fucoxanthin, showing enrichment for the genes/pathways for tetrapyrrole biosynthesis and for suites of genes directly related to photosynthesis. Only three genes were upregulated in the MEP (non-mevalonate) pathway to carotenoid biosynthesis pathway, suggesting either a strong influence of *IDI*, *CRTISO5* and *ZEP1* on fucoxanthin biosynthesis or a post-transcriptional or post-translational mechanism for the observed increase in fucoxanthin content.

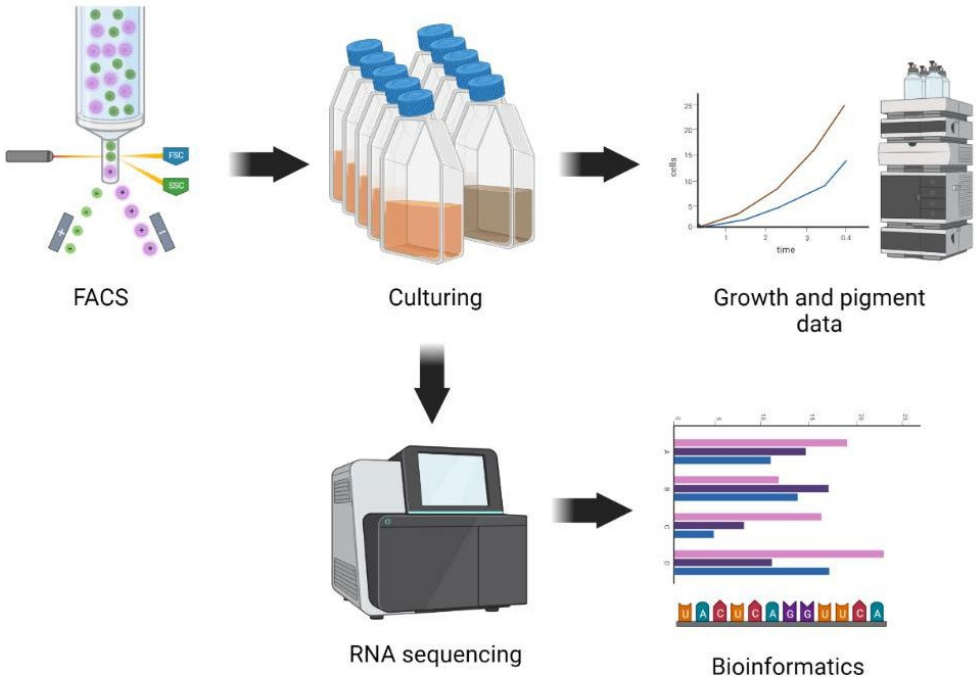

Figure 4.1. Conceptual diagram of workflow used in this study: from Fluorescence-Activated Cell Sorting (FACS) to culturing, pigment detection using High-Performance Liquid Chromatography (HPLC), and RNA sequencing and analysis.

4.2 Introduction

Microalgal biotechnology is a developing area of research with enormous potential as a contributing technology for a renewable agricultural industry[140,141]. Microalgae are single-celled eukaryotic organisms heavily responsible for Earth's oxygen production, nutrient cycling, and primary production[142-144]. The potential of these organisms as contributors to sustainable industry lies in their high growth rates, ability to be grown under a wide range of conditions, high nutritional value, use of non-arable land, and as a source of a suite of valuable compounds[18,145,146]. Microalgae have proven effective in many areas including the sequestration of carbon, as fertiliser in agriculture and as feed in aquaculture[10,56,143]. Valuable compounds like pigments are also being increasingly targeted using microalgae from a biotechnological perspective[147].

Microalgal pigments assist in the capture and transfer of light energy within the photosynthetic apparatus, but are currently used by humans as health compounds in the nutraceuticals and cosmetics industry, as well as for aquaculture feed[62,148,149]. Fucoxanthin is the main carotenoid pigment in the diatom *Phaeodactylum tricornutum*, and a target for biotechnological projects for its health benefits and use in terrestrial farming and aquaculture[92,93,150,151]. *P. tricornutum* is a model microalgal species with a sequenced genome and an advanced genetic toolkit. Fucoxanthin content in WT *P. tricornutum* can be orders of magnitude higher than in fucoxanthin-producing macroalgal species (up to 59.2 mg g^{-1} under specific culture conditions[44,152,153]). In addition, a variety of genetic manipulation techniques have been employed to improve baseline pigment content in *P. tricornutum*. Utilisation of physical and chemical mutagens have generated mutants with fucoxanthin content 1.7 × greater than WT, and genetic engineering efforts have produced transformant lines with 1.45 × WT fucoxanthin content by overexpressing the phytoene synthase gene[97-99].

Approaches that produce large libraries of mutants require high-throughput screening methods to select for elite strains. FACS is a high-throughput technique and has been used to screen for pigments in microalgae[100,136,154]. This method has also been used previously to isolate a population with a 1.25 × increase in fucoxanthin using *P. tricornutum*[106]. Screening of cell populations for pigment content by FACS eliminates the need for a time-consuming solvent extraction step and provides fluorescence, size, and cell volume data on a single-cell level[155]. In addition to high resolution measurements, FACS has the ability to sort cells based on combinations of these factors and with highly specific customised gating

arrangements. The technology can therefore not only be used as a screening method for various compounds, but also can be used as a method of artificial selection to separate populations with desirable phenotypes without the need for mutagenesis or complex laboratory evolution methodology.

However, there is very little exploration of the phenotypic and genetic differences of FACS-sorted (F) populations. Consequently, further study is needed to elucidate the true potential of FACS for microalgal research. This work included a theoretical industry-based growth regime for optimising fucoxanthin content in order to elucidate differences between WT and F populations. Furthermore, RNAseq analysis was incorporated to investigate changes occurring in the transcriptomes of F cells versus WT *P. tricornutum* cells. Cells sorted by the highest fluorescence using fucoxanthin gating were anticipated to exhibit elevated fucoxanthin content and differential gene expression in the carotenoid pathway, as well as related upstream pathways like the non-mevalonate (MEP) pathway. Additionally, other relevant pathways known to influence fucoxanthin biosynthesis, such as phytoene synthase (PSY), were expected to be involved. This would provide a comprehensive gene library potentially responsible for enhancing fucoxanthin production.

4.3 Materials and Methods

4.3.1 Stock culturing

Axenic *Phaeodactylum tricornutum* (CCAP 1055/1) stock cultures were grown in Artificial Sea Water (ASW) medium according to Darley and Volcani [133] under fluorescent incubator light (150 µmol photons m^{-2} s^{-1}) with a 24:0 light:dark cycle in shaking tissue culture flasks (140 rpm) kept at 21°C (Climo-Shaker ISF1-XC, Kuhner, Switzerland).

4.3.2 Sorting with FACS

FACS was performed using a BD FACSMelody (BD Biosciences, La Jolla, CA, USA) with the PerCP-Cy5.5 channel, as this laser arrangement had high correlation to fucoxanthin (Ex/Em 561/710 using CytoFlex LX, Beckman Coulter, USA) in our previous work[132]. To isolate cell populations, forward scatter (FSC) was first plotted against side scatter (SSC) to separate singlets. Gated single cells were then plotted using PerCP-Cy5.5 fluorescence against FSC to do further gating for fucoxanthin content. The gating strategy for selecting single cells using FACS is outlined: while manually generating a curve to follow the shape of the distribution and thereby select for high-fluorescing cells irrespective of cell volume (**Supplementary figure 4.1)**, it was found that despite doubling average fluorescence, the mean

FSC was approximately equal between the top 1% and the total population. However, a flat line / rectangle selected for higher cell volume in the top 1% (~3.6 × mean FSC) but this allowed for much higher fluorescence selection (~3.2 × mean fluorescence) than the total population. It was later observed that FSC and SSC were similar or identical between WT and F cultures, indicating that the rectangular gating strategy was appropriate. Therefore a straight line gate was used for sorting single cells into 384-well microplates. A rectangular gate was created which included the entire population to be sorted, and then was set at a threshold of ~1 % top fluorescing cells. Sorting was performed to a cell density of 20,000 cells mL^{-1} per sort and replicated 5 times at late exponential phase with sorting occurring once rather than iteratively.

4.3.3 Culture data

In order to simulate a theoretical product-favoured growth arrangement, sorted populations were grown to an inoculation density of 50,000 cells mL^{-1} and subcultured into fresh ASW under fluorescent light at 150 µmol photons m^{-2} s^{-1} with a 24:0 light cycle in shaking tissue culture flasks (140 rpm) kept at 21°C. Daily 1:1 dilutions were performed for 3 days to provide optimal growth conditions for maximising biomass, after which the flasks were placed in low light (< 10 µmol photons m^{-2} s^{-1}) without dilution for a further 5 days to maximise carotenoid content. Cell counts and fluorescence were measured daily using flow cytometry. At the end of the experimental period, cultures were centrifuged at 4°C, washed with chilled (4°C) Milli-Q water, flash-frozen in liquid nitrogen, and stored at -80°C for further analysis. All samples were centrifuged within 1 hr of each other and always remained chilled throughout collection.

4.3.4 HPLC

Freeze-dried pellets were weighed and re-suspended at 2-3 mg dry biomass per mL of chilled ethanol before being sonicated with 1-second pulses using an ultrasonic homogeniser (Qsonica Q125) at 100% amplitude and filtered once extraction was confirmed. Extracts were filtered using 0.2 µm PTFE syringe filters and stored at -80°C until analysis. High Performance Liquid Chromatography (HPLC) was conducted using an Agilent Technologies 1290 Infinity, equipped with a binary pump with integrated vacuum degasser, thermostated column compartment modules, Infinity 1290 auto-sampler and PDA detector. Column separation was performed using a 4.6 mm × 150 mm Zorbax Eclipse XDB-C8 reverse-phase column (Agilent Technologies, Inc.) and guard column using a gradient of TBAA: Methanol mix (30:70) (solvent A) and Methanol (Solvent B) as follows: 0–22 min, from 5 to 95% B; 22–29 min, 95% B; 29-31 min, 5% B; 31-40 min, column equilibration with 5% B. Column temperature was maintained at

55°C. A complete pigment profile from 270 to 700 nm was recorded using PDA detector with 3.4 nm bandwidth.

4.3.5 RNA extraction

RNA extractions were performed in triplicate using RNAse-free reagents. Flash-frozen pellets were resuspended in 1.5 mL of Trizol reagent and pipetted until homogenous before incubating at room temperature for 5 minutes. Then, 300 µl chloroform (Sigma-Aldrich, #C2432) was added and mixed by inverting tubes for 15 seconds before a second incubation at room temperature for 15 minutes. Tubes were centrifuged at 4°C and 12,000 RCF for 15 minutes. The aqueous phase was transferred to a clean 2 mL tube and an equal volume of molecular grade ethanol was added (Sigma-Aldrich, #E7023) before being inverted several times to mix. This was then transferred to a spin column in a 2 mL collection tube 650 µl at a time and centrifuged at 8,000 RCF for 30 seconds with discarding of flow-through, and this step was repeated until all of the liquid had passed through the column. Further purification was performed using a Qiagen RNeasy kit using the protocol recommended by manufacturer (Qiagen, Valencia, CA, USA). RNA concentration was measured using a NanoDrop spectrophotometer (Thermo Fisher Scientific, Waltham, MA, United States) and quality was evaluated via the presence of intact 18S and 28S ribosomal RNA bands using an Agilent 2100 BioAnalyzer (Agilent Technologies) prior to sequencing. Samples with RINS > 8.8 were included in sequencing.

4.3.6 Sequencing and assembly

Sequencing was undertaken at the Ramaciotti Centre for Genomics (University of New South Wales, Sydney, Australia). First, samples were converted to libraries using Illumina Stranded mRNA prep, ligation. Ribonucleic acid at 500 ng was used as input to the library prep with 10 PCR cycles. Libraries were pooled equimolar and the final pool was cleaned using 0.9 × AMPure XP beads. Sequencing was performed on an Illumina NextSeq 500 150 cycle High Output platform (Illumina, San Diego, CA, United States) in 2 × 75 bp strand-specific format. Fastq files were trimmed using TrimGalore! (Babraham Bioinformatics, v0.6.7) using default parameters. Quality control of fastq files was performed using FastQC v0.11.9[156] pre- and post-trimming, and reports compiled by MultiQC v1.11[157]. Fastq reads were then pseudo-aligned to the *P. tricornutum* ASM15095v2 transcriptome which was downloaded from ensemble genomes (http://protists.ensembl.org/Phaeodactylum_tricornutum/Info/Index) using kallisto v0.44.0[158] with the strand specific --rf-stranded option, to give read counts for each transcript. Counts were then combined for multiple transcripts of the same gene to give gene-level counts. Genes were

filtered for those with at least 10 counts in at least 3 samples. Gene-level differential expression was performed using Limma[159] and Voom[160]. All gene counts presented are Voom-transformed counts.

4.3.7 Pathway enrichment analysis

Genes with a logFC (log 2 fold change) threshold of 1 and p-value < 0.05 were input to ShinyGO v0.77[161] for enrichment of three GO aspects: Molecular Function (MF), Cellular Component (CC) and Biological Process (BP) with a minimum pathway size of 10.

4.3.8 Statistics and visualisation

One-way ANOVA with confidence level of 0.05 was performed followed by Tukey's post-hoc using GraphPad Prism version 9.0.2 for Windows (GraphPad Software, San Diego, California USA) for culture characteristics and pigment content data. Degust v4.2[162] was used to analyse Voom (variance modeling at the observational level) counts. Data visualisation was performed using Prism, Degust, Clustergrammer[163] and Kaluza Flow Cytometry Analysis Software version 2.1 (Beckman Coulter, USA).

4.4 Results

4.4.1 Growth and pigment phenotypes of FACS-sorted cultures

Because cell size did not significantly increase in the F cultures by the end of the experimental period (**Supplementary figure 4.2**), artificial selection for cell size can be excluded as the reason for increased fucoxanthin and chlorophyll *a* content in FACS cultures. Despite selecting for both fluorescence and cell volume (cells mL^{-1}), FACS and WT cultures throughout the experiment were similar for both geometric mean FSC and SSC (**Supplementary figure 4.2**).

FACS-sorted cultures had significantly higher cell counts than WT cultures at every time point, with the exception of day 0 ($p < 0.0003$ for days 1 - 3 and $p < 0.01$ for days 4 – 8 using t-tests). The highest mean cell count for F cultures was 4.7×10^6 mL^{-1} at day 2, whereas the maximum for WT was 3.1×10^6 mL^{-1} at day 3 (**Figure 4.2a**). Cultures sorted with FACS also exhibited a significantly higher ($p = 0.025$) mean specific growth rate during the optimal growth phase during days 0-3, which was 1.16 ± 0.06 for F cultures and 1.05 ± 0.05 for WT cultures (**Figure 4.2b**).

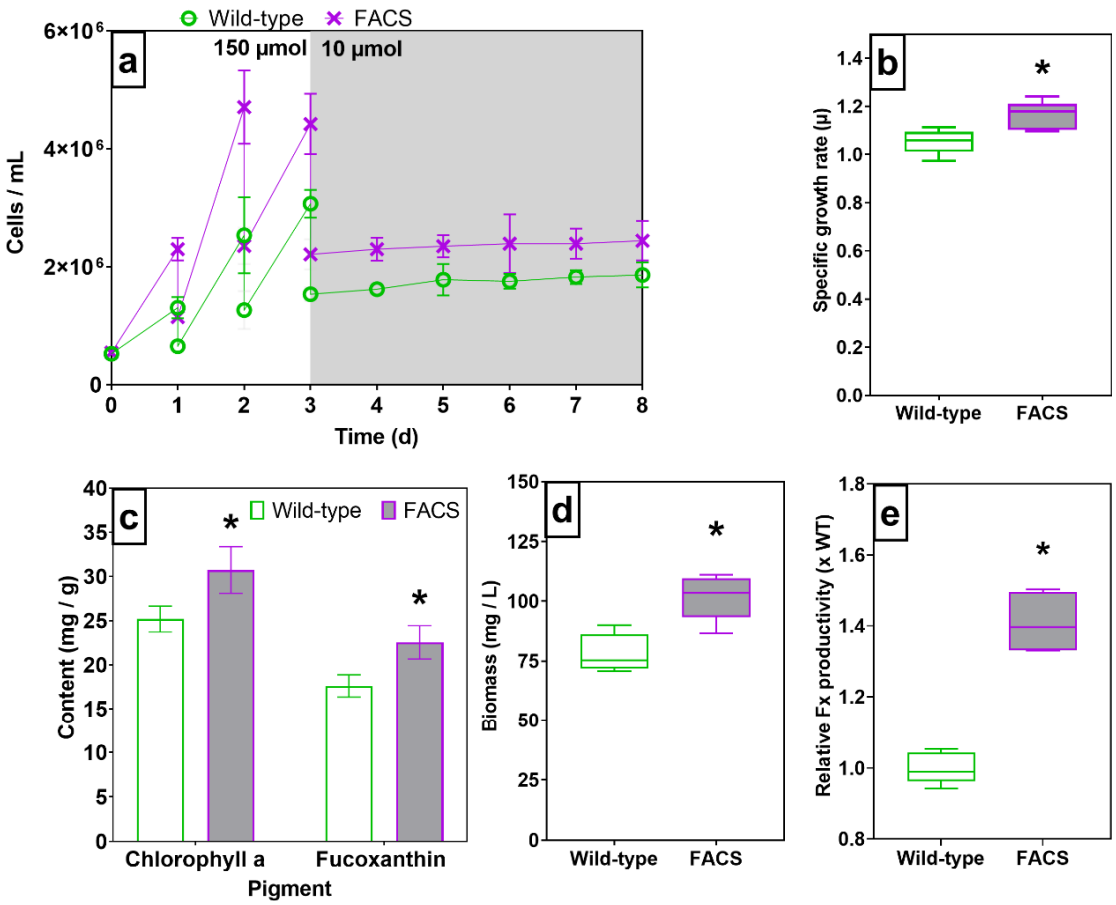

Figure 4.2. Biomass, growth and pigment data for WT and F cultures of *P. tricornutum*, with (**a**) cell counts measured using flow cytometry, (**b**) chlorophyll *a* and fucoxanthin pigment content measured using HPLC, (**c**) specific growth rate (µ), (**d**) relative fucoxanthin productivity and (**e**) biomass (mg per L). Asterisks denote statistical significance, $n = 5$.

After a period of low light from days 3 to 8, mean chlorophyll *a* and fucoxanthin content were both significantly higher in F cultures ($p = 0.024$ and 0.008, respectively) compared to WT (**Figure 4.2c**). Chlorophyll *a* content was 30.7 ± 2.6 for F cultures and 25.2 ± 1.5 mg g^{-1} for WT, while fucoxanthin was 22.5 ± 1.9 mg g^{-1} for F cultures and 17.6 ± 1.3 mg g^{-1} for WT.

Relative productivity was also significantly different ($p = 0.001$) with 1.41 × WT (± 0.08 ×) for F cultures (**Figure 4.2e**). Actual pellet weight for F cultures at the end of the experiment were between 1.11 – 1.42 × WT biomass (**Figure 4.2d**) with an average of 1.30 × WT (± 0.12 ×) and these were statistically different (t-test, $p = 0.003$).

These results show that not only did the F cultures grow faster under optimal conditions compared to WT cultures, they also had a higher chlorophyll *a* and fucoxanthin content after a period of low light that resulted in a significantly higher fucoxanthin productivity.

4.4.2 Gene expression

We performed RNA-seq on three samples for each F and control wild-type (WT), aligning to the reference *P. tricornutum* transcriptome to obtain gene expression levels. The MDS plot of normalised gene expression shows separation F and WT samples in dimension 1 (explaining 70% of sample variance), suggesting a clear difference in RNA expression in these conditions (**Figure 4.3**), yet heatmap visualisation illustrates an unclear definition between WT and F cultures in terms of total gene expression changes (**Supplementary figure 4.3**).

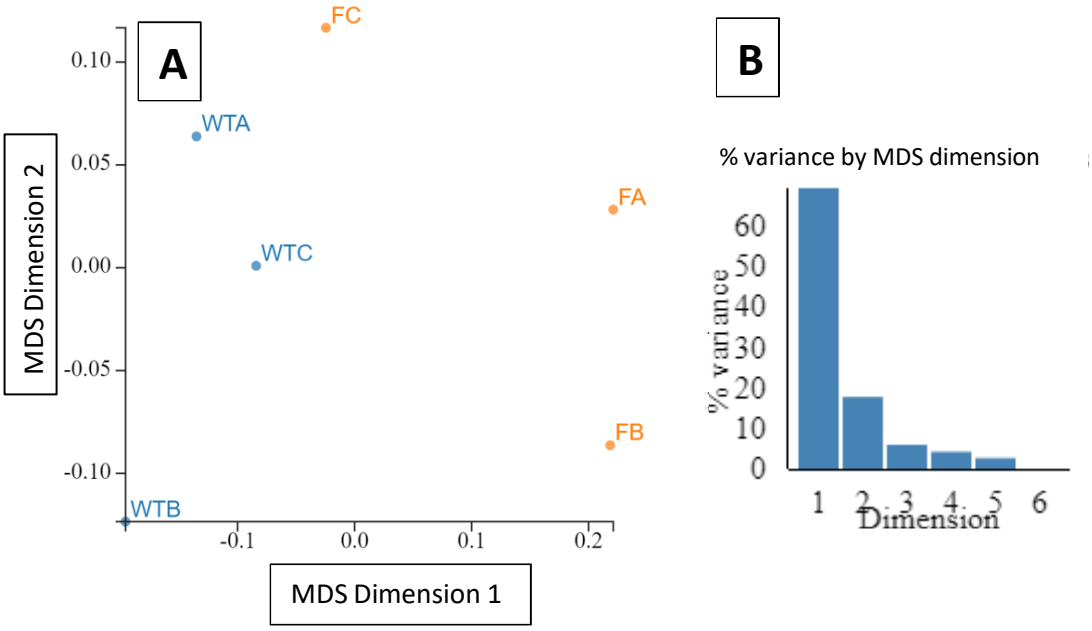

Figure 4.3. Multi-Dimensional Scaling (MDS) plot showing similarities between RNA samples (leading LogFC dimension 1 compared to leading LogFC dimension 2. WT = wild-type, F = FACS). Made using Degust.

A total of 312 genes were upregulated and 63 downregulated over a threshold of 1 logFC (p-value < 0.05) in F cultures compared to WT cultures over the whole transcriptome, however, all exhibited a false discovery rate (FDR) value between 0.11 and 0.18. The high number of genes with p values < 0.05 and FDR values > 0.05 indicated that gene enrichment analysis was a necessary step to elucidate enriched pathways. These 375 genes were used for gene enrichment analysis.

4.4.3 Gene enrichment analysis

Fifty-seven pathways were overrepresented in the gene set (FDR < 0.05) in F cultures compared to WT cultures as indicated by the ShinyGO platform; 18 related to biological processes, 19 to cellular components, and 20 related to molecular function (**Figure 4.4**, **supplementary Tables 1 - 3**).

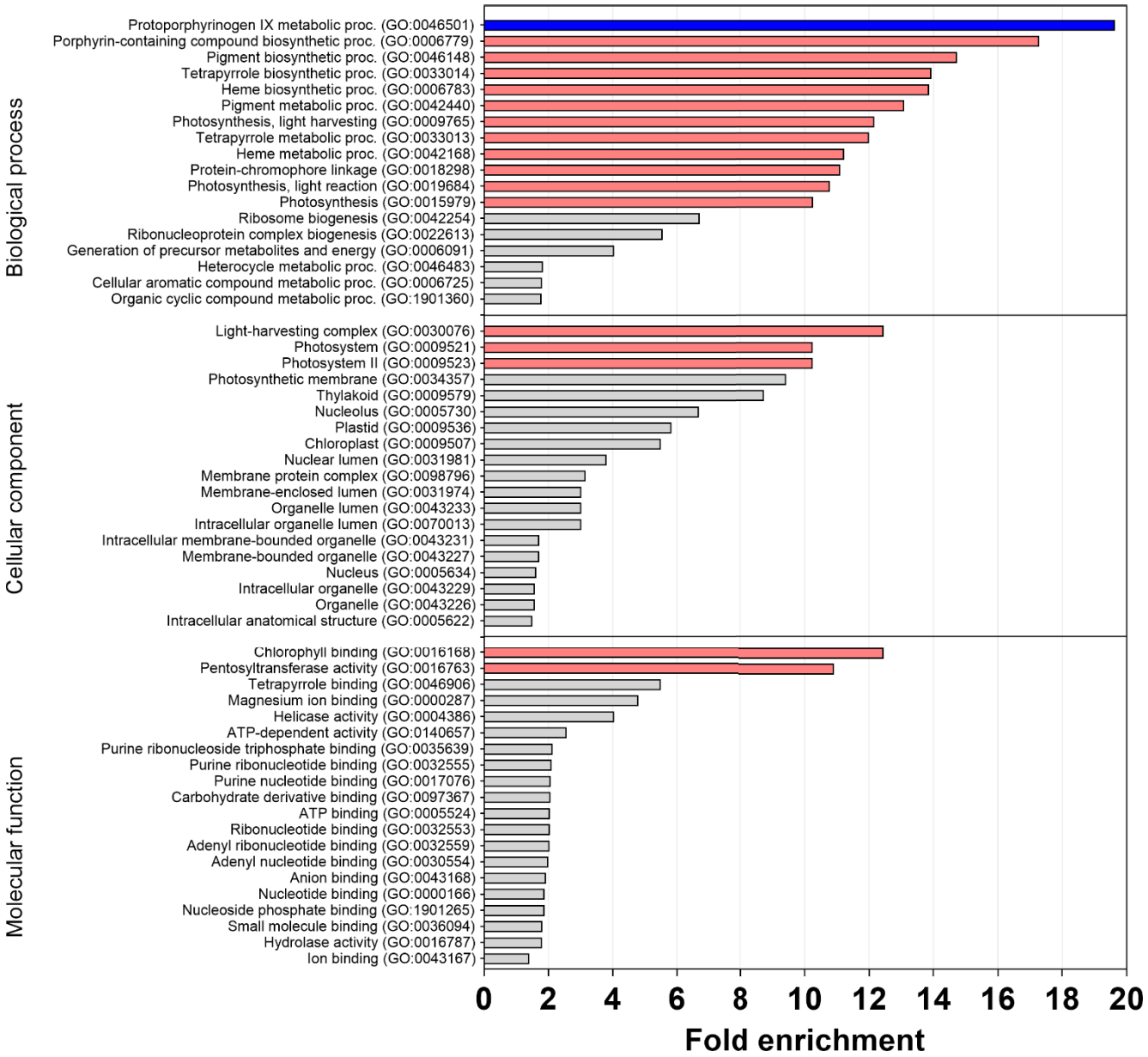

Figure 4.4. Gene Ontology (GO) enrichment analysis results with a minimum pathway size of 10 and FDR cut-off = 0.05. Pink bars indicate pathways with 25 – 50 % of genes in that pathway being represented by the gene set, blue indicates 50% of genes being represented. GO term IDs are in parentheses.

Of the 18 pathways related to biological processes, 12 had at least 25% of genes present being overexpressed. One pathway, the protoporphyrinogen IX metabolic process pathway (GO: 0046501), exhibited 50% of genes present being overexpressed. Three out of 19 pathways related to cellular

components had at least 25% of genes represented while 2 out of 20 related to molecular function had 25% of genes represented. All pathways with a minimum of 25% genes overexpressed corresponded to fold enrichment values between 10 – 15 (defined as the percentage of genes in a gene set belonging to a given pathway, divided by the corresponding percentage in the background). Meanwhile, the pathways that contained genes most overrepresented in the upregulated gene dataset were related to biological processes and were porphyrin-containing compound biosynthetic process (GO: 0006779) and protoporphyrinogen IX metabolic process pathway (GO: 0046501) at 17.3 and 19.6 fold enrichment, respectively. Gene Ontology (GO) ID terms directly associated with the tetrapyrrole biosynthetic pathway (protoporphyrinogen IX, porphyrins, pigments, tetrapyrroles, and heme pathways) were significantly enriched, as well as were other GO ID terms associated directly with pigments and photosynthesis (**Figure 4.4**, **supplementary Tables 1-3**).

4.4.4 Expression in pathways related to growth and pigmentation

We identified several differentially regulated genes -1 < logFC > 1 (downregulated and upregulated) and $p < 0.05$) within pathways related to pigmentation and growth. Despite FDR values between 0.11 – 0.18, 10 of the 13 genes in the tetrapyrrole pathway were upregulated above 1 logFC in the F cultures compared to WT cultures (**Figure 4.5**). One gene in the MEP pathway (*Phatr3_J12533* - isopentenyl-diphosphate delta-isomerase or *IDI*), which provides precursors for carotenoid biosynthesis as a fundamental step in isoprenoid biosynthesis, was found to be upregulated (1.07 logFC).[164,165] Two genes, *Phatr3_J9210* and *Phatr3_J45845*, corresponding to the carotenoid biosynthesis genes *CRTISO5* (carotenoid isomerase) and *ZEP1* (zeaxanthin epoxidase), were also upregulated by 1.04 and 1.80 logFC, respectively.

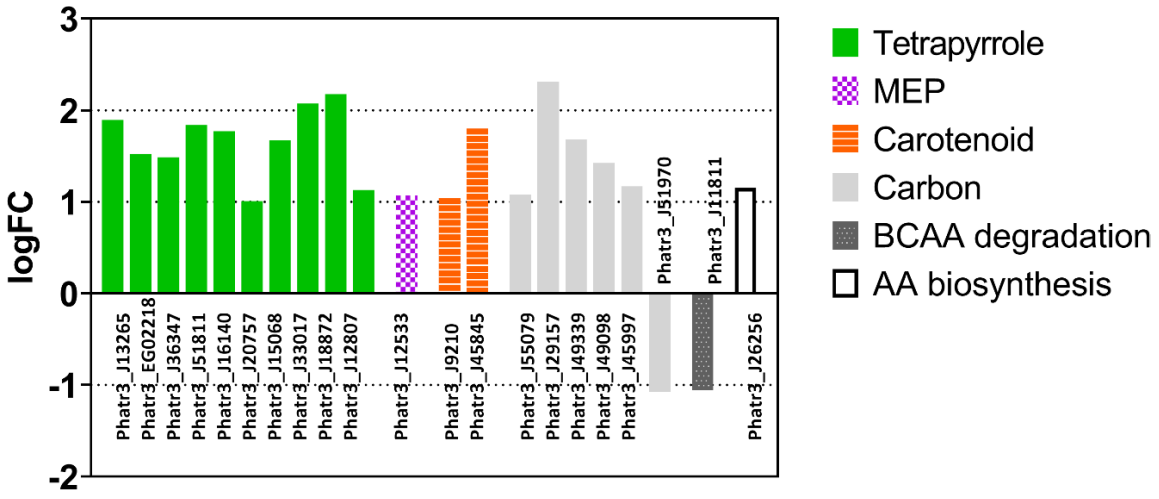

Figure 4.5. Genes differentially expressed over a threshold of 1 logFC and $p < 0.05$ in pathways related to pigment biosynthesis and growth. Nineteen genes were differentially regulated between F and WT populations.

Five genes involved in carbon metabolism (*Phatr3_J55079*, *Phatr3_J45997, Phatr3_J29157*, *Phatr3_J49339* and *Phatr3_J49098*) corresponding to *PK2, PK4* and *PK6* (pyruvate kinase), *PGK1*(phosphoglycerate kinase) and *PYC2* (precursor of carboxylase pyruvate carboxylase) are all related to glycolysis and were upregulated between 1.08 to 2.32 logFC. Another gene involved in carbon metabolism (*Phatr3_J51970*) was downregulated at -1.08 logFC. A gene related to branched-chain amino acid degradation (*Phatr3_J11811*) was downregulated (logFC -1.06), while a gene related to amino acid biosynthesis (*Phatr3_J26256*) was upregulated (logFC).

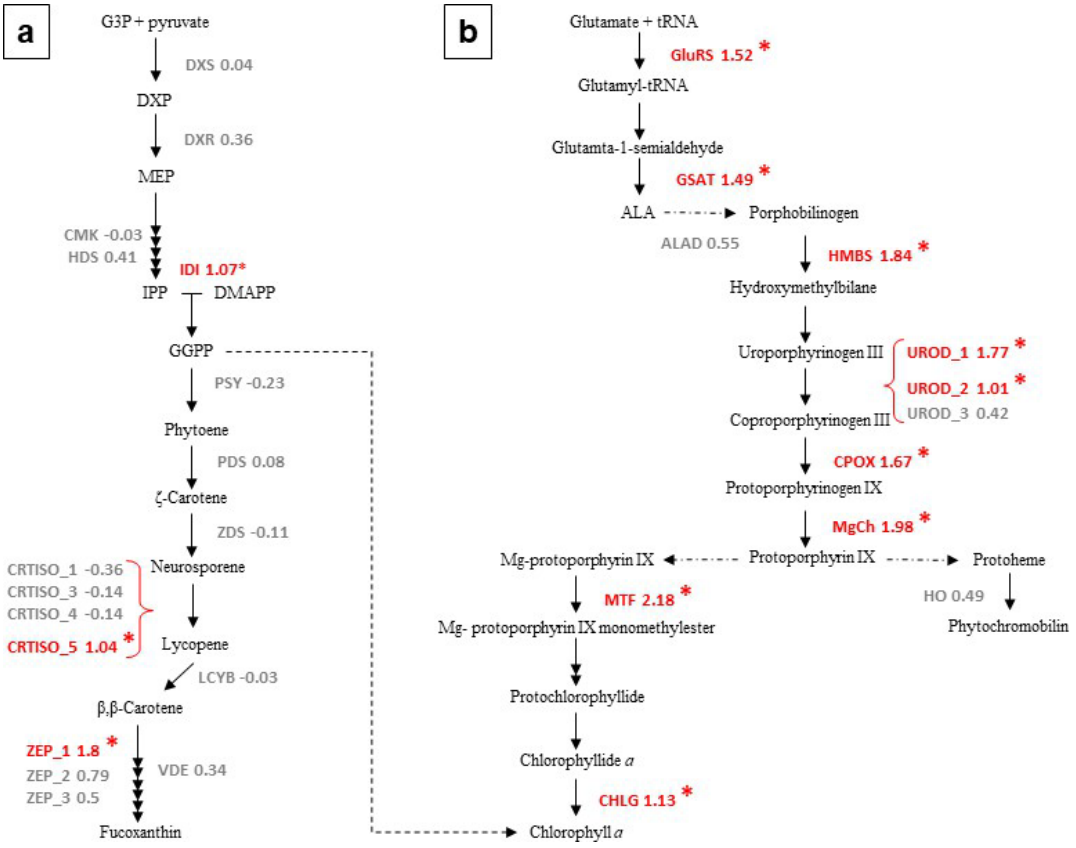

Figure 4.6. Pigment pathways with coinciding gene expression values comparing F cultures with WT cultures of *P. tricornutum*.. (**a**) Carotenoid / fucoxanthin pathway from upstream MEP pathway and (**b**) tetrapyrrole pathway to chlorophyll *a*. Red-coloured terms indicate genes over threshold of 1 logFC, while grey terms indicate genes within threshold of 1 logFC. Asterisks denote genes with expression p-value < 0.05. Reactions involving more than one gene are shown as averages unless p-values are either side of 0.05; e.g MgCh_H and MgCh_D are averaged to 1.98 and listed simply as MgCh as both had $p < 0.05$.

Given the significant increase in fucoxanthin content and productivity observed in F cultures (**Figure 4.2c,e**), it was expected that genes involved in carotenoid precursor supply and biosynthesis would be significantly upregulated. However, relatively few genes in these pathways were upregulated (**Figure 4.6a**). Instead, the tetrapyrrole to chlorophyll *a* pathway (**Figure 4.6b**) was upregulated and overrepresented in the enrichment analysis as indicated by the ShinyGO platform. Rate-limiting steps include *GSAT* (glutamate-1-semialdehyde aminotransferase, *Phatr3_J36347*) and *ALAD* (ALA dehydratase, *Phatr3_J41746*), of which F cultures exhibited 1.49 and 0.55 logFC compared to WT, respectively.

4.5 Discussion

The combined results suggest that FACS-sorting can be a powerful tool for enhancing production of pigments as well as other target compounds in microalgal cultures. Recent work has opted for sorting with the relationship to cell volume incorporated into the sorting method[106,154]. However, it is probable that differences in cell size during the initial sorting phase of the experiment are due to regular fluctuations over the *Phaeodactylum* life cycle, reducing the favouring of larger cells in sorted cultures downstream. Work on gating strategies for FACS-sorting in microalgal cultures is required to clarify best practices.

Results from the gene enrichment analysis showed that all pathways with a minimum of 25% of genes represented (also corresponding to >10 fold enrichment) primarily exist to serve functions of photosynthesis. The pathway with highest significant gene content (50% with 19.6 fold enrichment) was the protoporphyrinogen IX metabolic process pathway (GO: 0046501), an upstream system responsible for chlorophyll biosynthesis. This is reinforced by the increased chlorophyll *a* content and logFC of >1 for 10 out of 12 genes in the tetrapyrrole pathway to chlorophyll *a* for FACS cultures. Surprisingly, only 2 genes in the fucoxanthin pathway were significantly enriched with >1 logFC (*CRTISO5* and *ZEP1*). This gives mixed interpretations as *CRTISO* was previously seen to be downregulated under low light conditions, which was favorable for fucoxanthin biosynthesis, while ZEP had the opposite effect of being upregulated in correlation to increased fucoxanthin under low light [1,99,166]. More recent research has found that *CRTISO5* is directly responsible for fucoxanthin biosynthesis, and that knockdown of this gene removed *P. tricornutum* ability to synthesize fucoxanthin altogether.[167] Upregulation of this gene in F

cultures is therefore the likely cause of increased fucoxanthin content displayed in these cultures compared to WT.

It was reasoned that F cultures could display very large differences at the single gene level of expression but also that differences in gene expression could be smaller, yet distributed throughout multiple regions contributing to higher fucoxanthin. While there was a higher number of genes upregulated in the MEP to fucoxanthin pathway, the logFC increase was also generally higher. The 1.3 × WT increase of fucoxanthin in F cultures could therefore be a result of post-transcriptional or post-translational effects as seen elsewhere in *P. tricornutum* and other microalgae, but upregulation of one or more of *CRTISO5, IDI* and *ZEP1* along the MEP to fucoxanthin pathway are likely contributors[167-170].

Tetrapyrroles are synthesized in plastids and regulate nuclear gene expression[171,172]. It could be that tetrapyrrole signaling is responsible for altered gene expression across the nucleus. Enzymes along the tetrapyrrole pathway, *MgPMT* (Mg Protoporphyrin IX Methyltransferase), *MgCh* (Magnesium Chelatase) and ALA (5-Aminolevulinic acid), were upregulated in a tobacco line with enhanced expression of the gene *MTF* (Mg-Protoporphyrin IX methyltransferase) under low light.[173] The expression level of *MTF* in F cultures was 2.18 logFC higher than in WT cultures. While the tetrapyrrole pathway was highly enriched in F cultures, this gene is a key step in regulating downstream products, along with ALA synthesis (*GSAT*) [174-177]. Both of these genes were upregulated and may be the primary reason for increased chlorophyll *a* content in F cultures. It is likely that FACS cells will simply produce more pigments under all conditions, because cells exhibited higher chlorophyll *a* and fucoxanthin after experiencing low light conditions (days 4-8) despite being sorted under relatively high light (no adaptation before sorting).

The increased growth in F cultures is likely due in part to amplified photosynthetic activity from increased content of light harvesting pigments, as well as contributions from pyruvate kinase and phosphoglycerate kinase as vital contributors to carbon metabolism.[178,179] Genes associated with BCAA degradation have also been previously observed to be upregulated under conditions of TAG accumulation.[180,181] Increased AA synthesis and BCAA degradation are likely increasing carbon metabolism alongside *PK* and *PGK* for increased growth of F populations.[182]

4.6 Conclusion

Sorting out the top 1% fluorescing *P. tricornutum* cells resulted in cultures with faster growth, higher pigment content, and subsequently higher productivity. Analysis of RNA-seq data indicated that the underlying mechanisms for this improved functionality were upregulated pathways associated with photosynthesis, specifically upregulation of the tetrapyrrole pathway to chlorophyll *a*. The high utility of FACS as a method for artificial selection is clear, while the best gating strategies as well as accuracy for favouring specific pigments using FACS are yet to be determined and are likely species and condition specific. While this study provides a first comprehensive library of genes associated with a F population of cells showing increased production of fucoxanthin, future studies combining sequencing and FACS sorting of cells displaying different pigment fluorescence signatures under various conditions is clearly needed to elucidate the genetic mechanisms driving differences in microalgae pigment phenotypes. In conclusion, this study reveals the inherent presence of highly productive subpopulations within the *Phaeodactylum tricornutum* culture without modification using mutagenic agents. By employing Fluorescence-Activated Cell Sorting (FACS), these high-performing algae can be identified and selectively sub-cultured. The F cultures exhibited significant improvements in growth rate, biomass, and fucoxanthin productivity compared to the wild-type strain, demonstrating FACS as a powerful method that can be used to select desirable phenotypes that are distinguishable from the original (both phenotypically and from a gene expression standpoint) with as little as one selection event.

Chapter 5: Synthesis

This thesis developed understanding in three key areas of microalgal biotechnology, addressing more specifically three gaps for the natural production of pigments in microalgae: high-throughput screening, random mutagenesis and artificial selection - targeting the major pigment fucoxanthin and using the model diatom *Phaeodactylum tricornutum*. Firstly, two high-throughput screening technologies were highlighted as the most common and most promising: microplate reader and flow cytometry / FACS. One microplate reader method was adapted to detect fucoxanthin in live cultures without a solvent extraction step while maintaining axenic culture. This is the first time this has been achieved, and this work (**Chapter 2**) remains as a proof-of-concept for further studies looking to detect various pigment in other species. Secondly, random mutagenesis was utilised to increase fucoxanthin in *P. tricornutum*, with a superior subpopulation remaining four months after treatment with EMS. A central finding for **Chapter 3** is the critical need to incorporate temporal stability analysis in research projects investigating mutagenesis of microalgal culture in order to add depth to results. This chapter was also the first time ionising x-ray mutagenesis was utilised in microalgal biotechnology research. Lastly, artificial selection was undertaken using FACS, and this work supported the efficacy of the technology as well as resulted in pigment-enriched and faster-growing subpopulations of *P. tricornutum* in **Chapter 4**. This chapter also highlighted the enrichment of gene ontology terms associated with superior subpopulations and this is the first time RNAseq data was used alongside FACS in microalgal research.

5.1 The utility of spectrophotometry and FACS

Because high-throughput screening is an integral part of any project using an approach other than rational design (such as directed evolution), an investigation into the current status of high-throughput screening in microalgal cultures was performed. Spectrophotometry has been used widely for detecting pigments in algal cultures and there have been various methods produced based on the technology. These approaches often used modified equations founded on target

pigments, species and solvents [3,101,183,184]. Other works used spectrophotometry with the more mathematically complex spectral deconvolution alongside development of programming language scripts to aid researchers in making analysis relatively straight forward [4,102,103]. In recent years, FACS has been applied as an analytical tool for microalgal cultures and also as a screening and sorting method [100,106,154].

This thesis compared the two technologies and found that FACS enables high single-cell screening of strains at the single cell level that outperforms the comparatively low resolution of microplate readers. In addition, FACS enables single cell sorting, thus incorporating two vital steps in the directed evolution workload pipeline – screening and sorting, where microplate reader technology provides only one. However, the benefits of microplate reader technology are that it is low cost (often $1/10^{th}$ that of FACS hardware) as well as having substantially lower maintenance and expertise requirements. Another important consideration is that microplate readers require far less culture contact and thus cultures in plates can easily maintain sterility where FACS has a higher risk of contamination. Furthermore, cultures in plates can be assessed temporally while growing to density with little effort on behalf of the researcher, while FACS requires significant time for setup and calibration, performance and daily cleaning. There is also an increased use of associated disposables as well as increased occurrence of program errors due to the complexity of the system. Therefore, both methods should be incorporated into directed evolution projects – FACS being included where sorting cells is required (such as after mutagen treatment to separate newly-created strains), and microplate reader being included in other stages that require frequent culture measurement.

5.2 Random mutagenesis as a tool for strain development

Researchers using multiple mutagenic agents in their work should be careful to ensure rigorous examination of each before commencing any final treatment. The effects of various doses of UV and EMS are documented in the literature for some species [87,98,121]. However, there are still large knowledge gaps and researchers should be aware that dose-response varies hugely between species, even those closely related. Due to this gap, mortality curves, including not only

treatment dosage but also cell densities, growth phases, recovery methods (time in darkness and media components) and especially temporal analysis, will play a vital role in establishing the effects of mutagens on microalgal cultures.

In addition, further research should be conducted on mutagens including ionising agents like x-rays. The diversifying of specific mutagenic factors for DNA in algal culture could increase the genetic 'space' allowable for improved phenotypes. For example, UV primarily produces dimers at adjacent pyrimidines (cytosine and thymine), meaning ionising mutagens theoretically have a larger chromosomal reach to produce novel genetic forms. This, as well as secondary effects from ROS, should be investigated further in order to fully understand the effects of mutagens on microalgae.

5.3 Gene expression and the discovery of target genes

A number of genes associated with carotenoid biosynthesis have been identified and successfully manipulated to increase target pigments in microalgae [99,185,186]. Despite this, further studies are required to elucidate the vast network of genes and regulatory mechanisms associated with improved pigment content and interlinked outcomes like increased growth rate. Some gene ontology terms and specific genes associated with increased pigment content and growth are discussed in this thesis as is the overexpression of the tetrapyrrole pathway rather than the MEP and carotenoid to fucoxanthin pathway. Yet future work should be undertaken (i) to highlight further genes relevant to pigmentation in *P. tricornutum* and other model species, (ii) to reveal potential regulations at other level than transcriptional (e.g. post-translational) as well as (iii) to advance methods for improving cultures with industry applications.

5.4 Thesis limitations

Limitations to the first chapter are almost exclusively data-based. Because the high-throughput screening method was adapted to live cultures, absorbance at wavelengths between 400 – 550 nm was used as a measure for fucoxanthin absorbance in live cultures. This worked because fucoxanthin is the primary carotenoid and this screen is therefore a proxy screen using total

carotenoid content (or more precisely total cellular absorbance between 400 – 550 nm) as an indicator of fucoxanthin content per unit biomass. This is not entirely accurate and future studies should use knockdown strains and pigment-upregulated strains in order to characterise absorbance of a target pigment within a given strain. This way, accurate pigment profiles can be input into the spectral deconvolution method to firstly switch the screen from a proxy method back to a direct measurement method as the original work intended, and secondly to improve the resolution of the screen. Work from Cao, et al. [167] used a fucoxanthin knockdown mutant of *P. tricornutum* and this strain could be used to develop live culture pigment profiles for spectral deconvolution development.

The third chapter utilised UV, EMS and X-radiation to mutate cultures and the differences in mortality and downstream phenotype stability analysis showed that working with multiple mutagens is difficult. To compare mutagens statistically would be a very complicated endeavour and the only valuable conclusion arising from chapter two in this regard is that regardless of mutagen used in projects of this kind, high mortality (at least 90 – 95%) is critical in ensuring successful strain creation.

While FACS is an invaluable tool for work of this kind as demonstrated by Chapter 4, more complex methodology involving adaptive laboratory evolution, knockdown mutants and culture condition changes will likely multiply the power of FACS for creating and selecting superior strains of microalgae, especially when considering that this chapter did not have validation using specific genes relevant to photosynthesis and growth. Future work of this kind would ideally incorporate validation targeting the genes found in this work.

5.5 Combination methodology for directed evolution

A proposed directed evolution method is outlined below based on the findings in this thesis from Chapters 2, 3 and 4. Researchers start by sorting for improved strains using FACS (selection) to establish a higher benchmark from which to include further steps like mutagenesis. After the initial sort(s) and screening, researchers treat cells with mutagens at predetermined concentrations and intensities and, after a cell recovery period, sort again to separate the new strains. The iterative process in **Figure 5.1** is repeated – the newly sorted cells are grown to inoculation density and screened using plate reader before further mutagenesis, sorting and so on while the cycle continues for as long as the researcher deems appropriate.

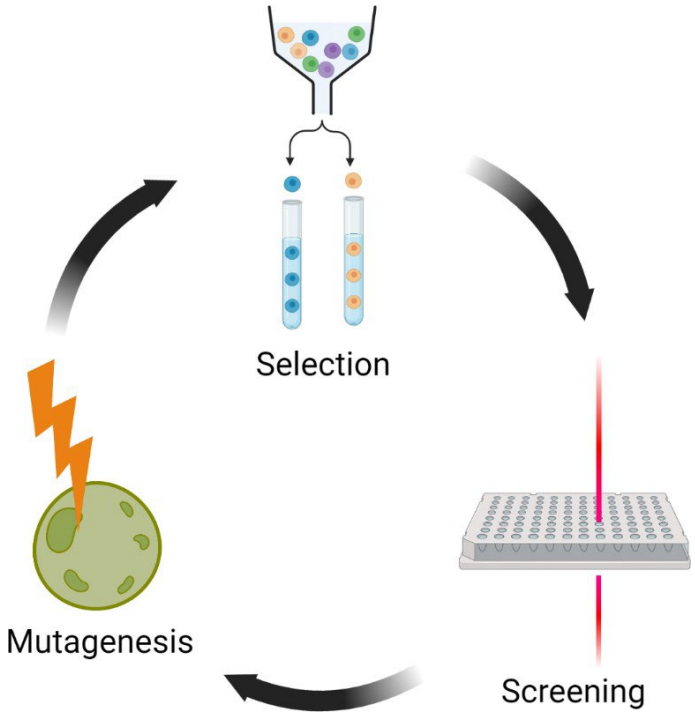

Figure 5.1. Hypothetical directed evolution methodology combining and repeating the three phases of selection, screening and mutagenesis for improving pigments in microalgal cultures. Once a starting population is established using FACS, cells are treated and sorted again, after which they are screened, mutated and sorted continually.

5.6 Concluding remarks

The main aims of this thesis were firstly to develop a high-throughput selection and screening method for fucoxanthin-improved mutants of *Phaeodactylum tricornutum* for further analysis. This was achieved by focusing on common microplate reader technology rather than FACS, and was successfully achieved with the outcome being development of a pigment screen that is able to determine fucoxanthin content differences between samples in 384-well microplate format. Not only does this new method enable high-throughput screening of fucoxanthin, it allows screening to be undertaken rapidly with minimal culture contact and little to moderate expertise. The second aim was to alter pigment biosynthesis in *Phaeodactylum tricornutum* using short UV radiation, EMS and X-radiation to create pigment hyper-producing strains. This was achieved at 4 months of subculture in a population of EMS-treated cells and highlights the necessity of including temporal stability analysis in mutagenesis projects. The third and final aim was to identify the gene expression changes responsible for improved non-mutant pigment phenotypes using FACS-sorting and Illumina RNA sequencing in *Phaeodactylum tricornutum*. This was achieved after confirming increased pigmentation and growth in a sorted population and highlighting of various overexpressed genes and associated enriched gene ontology terms. In addition, it was found that the tetrapyrrole pathway was overexpressed where the expected MEP to carotenoid pathway unexpectedly was not. Rather, only a few genes were upregulated and this indicates that fucoxanthin biosynthesis may be regulated by few rate-limiting steps. This also indicates that random mutagenesis and FACS are overlooked methods for discovering potentially unexpected biological pathways.

References

1 Manfellotto, F., Stella, G. R., Falciatore, A., Brunet, C. & Ferrante, M. I. Engineering the unicellular alga *Phaeodactylum tricornutum* for enhancing carotenoid production. *Antioxidants* **9**, 757 (2020).

2 Stiger-Pouvreau, V. & Zubia, M. Macroalgal diversity for sustainable biotechnological development in French tropical overseas territories. *Botanica marina* **63**, 17-41 (2020).

3 Wang, L.-J. *et al.* A rapid method for the determination of fucoxanthin in diatom. *Marine drugs* **16**, 33 (2018).

4 Thrane, J.-E. *et al.* Spectrophotometric analysis of pigments: a critical assessment of a high-throughput method for analysis of algal pigment mixtures by spectral deconvolution. *PloS one* **10**, e0137645 (2015).

5 Bacci, M. L. *A concise history of world population*. (John Wiley & Sons, 2017).

6 Raskin, I. *et al.* Plants and human health in the twenty-first century. *TRENDS in Biotechnology* **20**, 522-531 (2002).

7 Gomiero, T., Pimentel, D. & Paoletti, M. G. Is there a need for a more sustainable agriculture? *Critical reviews in plant sciences* **30**, 6-23 (2011).

8 Tanentzap, A. J., Lamb, A., Walker, S. & Farmer, A. Resolving conflicts between agriculture and the natural environment. *PLoS biology* **13**, e1002242 (2015).

9 Ahmad, A. L., Yasin, N. M., Derek, C. & Lim, J. Microalgae as a sustainable energy source for biodiesel production: a review. *Renewable and sustainable energy reviews* **15**, 584-593 (2011).

10 Renuka, N., Guldhe, A., Prasanna, R., Singh, P. & Bux, F. Microalgae as multi-functional options in modern agriculture: current trends, prospects and challenges. *Biotechnology advances* **36**, 1255-1273 (2018).

11 Sun, H. *et al.* Fucoxanthin from marine microalgae: A promising bioactive compound for industrial production and food application. *Critical Reviews in Food Science and Nutrition*, 1-17 (2022).

12 Rajkumar, R. & Yaakob, Z. The biology of microalgae. *Biotechnological Applications of Microalgae: Biodiesel and Value-Added Products*, 7-16 (2013).

13 Barsanti, L. *et al.* in *Algal toxins: nature, occurrence, effect and detection* 353-391 (Springer, 2008).

14 Falkowski, P., Barber, R. T. & Smetacek, V. Biogeochemical Controls and Feedbacks on Ocean Primary Production. *Science* **281**, 200-207 (1998).

15 Field, C. B., Behrenfeld, M. J., Randerson, J. T. & Falkowski, P. Primary production of the biosphere: integrating terrestrial and oceanic components. *science* **281**, 237-240 (1998).

16 Hopes, A. & Mock, T. Evolution of microalgae and their adaptations in different marine ecosystems. *eLS*, 1-9 (2015).

17 Dmytryk, A., Tuhy, Ł. & Chojnacka, K. in *Prospects and Challenges in Algal Biotechnology* 295-310 (Springer, 2017).

18 Khan, M. I., Shin, J. H. & Kim, J. D. The promising future of microalgae: current status, challenges, and optimization of a sustainable and renewable industry for biofuels, feed, and other products. *Microbial cell factories* **17**, 1-21 (2018).

19 Benedetti, M., Vecchi, V., Barera, S. & Dall'Osto, L. Biomass from microalgae: the potential of domestication towards sustainable biofactories. *Microbial cell factories* **17**, 1-18 (2018).

20 Ribeiro, A. R. *et al. Phaeodactylum tricornutum* in finishing diets for gilthead seabream: effects on skin pigmentation, sensory properties and nutritional value. *Journal of Applied Phycology* **29**, 1945-1956 (2017).

21 Chen, C.-Y., Yeh, K.-L., Aisyah, R., Lee, D.-J. & Chang, J.-S. Cultivation, photobioreactor design and harvesting of microalgae for biodiesel production: a critical review. *Bioresource technology* **102**, 71-81 (2011).
22 Hamed, I. The evolution and versatility of microalgal biotechnology: a review. *Comprehensive Reviews in Food Science and Food Safety* **15**, 1104-1123 (2016).
23 Bhola, V., Swalaha, F., Kumar, R. R., Singh, M. & Bux, F. Overview of the potential of microalgae for CO 2 sequestration. *International Journal of Environmental Science and Technology* **11**, 2103-2118 (2014).
24 Hosikian, A., Lim, S., Halim, R. & Danquah, M. K. Chlorophyll extraction from microalgae: a review on the process engineering aspects. *International journal of chemical engineering* **2010** (2010).
25 Rasmussen, R. S. & Morrissey, M. T. Marine biotechnology for production of food ingredients. *Advances in food and nutrition research* **52**, 237-292 (2007).
26 Ng, D. H., Ng, Y. K., Shen, H. & Lee, Y. K. in *Handbook of Marine Microalgae* 69-80 (Elsevier, 2015).
27 Wichuk, K., Brynjólfsson, S. & Fu, W. Biotechnological production of value-added carotenoids from microalgae: Emerging technology and prospects. *Bioengineered* **5**, 204-208 (2014).
28 Leu, S. & Boussiba, S. (2013).
29 Mann, D. G. & Vanormelingen, P. An inordinate fondness? The number, distributions, and origins of diatom species. *Journal of eukaryotic microbiology* **60**, 414-420 (2013).
30 Ovide, C. *et al.* Comparative in depth RNA sequencing of P. tricornutum's morphotypes reveals specific features of the oval morphotype. *Scientific reports* **8**, 14340 (2018).
31 Lewin, J. C., Lewin, R. & Philpott, D. Observations on *Phaeodactylum tricornutum*. *Microbiology* **18**, 418-426 (1958).
32 Bowler, C. *et al.* The *Phaeodactylum genome* reveals the evolutionary history of diatom genomes. *Nature* **456**, 239-244 (2008).
33 De Riso, V. *et al.* Gene silencing in the marine diatom *Phaeodactylum tricornutum*. *Nucleic acids research* **37**, e96-e96 (2009).
34 Taddei, L. *et al.* Multisignal control of expression of the LHCX protein family in the marine diatom *Phaeodactylum tricornutum*. *Journal of experimental botany* **67**, 3939-3951 (2016).
35 Bañuelos-Hernández, B., Beltrán-López, J. I. & Rosales-Mendoza, S. in *Handbook of Marine Microalgae* 281-298 (Elsevier, 2015).
36 Perfeito, C., Ambrósio, M., Santos, R. B., Afonso, C. N. & Abranches, R. in *Front Mar Sci Conference Abstract: IMMR'18| International Meeting on Marine Research.*
37 Hamilton, M. L., Haslam, R. P., Napier, J. A. & Sayanova, O. Metabolic engineering of *Phaeodactylum tricornutum* for the enhanced accumulation of omega-3 long chain polyunsaturated fatty acids. *Metabolic engineering* **22**, 3-9 (2014).
38 Chauton, M. S., Winge, P., Brembu, T., Vadstein, O. & Bones, A. M. Gene regulation of carbon fixation, storage, and utilization in the diatom *Phaeodactylum tricornutum* acclimated to light/dark cycles. *Plant physiology* **161**, 1034-1048 (2013).
39 Nicoletti, M. Microalgae nutraceuticals. *Foods* **5**, 54 (2016).
40 Butler, T., Kapoore, R. V. & Vaidyanathan, S. *Phaeodactylum tricornutum*: a diatom cell factory. *Trends in biotechnology* **38**, 606-622 (2020).
41 Kim, S. M. *et al.* A potential commercial source of fucoxanthin extracted from the microalga *Phaeodactylum tricornutum*. *Applied biochemistry and biotechnology* **166**, 1843-1855 (2012).
42 Koo, S. Y. *et al.* Anti-obesity effect of standardized extract of microalga P*haeodactylum tricornutum* containing fucoxanthin. *Marine drugs* **17**, 311 (2019).

43 Guo, B. *et al.* Screening of diatom strains and characterization of Cyclotella cryptica as a potential fucoxanthin producer. *Marine Drugs* **14**, 125 (2016).
44 McClure, D. D., Luiz, A., Gerber, B., Barton, G. W. & Kavanagh, J. M. An investigation into the effect of culture conditions on fucoxanthin production using the marine microalgae *Phaeodactylum tricornutum*. *Algal Research* **29**, 41-48 (2018).
45 Maoka, T. Carotenoids as natural functional pigments. *Journal of natural medicines* **74**, 1-16 (2020).
46 Simkin, A. J. *et al.* The role of photosynthesis related pigments in light harvesting, photoprotection and enhancement of photosynthetic yield in planta. *Photosynthesis Research* **152**, 23-42 (2022).
47 Nagao, R. *et al.* Structural basis for assembly and function of a diatom photosystem I-light-harvesting supercomplex. *Nature communications* **11**, 1-12 (2020).
48 Papagiannakis, E., HM van Stokkum, I., Fey, H., Büchel, C. & Van Grondelle, R. Spectroscopic characterization of the excitation energy transfer in the fucoxanthin–chlorophyll protein of diatoms. *Photosynthesis Research* **86**, 241-250 (2005).
49 Büchel, C. Fucoxanthin-chlorophyll proteins in diatoms: 18 and 19 kDa subunits assemble into different oligomeric states. *Biochemistry* **42**, 13027-13034 (2003).
50 Gelzinis, A. *et al.* Mapping energy transfer channels in fucoxanthin–chlorophyll protein complex. *Biochimica et Biophysica Acta (BBA)-Bioenergetics* **1847**, 241-247 (2015).
51 Kira, N. *et al.* Expression profile of genes involved in isoprenoid biosynthesis in the marine diatom *Phaeodactylum tricornutum*. *Environmental Control in Biology* **54**, 31-37 (2016).
52 Nisar, N., Li, L., Lu, S., Khin, N. C. & Pogson, B. J. Carotenoid metabolism in plants. *Molecular plant* **8**, 68-82 (2015).
53 Lourenço-Lopes, C. *et al.* Biological action mechanisms of fucoxanthin extracted from algae for application in food and cosmetic industries. *Trends in Food Science & Technology* **117**, 163-181 (2021).
54 Wang, S. *et al.* A review on the progress, challenges and prospects in commercializing microalgal fucoxanthin. *Biotechnology advances* **53**, 107865 (2021).
55 Adeel, S., Amin, N., Ahmad, T., Batool, F. & Hassan, A. Sustainable isolation of natural dyes from plant wastes for textiles. *Recycling from waste in fashion and textiles: a sustainable and circular economic approach*, 363-390 (2020).
56 Shah, M. R. *et al.* Microalgae in aquafeeds for a sustainable aquaculture industry. *Journal of applied phycology* **30**, 197-213 (2018).
57 Eggersdorfer, M. & Wyss, A. Carotenoids in human nutrition and health. *Archives of biochemistry and biophysics* **652**, 18-26 (2018).
58 Dissing, B. S., Nielsen, M. E., Ersbøll, B. K. & Frosch, S. Multispectral imaging for determination of astaxanthin concentration in salmonids. *PloS one* **6**, e19032 (2011).
59 Shahidi, F. & Brown, J. A. Carotenoid pigments in seafoods and aquaculture. *Critical Reveiws in Food Science* **38**, 1-67 (1998).
60 Li, J., Zhu, D., Niu, J., Shen, S. & Wang, G. An economic assessment of astaxanthin production by large scale cultivation of *Haematococcus pluvialis*. *Biotechnology advances* **29**, 568-574 (2011).
61 Milledge, J. J. Commercial application of microalgae other than as biofuels: a brief review. *Reviews in Environmental Science and Bio/Technology* **10**, 31-41 (2011).
62 Silva, S. C., Ferreira, I. C., Dias, M. M. & Barreiro, M. F. Microalgae-derived pigments: A 10-year bibliometric review and industry and market trend analysis. *Molecules* **25**, 3406 (2020).
63 Muller, P., Li, X.-P. & Niyogi, K. K. Non-photochemical quenching. A response to excess light energy. *Plant physiology* **125**, 1558-1566 (2001).

64 Borowitzka, M., Beardall, J. & Raven, J. The physiology of microalgae, developments in applied phycology. *Springer International Publishing* **10**, 978-973 (2016).
65 Büchel, C. Fucoxanthin-chlorophyll-proteins and non-photochemical fluorescence quenching of diatoms. *Non-photochemical quenching and energy dissipation in plants, algae and cyanobacteria*, 259-275 (2014).
66 Veith, T. & Büchel, C. The monomeric photosystem I-complex of the diatom *Phaeodactylum tricornutum* binds specific fucoxanthin chlorophyll proteins (FCPs) as light-harvesting complexes. *Biochimica et Biophysica Acta (BBA)-Bioenergetics* **1767**, 1428-1435 (2007).
67 Peng, J., Yuan, J.-P., Wu, C.-F. & Wang, J.-H. Fucoxanthin, a marine carotenoid present in brown seaweeds and diatoms: metabolism and bioactivities relevant to human health. *Marine drugs* **9**, 1806-1828 (2011).
68 Sachindra, N. M. *et al.* Radical scavenging and singlet oxygen quenching activity of marine carotenoid fucoxanthin and its metabolites. *Journal of agricultural and food chemistry* **55**, 8516-8522 (2007).
69 Nomura, T., Kikuchi, M., Kubodera, A. & Kawakami, Y. Proton-donative antioxidant activity of fucoxanthin with 1, 1-diphenyl-2-picrylhydrazyl (DPPH). *IUBMB Life* **42**, 361-370 (1997).
70 Sangeetha, R., Bhaskar, N. & Baskaran, V. Comparative effects of β-carotene and fucoxanthin on retinol deficiency induced oxidative stress in rats. *Molecular and cellular biochemistry* **331**, 59-67 (2009).
71 Miyashita, K., Beppu, F., Hosokawa, M., Liu, X. & Wang, S. Nutraceutical characteristics of the brown seaweed carotenoid fucoxanthin. *Archives of biochemistry and biophysics* **686**, 108364 (2020).
72 Maeda, H., Hosokawa, M., Sashima, T. & Miyashita, K. Dietary combination of fucoxanthin and fish oil attenuates the weight gain of white adipose tissue and decreases blood glucose in obese/diabetic KK-Ay mice. *J. of Agricultural and Food Chemistry* **55**, 7701-7706 (2007).
73 Kozak, L. & Anunciado-Koza, R. UCP1: its involvement and utility in obesity. *International journal of obesity* **32**, S32-S38 (2008).
74 Patil, V., Tran, K.-Q. & Giselrød, H. R. Towards sustainable production of biofuels from microalgae. *International journal of molecular sciences* **9**, 1188-1195 (2008).
75 Trovão, M. *et al.* Random mutagenesis as a promising tool for microalgal strain improvement towards industrial production. *Marine drugs* **20**, 440 (2022).
76 Grama, S. B., Liu, Z. & Li, J. Emerging trends in genetic engineering of microalgae for commercial applications. *Marine Drugs* **20**, 285 (2022).
77 Friedberg, E. C., Walker, G. C., Siede, W. & Wood, R. D. *DNA repair and mutagenesis*. (American Society for Microbiology Press, 2005).
78 Amos, W. & Harwood, J. Factors affecting levels of genetic diversity in natural populations. *Philosophical Transactions of the Royal Society* **353**, 177-186 (1998).
79 Gatew, H. Genetically modified foods (GMOs); a review of genetic engineering. *Journal of World's Poultry Research* **9**, 157-163, doi:10.36380/scil.2019.jlsb25 (2019).
80 Liu, B. *et al.* Mechanisms of mutagenesis: DNA replication in the presence of DNA damage. *Mutat Res Rev Mutat Res* **768**, 53-67, doi:10.1016/j.mrrev.2016.03.006 (2016).
81 Ikehata, H. & Ono, T. The mechanisms of UV mutagenesis. *J Radiat Res* **52**, 115-125, doi:10.1269/jrr.10175 (2011).
82 Despic, V., Dejung, M., Butter, F. & Neugebauer, K. M. Analysis of RNA-protein interactions in vertebrate embryos using UV crosslinking approaches. *Methods* **126**, 44-53, doi:10.1016/j.ymeth.2017.07.013 (2017).

83 Livneh, Z., Cohen-Fix, O., Skaliter, R. & Elizur, T. Replication of damaged DNA and the molecular mechanism of ultraviolet light mutagenesis. *Crit Rev Biochem Mol Biol* **28**, 465-513, doi:10.3109/10409239309085136 (1993).
84 Friedberg, E. C. *et al. DNA Repair and Mutagenesis*. 2 edn, (American Society for Microbiology, 2005).
85 Choi, J. H., Besaratinia, A., Lee, D. H., Lee, C. S. & Pfeifer, G. P. The role of DNA polymerase iota in UV mutational spectra. *Mutat Res* **599**, 58-65, doi:10.1016/j.mrfmmm.2006.01.003 (2006).
86 Sega, G. A. A review of the genetic effects of ethyl methanesulfonate. *Mutation Research/Reviews in Genetic Toxicology* **134**, 113-142 (1984).
87 Kim, Y., Schumaker, K. S. & Zhu, J.-K. EMS Mutagenesis of Arabidopsis. *Methods in Molecular Biology* **323**, 101-103 (2006).
88 Borrego-Soto, G., Ortiz-López, R. & Rojas-Martínez, A. Ionizing radiation-induced DNA injury and damage detection in patients with breast cancer. *Genetics and molecular biology* **38**, 420-432 (2015).
89 Ward, J. The yield of DNA double-strand breaks produced intracellularly by ionizing radiation: a review. *International journal of radiation biology* **57**, 1141-1150 (1990).
90 Nikjoo, H., Munson, R. J. & Bridges, B. A. RBE-LET relationships in mutagenesis by ionizing radiation. *Journal of radiation research* **40**, S85-S105 (1999).
91 Matsuno, T. Aquatic animal carotenoids. *Fisheries science* **67**, 771-783 (2001).
92 Bae, M., Kim, M.-B., Park, Y.-K. & Lee, J.-Y. Health benefits of fucoxanthin in the prevention of chronic diseases. *Biochimica et Biophysica Acta (BBA)-Molecular and Cell Biology of Lipids* **1865**, 158618 (2020).
93 Karpiński, T. M. & Adamczak, A. Fucoxanthin—An antibacterial carotenoid. *Antioxidants* **8**, 239 (2019).
94 Satomi, Y. Antitumor and cancer-preventative function of fucoxanthin: A marine carotenoid. *Anticancer research* **37**, 1557-1562 (2017).
95 Miyashita, K. *et al.* The allenic carotenoid fucoxanthin, a novel marine nutraceutical from brown seaweeds. *Journal of the Science of Food and Agriculture* **91**, 1166-1174 (2011).
96 Fabris, M. *et al.* Extrachromosomal genetic engineering of the marine diatom *Phaeodactylum tricornutum* enables the heterologous production of monoterpenoids. *ACS synthetic biology* **9**, 598-612 (2020).
97 Yi, Z. *et al.* Photo-oxidative stress-driven mutagenesis and adaptive evolution on the marine diatom *Phaeodactylum tricornutum* for enhanced carotenoid accumulation. *Marine drugs* **13**, 6138-6151 (2015).
98 Yi, Z. *et al.* Chemical mutagenesis and fluorescence-based high-throughput screening for enhanced accumulation of carotenoids in a model marine diatom *Phaeodactylum tricornutum*. *Marine drugs* **16**, 272 (2018).
99 Kadono, T. *et al.* Effect of an introduced phytoene synthase gene expression on carotenoid biosynthesis in the marine diatom *Phaeodactylum tricornutum*. *Marine drugs* **13**, 5334-5357 (2015).
100 Gao, F., Teles, I., Ferrer-Ledo, N., Wijffels, R. H. & Barbosa, M. J. Production and high throughput quantification of fucoxanthin and lipids in *Tisochrysis lutea* using single-cell fluorescence. *Bioresource Technology* **318**, 124104 (2020).
101 Ritchie, R. J. Universal chlorophyll equations for estimating chlorophylls a, b, c, and d and total chlorophylls in natural assemblages of photosynthetic organisms using acetone, methanol, or ethanol solvents. *Photosynthetica* **46**, 115-126 (2008).
102 Küpper, H., Spiller, M. & Küpper, F. C. Photometric method for the quantification of chlorophylls and their derivatives in complex mixtures: fitting with Gauss-peak spectra. *Analytical Biochemistry* **286**, 247-256 (2000).

103 Küpper, H., Seibert, S. & Parameswaran, A. Fast, sensitive, and inexpensive alternative to analytical pigment HPLC: quantification of chlorophylls and carotenoids in crude extracts by fitting with Gauss peak spectra. *Analytical chemistry* **79**, 7611-7627 (2007).
104 Li, W., Gao, K. & Beardall, J. Interactive effects of ocean acidification and nitrogen-limitation on the diatom *Phaeodactylum tricornutum*. *PloS one* **7**, e51590 (2012).
105 Premvardhan, L. *et al.* The charge-transfer properties of the S2 state of fucoxanthin in solution and in fucoxanthin chlorophyll-a/c2 protein (FCP) based on stark spectroscopy and molecular-orbital theory. *The Journal of Physical Chemistry B* **112**, 11838-11853 (2008).
106 Fan, Y. *et al.* Rapid Sorting of Fucoxanthin-Producing *Phaeodactylum tricornutum* Mutants by Flow Cytometry. *Marine drugs* **19**, 228 (2021).
107 Hunter, M. C., Smith, R. G., Schipanski, M. E., Atwood, L. W. & Mortensen, D. A. Agriculture in 2050: recalibrating targets for sustainable intensification. *Bioscience* **67**, 386-391 (2017).
108 Sabiha, N.-E., Salim, R., Rahman, S. & Rola-Rubzen, M. F. Measuring environmental sustainability in agriculture: A composite environmental impact index approach. *Journal of environmental management* **166**, 84-93 (2016).
109 Fróna, D., Szenderák, J. & Harangi-Rákos, M. The challenge of feeding the world. *Sustainability* **11**, 5816 (2019).
110 Alvarez, A. L., Weyers, S. L., Goemann, H. M., Peyton, B. M. & Gardner, R. D. Microalgae, soil and plants: A critical review of microalgae as renewable resources for agriculture. *Algal Research* **54**, 102200 (2021).
111 Barolo, L. *et al.* Perspectives for glyco-engineering of recombinant biopharmaceuticals from microalgae. *Cells* **9**, 633 (2020).
112 Ambati, R. R. *et al.* Industrial potential of carotenoid pigments from microalgae: Current trends and future prospects. *Critical reviews in food science and nutrition* **59**, 1880-1902 (2019).
113 Khan, M. I., Shin, J. H. & Kim, J. D. The promising future of microalgae: current status, challenges, and optimization of a sustainable and renewable industry for biofuels, feed, and other products. *Microbial cell factories* **17**, 36 (2018).
114 Gong, M. & Bassi, A. Carotenoids from microalgae: A review of recent developments. *Biotechnology advances* **34**, 1396-1412 (2016).
115 Nuhma, M. J., Alias, H., Tahir, M. & Jazie, A. A. Microalgae biomass conversion into biofuel using modified HZSM-5 zeolite catalyst: a review. *Materials Today: Proceedings* **42**, 2308-2313 (2021).
116 Calijuri, M. L. *et al.* Bioproducts from microalgae biomass: Technology, sustainability, challenges and opportunities. *Chemosphere*, 135508 (2022).
117 Fabris, M. *et al.* Emerging Technologies in Algal Biotechnology: Toward the Establishment of a Sustainable, Algae-Based Bioeconomy. *Frontiers in Plant Science* **11** (2020).
118 Dragosits, M. & Mattanovich, D. Adaptive laboratory evolution–principles and applications for biotechnology. *Microbial cell factories* **12**, 1-17 (2013).
119 Portnoy, V. A., Bezdan, D. & Zengler, K. Adaptive laboratory evolution—harnessing the power of biology for metabolic engineering. *Current opinion in biotechnology* **22**, 590-594 (2011).
120 Wang, M. *et al.* Removal of nutrients from undiluted anaerobically treated piggery wastewater by improved microalgae. *Bioresource Technology* **222**, 130-138 (2016).
121 Beacham, T., Macia, V. M., Rooks, P., White, D. & Ali, S. Altered lipid accumulation in *Nannochloropsis salina* CCAP849/3 following EMS and UV induced mutagenesis. *Biotechnology reports* **7**, 87-94 (2015).

122 Meireles, L. A., Guedes, A. C. & Malcata, F. X. Increase of the yields of eicosapentaenoic and docosahexaenoic acids by the microalga Pavlova lutheri following random mutagenesis. *Biotechnology and bioengineering* **81**, 50-55 (2003).
123 Li, F.-F. *et al.* Microalgae capture of CO2 from actual flue gas discharged from a combustion chamber. *Industrial & Engineering Chemistry Research* **50**, 6496-6502 (2011).
124 Price, S., Kuzhiumparambil, U., Pernice, M. & Ralph, P. J. Cyanobacterial polyhydroxybutyrate for sustainable bioplastic production: Critical review and perspectives. *Journal of Environmental Chemical Engineering* **8**, doi:10.1016/j.jece.2020.104007 (2020).
125 Yi, Z. *et al.* Chemical Mutagenesis and Fluorescence-Based High-Throughput Screening for Enhanced Accumulation of Carotenoids in a Model Marine *Diatom Phaeodactylum tricornutum*. *Mar Drugs* **16**, doi:10.3390/md16080272 (2018).
126 Nybom, N. Some experiences from mutation experiments in Chlamydomonas. *Hereditas* **39**, 317-324 (1953).
127 Halberstaedter, L. & Back, A. The Effect of X Rays on Single Colonies of Pandorina. *The British Journal of Radiology* **15**, 124-128 (1942).
128 Kumar, H. Effects of Radiations on Blue-green Algae: II. Effects in Growth. *Annals of Botany* **28**, 555-564 (1964).
129 Hashimoto, H., Uragami, C. & Cogdell, R. J. Carotenoids and photosynthesis. *Carotenoids in nature*, 111-139 (2016).
130 Henríquez, V., Escobar, C., Galarza, J. & Gimpel, J. Carotenoids in microalgae. *Carotenoids in Nature*, 219-237 (2016).
131 Gammone, M. A., Riccioni, G. & D'Orazio, N. Marine carotenoids against oxidative stress: effects on human health. *Marine Drugs* **13**, 6226-6246 (2015).
132 Macdonald Miller, S. *et al.* Comparative Study Highlights the Potential of Spectral Deconvolution for Fucoxanthin Screening in Live *Phaeodactylum tricornutum* Cultures. *Marine drugs* **20**, 19 (2021).
133 Darley, W. M. & Volcani, B. Role of silicon in diatom metabolism: a silicon requirement for deoxyribonucleic acid synthesis in the diatom *Cylindrotheca fusiformis* Reimann and Lewin. *Experimental Cell Research* **58**, 334-342 (1969).
134 Bulankova, P. *et al.* Mitotic recombination between homologous chromosomes drives genomic diversity in diatoms. *Current Biology* **31**, 3221-3232. e3229 (2021).
135 Myung, K. & Kolodner, R. D. Induction of genome instability by DNA damage in Saccharomyces cerevisiae. *DNA repair* **2**, 243-258 (2003).
136 Pereira, H. *et al.* Fluorescence activated cell-sorting principles and applications in microalgal biotechnology. *Algal research* **30**, 113-120 (2018).
137 Gao, F., Cabanelas, I. T. D., Wijffels, R. H. & Barbosa, M. J. Fucoxanthin and docosahexaenoic acid production by cold-adapted Tisochrysis lutea. *New Biotechnology* **66**, 16-24 (2022).
138 Tominaga, H., Kodama, S., Matsuda, N., Suzuki, K. & Watanabe, M. Involvement of reactive oxygen species (ROS) in the induction of genetic instability by radiation. *Journal of radiation research* **45**, 181-188 (2004).
139 Patel, M., Jiang, Q., Woodgate, R., Cox, M. M. & Goodman, M. F. A new model for SOS-induced mutagenesis: how RecA protein activates DNA polymerase V. *Critical reviews in biochemistry and molecular biology* **45**, 171-184 (2010).
140 Fabris, M. *et al.* Emerging technologies in algal biotechnology: toward the establishment of a sustainable, algae-based bioeconomy. *Frontiers in plant science* **11**, 279 (2020).
141 Sahu, S. K., Mantri, V. A., Zheng, P. & Yao, N. Algae Biotechnology: Current Status, Potential and Impediments. *Encyclopedia of Marine Biotechnology* **1**, 1-31 (2020).

142 Moroney, J. V. Algal photosynthesis. *e LS* (2001).
143 Singh, U. B. & Ahluwalia, A. Microalgae: a promising tool for carbon sequestration. *Mitigation and Adaptation Strategies for Global Change* **18**, 73-95 (2013).
144 Prata, J. C., da Costa, J. P., Lopes, I., Duarte, A. C. & Rocha-Santos, T. Effects of microplastics on microalgae populations: a critical review. *Science of The Total Environment* **665**, 400-405 (2019).
145 Spolaore, P., Joannis-Cassan, C., Duran, E. & Isambert, A. Commercial applications of microalgae. *Journal of bioscience and bioengineering* **101**, 87-96 (2006).
146 Dragone, G., Fernandes, B. D., Vicente, A. A. & Teixeira, J. A. Third generation biofuels from microalgae. (2010).
147 Brennan, L. & Owende, P. Biofuels from microalgae—a review of technologies for production, processing, and extractions of biofuels and co-products. *Renewable and sustainable energy reviews* **14**, 557-577 (2010).
148 Pérez-Legaspi, I. A., Valadez-Rocha, V., Ortega-Clemente, L. A. & Jiménez-García, M. I. Microalgal pigment induction and transfer in aquaculture. *Reviews in Aquaculture* **12**, 1323-1343 (2020).
149 Nwoba, E. G., Ogbonna, C. N., Ishika, T. & Vadiveloo, A. in *Microalgae biotechnology for food, health and high value products* 81-123 (Springer, 2020).
150 Zhang, H. *et al.* Fucoxanthin: A promising medicinal and nutritional ingredient. *Evidence-based complementary and alternative medicine* **2015** (2015).
151 Xia, S. *et al.* Production, characterization, and antioxidant activity of fucoxanthin from the marine diatom Odontella aurita. *Marine drugs* **11**, 2667-2681 (2013).
152 Pocha, C. K. R., Chia, W. Y., Chew, K. W., Munawaroh, H. S. H. & Show, P. L. Current advances in recovery and biorefinery of fucoxanthin from *Phaeodactylum tricornutum*. *Algal Research* **65**, 102735 (2022).
153 Khaw, Y. S. *et al.* Fucoxanthin Production of Microalgae under Different Culture Factors: A Systematic Review. *Marine Drugs* **20**, 592 (2022).
154 Gao, F., Sá, M., Cabanelas, I. T. D., Wijffels, R. H. & Barbosa, M. J. Improved fucoxanthin and docosahexaenoic acid productivities of a sorted self-settling *Tisochrysis lutea* phenotype at pilot scale. *Bioresource Technology* **325**, 124725 (2021).
155 Gerashchenko, B. I. Fluorescence-Activated Cell Sorting (FACS)-Based Characterization of Microalgae. *Monitoring artificial materials and microbes in marine ecosystems: Interactions and assessment methods*, 148-160 (2020).
156 Andrews, S. *FastQC: A Quality Control Tool for High Throughput Sequence Data [Online].* <http://www.bioinformatics.babraham.ac.uk/projects/fastqc/> (2010).
157 Ewels, P., Magnusson, M., Lundin, S. & Käller, M. MultiQC: summarize analysis results for multiple tools and samples in a single report. *Bioinformatics* **32**, 3047-3048 (2016).
158 Bray, N. L., Pimentel, H., Melsted, P. & Pachter, L. Near-optimal probabilistic RNA-seq quantification. *Nature biotechnology* **34**, 525-527 (2016).
159 Smyth, G. K. Limma: linear models for microarray data. *Bioinformatics and computational biology solutions using R and Bioconductor*, 397-420 (2005).
160 Law, C. W., Chen, Y., Shi, W. & Smyth, G. K. voom: Precision weights unlock linear model analysis tools for RNA-seq read counts. *Genome biology* **15**, 1-17 (2014).
161 Ge, S. X., Jung, D. & Yao, R. ShinyGO: a graphical gene-set enrichment tool for animals and plants. *Bioinformatics* **36**, 2628-2629 (2020).
162 Powell, D. *Degust: interactive RNA-seq analysis*, <https://degust.erc.monash.edu/> (2015).
163 Fernandez, N. F. *et al.* Clustergrammer, a web-based heatmap visualization and analysis tool for high-dimensional biological data. *Scientific data* **4**, 1-12 (2017).
164 Berthelot, K., Estevez, Y., Deffieux, A. & Peruch, F. Isopentenyl diphosphate isomerase: a checkpoint to isoprenoid biosynthesis. *Biochimie* **94**, 1621-1634 (2012).

165 Jaramillo-Madrid, A. C., Ashworth, J., Fabris, M. & Ralph, P. J. The unique sterol biosynthesis pathway of three model diatoms consists of a conserved core and diversified endpoints. *Algal research* **48**, 101902 (2020).
166 Kwon, D. Y. *et al.* Fucoxanthin biosynthesis has a positive correlation with the specific growth rate in the culture of microalga *Phaeodactylum tricornutum*. *Journal of Applied Phycology* **33**, 1473-1485 (2021).
167 Cao, T. *et al.* An unexpected hydratase synthesizes the green light-absorbing pigment fucoxanthin. *The Plant Cell*, koad116 (2023).
168 Huang, R. *et al.* A potential role for epigenetic processes in the acclimation response to elevated p CO2 in the model diatom *Phaeodactylum tricornutum*. *Frontiers in Microbiology* **9**, 3342 (2019).
169 Bacova, R., Kolackova, M., Klejdus, B., Adam, V. & Huska, D. Epigenetic mechanisms leading to genetic flexibility during abiotic stress responses in microalgae: A review. *Algal Research* **50**, 101999 (2020).
170 Veluchamy, A. *et al.* An integrative analysis of post-translational histone modifications in the marine diatom *Phaeodactylum tricornutum*. *Genome biology* **16**, 1-18 (2015).
171 Larkin, R. M. Tetrapyrrole signaling in plants. *Frontiers in Plant Science* **7**, 1586 (2016).
172 Terry, M. J. & Smith, A. G. A model for tetrapyrrole synthesis as the primary mechanism for plastid-to-nucleus signaling during chloroplast biogenesis. *Frontiers in Plant Science* **4**, 14 (2013).
173 Alawady, A. E. & Grimm, B. Tobacco Mg protoporphyrin IX methyltransferase is involved in inverse activation of Mg porphyrin and protoheme synthesis. *The Plant Journal* **41**, 282-290 (2005).
174 Zhang, K., Li, J., Zhou, Z., Huang, R. & Lin, S. Roles of Alkaline Phosphatase PhoA in Algal Metabolic Regulation under Phosphorus-replete Conditions. *Journal of Phycology* **57**, 703-707 (2021).
175 Czarnecki, O. & Grimm, B. Post-translational control of tetrapyrrole biosynthesis in plants, algae, and cyanobacteria. *Journal of Experimental Botany* **63**, 1675-1687 (2012).
176 Sinha, N., Eirich, J., Finkemeier, I. & Grimm, B. Glutamate 1-semialdehyde aminotransferase is connected to GluTR by GluTR-binding protein and contributes to the rate-limiting step of 5-aminolevulinic acid synthesis. *The Plant Cell* **34**, 4623-4640 (2022).
177 Wang, P., Ji, S. & Grimm, B. Post-translational regulation of metabolic checkpoints in plant tetrapyrrole biosynthesis. *Journal of Experimental Botany* **73**, 4624-4636 (2022).
178 Bosco, M. B., Aleanzi, M. C. & Iglesias, A. Á. Plastidic phosphoglycerate kinase from *Phaeodactylum tricornutum*: on the critical role of cysteine residues for the enzyme function. *Protist* **163**, 188-203 (2012).
179 Ma, Y.-H. *et al.* Antisense knockdown of pyruvate dehydrogenase kinase promotes the neutral lipid accumulation in the diatom *Phaeodactylum tricornutum*. *Microbial cell factories* **13**, 1-9 (2014).
180 Ge, F. *et al.* Methylcrotonyl-CoA carboxylase regulates triacylglycerol accumulation in the model diatom *Phaeodactylum tricornutum*. *The Plant Cell* **26**, 1681-1697 (2014).
181 Conte, M. *et al.* Screening for biologically annotated drugs that trigger triacylglycerol accumulation in the diatom *Phaeodactylum*. *Plant physiology* **177**, 532-552 (2018).
182 Pan, Y. *et al.* Amino acid catabolism during nitrogen limitation *in Phaeodactylum tricornutum*. *Frontiers in Plant Science* **11**, 589026 (2020).
183 Ritchie, R. J. Consistent sets of spectrophotometric chlorophyll equations for acetone, methanol and ethanol solvents. *Photosynthesis research* **89**, 27-41 (2006).

184 Dere, Ş., Gunes, T. & Sivaci, R. Spectrophotometric determination of chlorophyll-A, B and total carotenoid contents of some algae species using different solvents. *Turkish Journal of Botany* **22**, 13-18 (1998).
185 Aswini, V. & Gothandam, K. Genetic manipulation for carotenoid production in microalgae an overview. *Current Research in Biotechnology* (2022).
186 Liu, M., Ding, W., Yu, L., Shi, Y. & Liu, J. Functional characterization of carotenogenic genes provides implications into carotenoid biosynthesis and engineering in the marine alga *Nannochloropsis oceanica*. *Algal Research* **67**, 102853 (2022).
187 Fernandes, A. S., do Nascimento, T. C., Jacob-Lopes, E., De Rosso, V. V., & Zepka, L. Q. (2018). Carotenoids: A brief overview on its structure, biosynthesis, synthesis, and applications. *Progress in carotenoid research*, *1*, 1-17.
188 Levasseur M, Thompson PA, Harrison PJ (1993) Physiological acclimation of marine phytoplankton to different nitrogen sources 1. Journal of Phycology 29 (5):587-595
189 Susanto E, Fahmi AS, Abe M, Hosokawa M, Miyashita K (2016) Lipids, fatty acids, and fucoxanthin content from temperate and tropical brown seaweeds. Aquatic Procedia 7:66-75

Supplementary Material

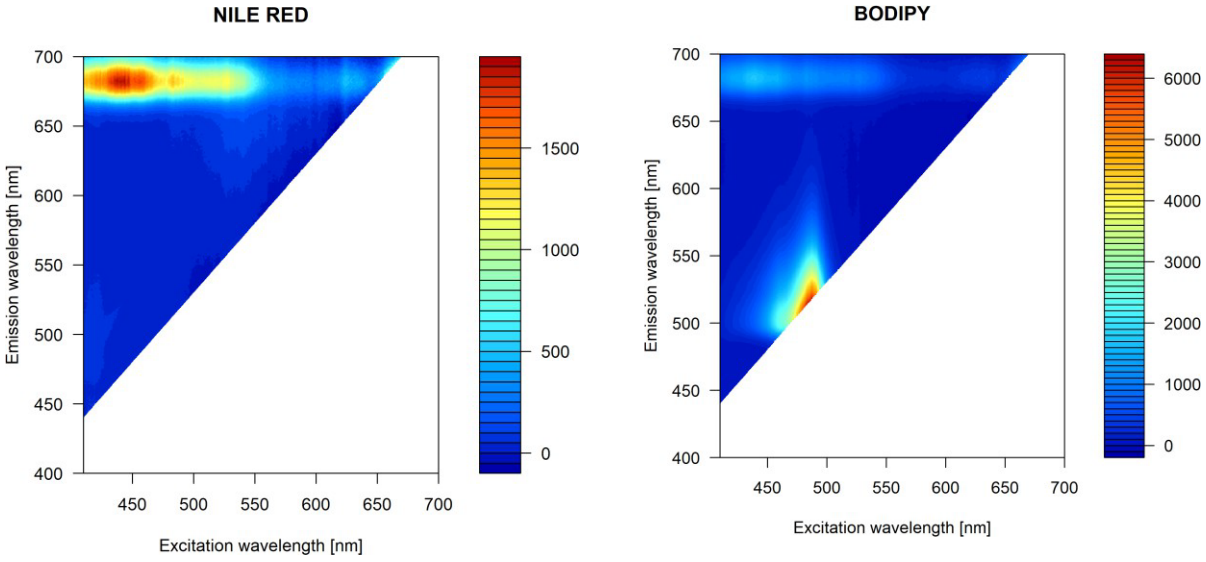

Supplementary figure 2.1. Nile red and BODIPY optimal concentrations at excitation/emission wavelengths of 484/583 and 490/512, respectively, without washing media after staining.

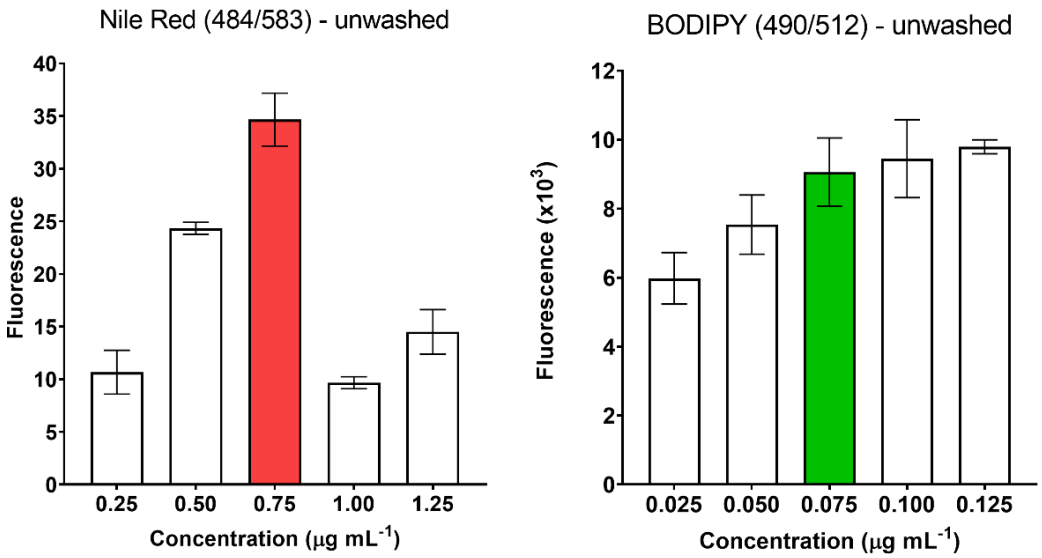

Supplementary figure 2.2. Nile red and BODIPY excitation/emission matrices showing fluorescence characteristics of stained cell of *Phaeodactylum tricornutum*.

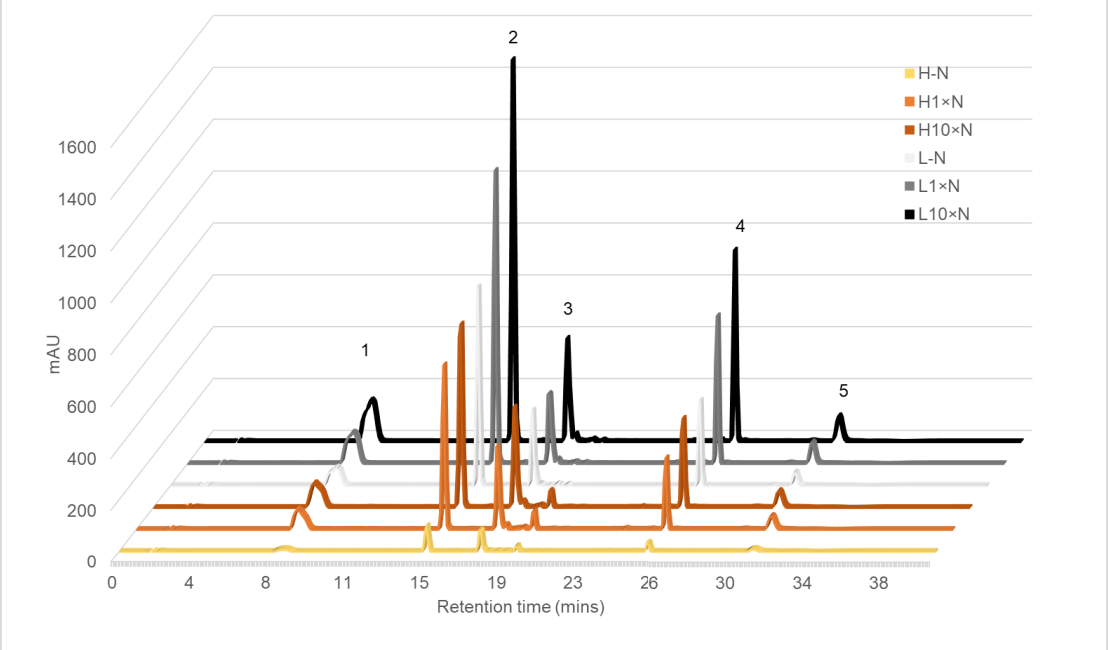

Supplementary figure 2.3. Representative HPLC chromatograms *of Phaeodactylum tricornutum* extract from each treatment group. Treatment abbreviations are as follows: nitrate-free ASW media (-N), standard (1xN) nitrate media or media with 10× nitrate (10xN) and either 10 (LL) or 200 (HL) µmol photons m^{-2} s^{-1}. Peaks numbers are represented as follows: 1: Chlorophyll *c*; 2: Fucoxanthin; 3: Diadinoxanthin; 4: Chlorophyll *a*; 5: β-carotene.

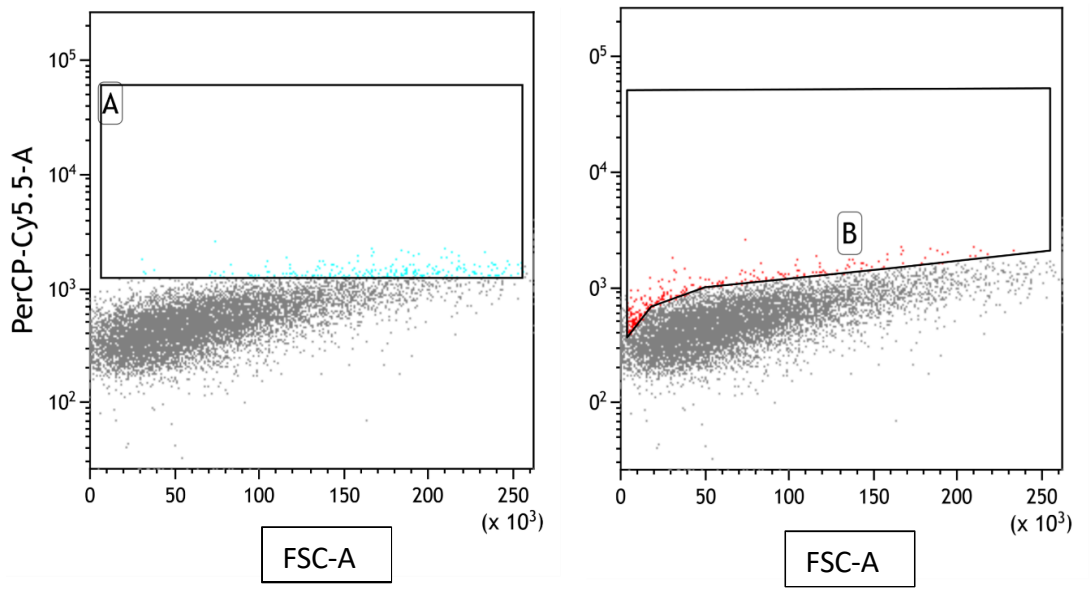

Supplementary figure 4.1 Example of gating strategy used (rectangle – A) to sort top ~1% fluorescing cells of *P. tricornutum* with FACS.

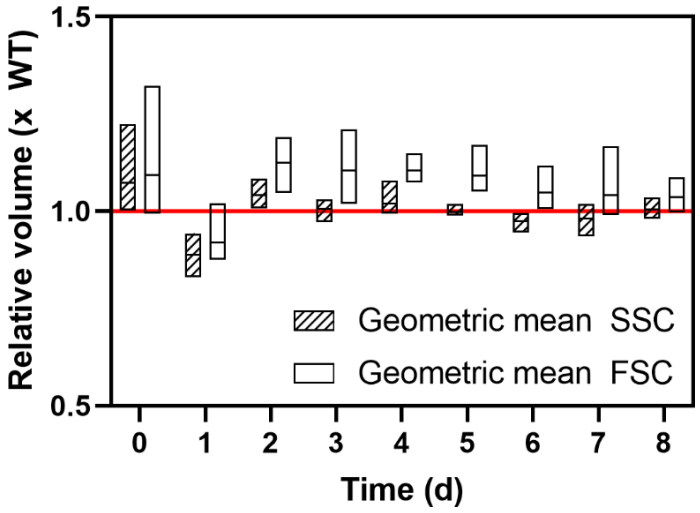

Supplementary figure 4.2. Cell volume measured using the geometric mean of FSC (Forward Scatter) and SSC (Side Scatter) over the experimental period. Values are FACS replicates divided by WT mean with floating bars from minimum to maximum, $n = 5$.

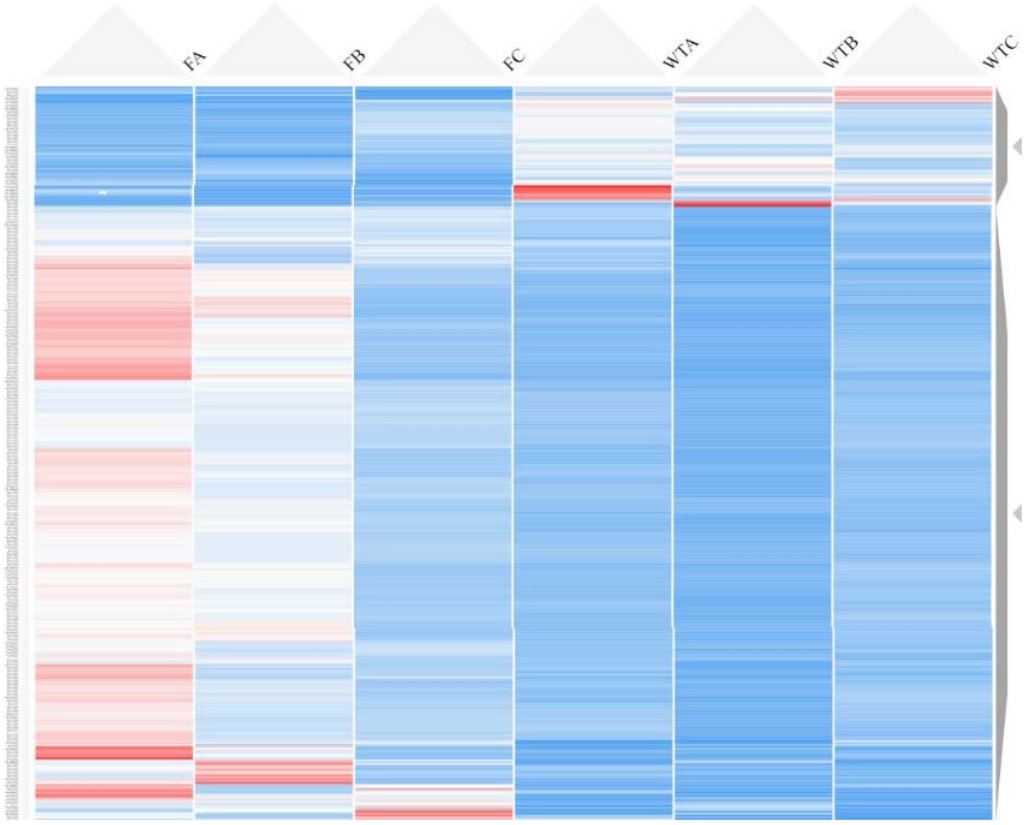

Supplementary figure 4.3. Heatmap showing relative gene expression between WT and FACS-sorted cultures of *P. tricornutum* expressed as z-scores. Genes are grouped by GO aspect term with minimum gene pool of 4. Made using Clustergrammer https://maayanlab.cloud/clustergrammer/.

Supplementary table 4.1. Enrichment analysis results depicting fold enrichment and FDR for GO aspect Biological Processes, sorted by fold enrichment 1.

GO aspect	Pathway	Fold Enrichment	FDR
BP	Protoporphyrinogen IX metabolic process	19.64	<0.001
BP	Protoporphyrinogen IX biosynthetic process	19.64	<0.001
BP	Porphyrin-containing compound biosynthetic process	17.28	<0.001
BP	Porphyrin-containing compound metabolic process	14.90	<0.001
BP	Pigment biosynthetic process	14.73	<0.001
BP	Tetrapyrrole biosynthetic process	13.94	<0.001
BP	Heme biosynthetic process	13.86	<0.001
BP	Pigment metabolic process	13.09	<0.001
BP	Photosynthesis, light harvesting	12.16	<0.001
BP	Tetrapyrrole metabolic process	12.00	<0.001
BP	Heme metabolic process	11.22	<0.001
BP	Protein-chromophore linkage	11.10	<0.001
BP	Photosynthesis, light reaction	10.78	<0.001
BP	Photosynthesis	10.27	<0.001
BP	Ribosome biogenesis	6.71	<0.001
BP	RRNA processing	5.82	0.001

BP	RRNA metabolic process	5.71	0.001
BP	Ribonucleoprotein complex biogenesis	5.56	<0.001
BP	Generation of precursor metabolites and energy	4.04	<0.001
BP	Cellular component biogenesis	3.43	<0.001
BP	NcRNA processing	3.06	0.012
BP	Purine-containing compound metabolic process	3.02	0.048
BP	Cellular component organization or biogenesis	2.63	0.001
BP	NcRNA metabolic process	2.58	0.018
BP	Nucleobase-containing small molecule metabolic process	2.38	0.047
BP	Aromatic compound biosynthetic process	2.13	0.003
BP	Heterocycle biosynthetic process	2.07	0.005
BP	Organic cyclic compound biosynthetic process	1.99	0.008
BP	Organonitrogen compound biosynthetic process	1.87	0.018
BP	Heterocycle metabolic process	1.82	<0.001
BP	Cellular aromatic compound metabolic process	1.80	<0.001
BP	Organic cyclic compound metabolic process	1.79	<0.001
BP	Small molecule metabolic process	1.79	0.032
BP	Organonitrogen compound metabolic process	1.62	0.001
BP	Organic substance biosynthetic process	1.60	0.014
BP	Cellular nitrogen compound metabolic process	1.55	0.007
BP	Biosynthetic process	1.55	0.024
BP	Cellular biosynthetic process	1.54	0.038

Supplementary table 4.2. Enrichment analysis results depicting fold enrichment and FDR for GO aspect Cellular Component, sorted by fold enrichment 2.

GO aspect	Pathway	Fold Enrichment	FDR
CC	Light-harvesting complex	12.46	<0.001
CC	Photosystem	10.25	<0.001
CC	Photosystem II	10.25	<0.001
CC	Photosynthetic membrane	9.43	<0.001
CC	Thylakoid	8.73	<0.001
CC	Nucleolus	6.67	<0.001
CC	Plastid	5.82	<0.001
CC	Chloroplast	5.50	<0.001
CC	Nuclear lumen	3.80	0.003
CC	Membrane protein complex	3.16	0.003
CC	Membrane-enclosed lumen	3.02	0.011
CC	Organelle lumen	3.02	0.011
CC	Intracellular organelle lumen	3.02	0.011
CC	Intracellular membrane-bounded organelle	1.72	0.002
CC	Membrane-bounded organelle	1.72	0.002
CC	Nucleus	1.62	0.044
CC	Intracellular organelle	1.58	0.005
CC	Organelle	1.57	0.005

CC	Intracellular anatomical structure	1.49	0.005

Supplementary table 4.3. Enrichment analysis results depicting fold enrichment and FDR for GO aspect Molecular Function, sorted by fold enrichment 3.

GO aspect	Pathway	Fold Enrichment	FDR
MF	Chlorophyll binding	12.46	<0.001
MF	Pentosyltransferase activity	10.91	0.001
MF	Tetrapyrrole binding	5.50	<0.001
MF	Magnesium ion binding	4.79	0.034
MF	Helicase activity	4.04	0.017
MF	ATP-dependent activity	2.57	0.013
MF	Purine ribonucleoside triphosphate binding	2.12	<0.001
MF	Purine ribonucleotide binding	2.11	<0.001
MF	Purine nucleotide binding	2.07	<0.001
MF	Carbohydrate derivative binding	2.06	<0.001
MF	ATP binding	2.05	<0.001
MF	Ribonucleotide binding	2.04	<0.001
MF	Adenyl ribonucleotide binding	2.03	<0.001
MF	Adenyl nucleotide binding	1.99	<0.001
MF	Anion binding	1.92	<0.001
MF	Nucleotide binding	1.89	<0.001
MF	Nucleoside phosphate binding	1.89	<0.001
MF	Small molecule binding	1.81	<0.001
MF	Hydrolase activity	1.80	0.001
MF	Ion binding	1.40	0.030